



PONTIFICIA UNIVERSIDAD CATÓLICA DE CHILE
DIRECCION DE INVESTIGACION Y DOCTORADO
ESCUELA DE MEDICINA

REVERSE TRIGGERING DYSSYNCHRONY AND ITS IMPACT ON DIAPHRAGM INJURY DURING MECHANICAL VENTILATION

POR

L. FELIPE DAMIANI REBOLLEDO

Tesis presentada a la Pontificia Universidad Católica de Chile

Para optar al grado de Doctor en Ciencias Médicas

Profesores Guía:

Alejandro Bruhn Cruz

Profesor titular

Pontificia Universidad Católica de Chile

Laurent Brochard

Interdepartmental Division of Critical Care Medicine

University of Toronto, Canada

2020

Santiago de Chile

©2020, L. Felipe Damiani Rebolledo

TODO TIENE SU TIEMPO

Todo tiene su tiempo, y todo lo que se quiere debajo del cielo tiene su hora.

Tiempo de nacer, y tiempo de morir; tiempo de plantar, y tiempo de arrancar lo plantado;

tiempo de matar, y tiempo de curar; tiempo de destruir, y tiempo de edificar;

tiempo de llorar, y tiempo de reír; tiempo de endechar, y tiempo de bailar;

tiempo de esparcir piedras, y tiempo de juntar piedras; tiempo de abrazar, y tiempo de abstenerse de abrazar;

tiempo de buscar, y tiempo de perder; tiempo de guardar, y tiempo de desechar;

tiempo de romper, y tiempo de coser; tiempo de callar, y tiempo de hablar;

tiempo de amar, y tiempo de aborrecer; tiempo de guerra, y tiempo de paz.

(Eclesiastés 3:1-8)

All this work is dedicated to:

Brian P. Kavanagh my former mentor who left a tremendous and invaluable mark in my
scientific and personal life.

AGRADECIMIENTOS PERSONALES

La planificación, ejecución y finalización de este trabajo no sería posible sin la acción de diferentes personas que de alguna u otra forma aportaron en la consecución de este manuscrito. Así, agradezco a:

Carina, mi señora y compañera de vida por su apoyo incondicional y amor sincero.

Mis amadas hijas, Rafaella y Simona, que llegaron en medio de este proceso para convertirse en el sentido de mi vida e inspiración.

Mis padres, Carmen Gloria y Luis, por entregarme un amor incomprensible y valores que me convierten en la persona que soy.

Mis hermanos, Renzo y Loredanna, por su compañía cariñosa y verdadera a lo largo de mi vida.

Mis abuelos, Jaime y Gloria, por su apoyo desinteresado y genuino en los primeros pasos de mi formación profesional.

Mis queridas sobrinas y sobrinos, Josefa, Colomba, José Tomás, Victoria, Ian e Iñigo por entregar alegría al mundo de manera noble e inocente recordándonos la belleza de lo simple y cotidiano.

Mi amigo y compañero de viajes Yorschua, por su compañía cariñosa y sencillez de corazón.

Mis compañeros de trabajo y amigos de diferentes partes del mundo, Thomas, Ricard, Tai, Irene, Ignacio, Doreen, Luca, Kohei, Bhushan, Gail; nada de esto sería posible sin la ayuda de ustedes.

Mis maestros y mentores, Alejandro, Laurent y Brian, por enseñarme el “arte” de la ciencia a través de sabios consejos de vida; sin duda son imprescindibles.

Finalmente, a todos aquellos pacientes y animales que cumplieron un rol clave en la realización de esta tesis.

AGRADECIMIENTOS INSTITUCIONALES

Agradezco a la escuela de Medicina de la Pontificia Universidad Católica de Chile, por haber seleccionado mi postulación al Programa de Doctorado en Ciencias Médicas, incluyendo así, por primera vez a un kinesiólogo en la historia de su programa. Además, les agradezco sinceramente el haber aportado a mi ingreso económico mensual durante los 4 años del doctorado.

Agradezco a las instituciones del gobierno, ANID (ex CONICYT), por haber hecho posible la realización de este doctorado, aportando la mayor parte de mi ingreso económico mensual durante los últimos 3 años de estudio tanto en Chile como en Canadá.

Agradezco a los distintos directores que este programa de doctorado ha tenido durante estos años, Jaime Pereira, Claudia Sáez, Silvana Zanlungo, Jorge Carvajal y Andrea Leiva, quienes me apoyaron sin dudar durante todo el proceso de mi formación. Del mismo modo, quisiera agradecer a cada uno de los docentes que con excelencia y pasión aportaron en mi formación científica.

Finalmente, agradezco muy cariñosamente a los miembros de mi comisión de tesis, los doctores Rodrigo Cornejo y Jaime Retamal, por creer en la idea y apoyarme de manera paciente y desinteresada.

TABLE OF CONTENTS

(Hyperlinks available)

LIST OF FIGURES AND ANNEXES	1
LIST OF TABLES	3
SUMMARY	4
INTRODUCTION	7
1.Mechanical ventilation and Acute Respiratory Distress Syndrome	7
2.Understanding Patient-Ventilator Interaction	7
2.1 Synchrony between the patient and the ventilator.....	7
2.2 Mechanical ventilation modes.....	8
2.3 Pressures applied in the respiratory system.....	8
2.4 Importance of the respiratory drive and level of breathing effort	10
3. Reverse triggering dyssynchrony	10
3.1 Definition.....	10
3.2 How frequently does reverse triggering occur?	11
3.3 Pathophysiology	12
3.4 Potential mechanisms	12
3.5 Monitoring patient-ventilator dyssynchronies	13
4. Understanding how patient ventilator dyssynchrony may be harmful for the diaphragm	14
4.1 Myotrauma and Ventilation induced diaphragm dysfunction.....	14
4.2 Diaphragm dysfunction and outcomes.....	15
4.3 Mechanisms of Myotrauma	16
4.4 Potentials biomarkers of respiratory muscle injury.....	19
4.5 How specifically reverse triggering may affect diaphragm function?	20
HYPOTHESIS.....	22

GOALS OF THE THESIS	23
MATERIALS AND METHODS	25
1. Incidence of reverse triggering	25
1.1 Data collection and study design	25
1.2 Derivation of the automated detection of reverse triggering	25
1.3 Validation of the automated detection of reverse triggering.....	28
1.4 Incidence of reverse triggering	28
1.5 Statistical analysis	29
2. Development of a porcine model of reverse triggering during ARDS	30
2.1 ARDS model.....	30
2.2 Experimental protocol and study groups.....	32
2.3 Induction of reverse triggering dyssynchrony	34
2.4 Physiological measurements and sample collection	34
2.5 Statistical analysis	36
3. Measurements of function and structure of the diaphragm	36
3.1 Breathing effort and study groups.....	36
3.2 Diaphragm function	38
3.3 Diaphragm morphology	39
3.4 Biomarkers of muscle injury	41
3.5 Statistical analysis	41
RESULTS	42
1. Incidence of reverse triggering	42
1.1 Detection of reverse triggering	42
1.2 Validation of the automated detection of reverse triggering	43
1.3 Incidence of reverse triggering	43
1.4 Entrainment and within subject analysis	50
1.5 Factors associated with high incidence of reverse triggering.....	52
2. Porcine model of reverse triggering during ARDS	55

2.1 ARDS model.....	55
2.2 Development of reverse triggering model.....	55
2.3 Characteristics reverse triggering model	57
3. Impact of reverse triggering on diaphragm function and structure	64
3.1 Pressure time product and study groups.....	64
3.2 Diaphragm force generating capacity.....	65
3.3 Histological evidence of diaphragm injury.....	69
3.4 Serum skeletal troponin I.....	73
DISCUSSION	75
1. Incidence of reverse triggering	75
2. Reverse triggering model	78
3. Impact of reverse triggering on function and structure of the diaphragm.....	82
4. Conclusion, limitations and future projections.....	88
ABBREVIATIONS	91
REFERENCES.....	94
ANNEXES.....	104

LIST OF FIGURES AND ANNEXES

(Hyperlinks available)

[Figure 1. Reverse triggering dyssynchrony](#)

[Figure 2. Reverse triggering leading to eccentric contraction of the diaphragm](#)

[Figure 3. Study protocol and experimental groups](#)

[Figure 4. Example of force/frequency curve](#)

[Figure 5. Comparison of reverse triggering incidence](#)

[Figure 6. Flow diagram of the study population](#)

[Figure 7. Incidence of reverse triggering using EAdi cut-off > 1 \$\mu\$ V](#)

[Figure 8. Incidence of reverse triggering using EAdi cut-off >3 and >5 \$\mu\$ V](#)

[Figure 9. Correlation between amount RT breaths and 1:1 entrainment](#)

[Figure 10. Representative tracing of one animal with reverse triggering dyssynchrony](#)

[Figure 11. Cumulative doses of sedatives in passive and RT group](#)

[Figure 12. Anesthesia depth in passive and RT group](#)

[Figure 13. Wet-dry weight ratio in passive and RT group](#)

[Figure 14. BAL total protein content in passive and RT group](#)

[Figure 15. PTP_{min} values and experimental groups](#)

[Figure 16. Transdiaphragmatic twitch pressure \(P_{diTw}\)](#)

[Figure 17. Force/frequency curves](#)

[Figure 18. Transdiaphragmatic twitch pressure \(P_{diTw}\) normalized to baseline](#)

Figure 19. Transdiaphragmatic pressure (P_{di}) normalized to baseline

Figure 20. Myofiber cross-sectional area of diaphragm muscle

Figure 21. Histologic assessment of diaphragm fibers

Figure 22. Relative change of Fast skeletal troponin I as a marker of diaphragm injury

Annex 1. Reverse triggering detection based on expiratory time (T_e)

Annex 2. Diagram of the experiment set up and cuff electrodes

Annex 3. Calculation of Pressure-Time-Product in reverse triggered breaths

Annex 4. Western blot protocol for troponin I in serum samples

LIST OF TABLES

(Hyperlinks available)

[Table 1. Definitions and criteria used for visual and automated detection of reverse triggering](#)

[Table 2. Criteria for abnormal fibers of haematoxylin and eosin stained cross-sections of the diaphragm](#)

[Table 3. Sensitivity analysis on 2000 breaths \(n=10\) in order to estimate variability of diagnostic value of proposed algorithm](#)

[Table 4. Baseline patient characteristics](#)

[Table 5. Within-subject analysis of EAdi and phase angle in patients with a high incidence of entrainment](#)

[Table 6. Ventilatory variables in RT and passive ventilation](#)

[Table 7. Respiratory mechanics \(static conditions\) in RT and passive group](#)

[Table 8. Hemodynamic and metabolic variables in RT and passive group](#)

SUMMARY

Mechanical ventilation (MV) is used to sustain life in patients admitted to the intensive care unit for a wide spectrum of indications such as elective surgical procedures, septic shock, multiple organic failure and acute respiratory distress syndrome. Safe and effective ventilation depends on a smooth interaction between these two independent systems: the patient and the mechanical ventilator. Any mismatch between the patient and mechanical ventilator in terms of breath delivery timing, as well as the inability of the ventilator's flow delivery to match the patient's flow demand, is referred to as patient-ventilator dyssynchrony (PVD). Reverse Triggering (RT) is a type of PVD where muscle contractions are delayed, starting a certain amount of time after the machine triggered breath and occurring under different entrainment patterns. RT was originally described in 2013, in sedated patients admitted to the intensive care unit. Unfortunately, data about RT until now is scarce and its relevance remains totally uncertain. If any, the relevance of RT might be attributed to 2 main factors: the frequency of this PVD and its potential consequences in both lung and diaphragm injury. The group of different adverse patient-ventilator interactions leading to diaphragm atrophy and injury and resulting in a final common pathway of diaphragm weakness are denominated myotrauma. Particularly, RT is thought to cause eccentric myotrauma, which is a muscle contraction while muscle is lengthening during the ventilator's expiratory phase while lung volume is decreasing. Based on animal and human studies, the impact of RT (if any) might be mediated by the level of breathing effort.

In this thesis we aimed to describe the incidence of RT in patients early after intubation and admission to the intensive care unit and also to study the impact of RT with different levels of breathing effort on diaphragm injury (function and structure) in an animal model of RT with acute respiratory distress syndrome.

To determine RT incidence, we conducted ancillary study in patients with continuous monitorization of the electrical activity of the diaphragm (EAdi). We developed a method

for automatic detection of reverse triggering using EAdi and airway pressure curve. We additionally compared patients' demographics, sedation depth and ventilation settings according to the median rate of reverse triggering, including time to transition to assisted ventilation or extubation. We found that our new automatic method presented a good diagnostic accuracy (98% total accuracy). Using a threshold of 1 μ V for EAdi, median reverse triggering rate was 8% (range 0.1 to 75) with 44% (17 out of 39) of patients having $\geq 10\%$ of breaths with reverse triggering. With 3 μ V threshold, 26% (10 out of 39) of patients had $\geq 10\%$ reverse triggered breaths. Importantly, patients who resented more reverse triggering were more likely to be on an assisted mode or extubated in the following 24 hours than patients who had low rate of RT (68% vs 35%; $p=0.039$).

We also developed a 3 hours model of reverse triggering in pigs by modifying tidal volume, respiratory rate and level of sedation. Our approach to induce reverse triggering was not only feasible, but consistently reproducible in all animals, although with different presentations in terms of breathing effort and entrainment pattern. The most frequent entrainment pattern observed was 1:1, occurring in 83% of the total animals. Compared to passive ventilation (no breathing effort), RT group had significantly lower tidal volume (7 vs 10 ml/kg) and higher respiratory rate (45 vs 31 bpm) whereas no differences were found in other cardiorespiratory and sedation variables, nor in lung injury indicators after the study period.

In order to study the impact of RT on diaphragm injury, we divided the RT group in 3 sub-groups based on the level of breathing effort calculated by the pressure time product. Thus, 4 experimental groups were analyzed: Passive (no breathing effort), RT with low effort, RT with middle effort and RT with high effort. Function of the diaphragm was assessed by the ability to generate force, which correspond to the transdiaphragmatic pressure whilst diaphragm structure was evaluated using histological samples and serum troponin I as biomarker of muscle injury.

We found that RT affects diaphragm function in two opposite directions. On one hand, animals with RT and low breathing effort showed a significant increase in force of 10% as compared to baseline. On the other hand, animals with RT and high breathing effort showed a larger decrease in force (34%) as compared to baseline. This difference was significantly different with the other experimental groups. Moreover, histologic analysis of diaphragm myofibers showed that RT with high breathing effort had significant lower myofiber cross-sectional area than passive group. Also, when comparing abnormal myofibers between groups, a significantly lower proportion of small fiber size were found in RT with high breathing effort in comparison to passive group. No differences were found in serum troponin I neither overtime nor between groups.

In conclusion, an EAdi-based automated reverse triggering detection showed that this asynchrony is highly prevalent early after intubation under assist-control ventilation; the incidence depends on the magnitude of the activity detected and that reverse triggering seems to occur during the transition phase between deep sedation and the onset of patient triggering. In addition, the creation of a reverse triggering model revealed this phenomenon very complex, with high variability in terms of entrainment pattern and level of breathing effort. Finally, we have confirmed that RT dyssynchrony affects diaphragm function and this effect is modulated by the level of respiratory effort. Reverse triggering with low breathing effort seems to have a protective role on diaphragm function whereas reverse triggering with high breathing effort may favor eccentric myotrauma.

INTRODUCTION

1. Mechanical ventilation and Acute Respiratory Distress Syndrome

Mechanical ventilation (MV) is a life support technique capable to provide airflow and positive pressure to the lungs. It has been described that patients who required invasive MV represent 2.8% of total hospital admissions in United States and around 60% of all admitted patients to intensive care units (ICU)^{1,2}. MV is usually applied for a wide spectrum of indications such as elective surgical procedures, multiple organic failure and acute respiratory distress syndrome (ARDS)^{1,3}. ARDS is a type of acute, diffuse and inflammatory lung injury, leading to increased pulmonary vascular permeability, increased lung weight, and loss of aerated lung tissue. The clinical hallmarks are hypoxemia and bilateral radiographic opacities, associated with increased venous admixture, increased physiological dead space, and decreased lung compliance. The morphological hallmark of the acute phase is diffuse alveolar damage (*i.e.*, edema, inflammation, hyaline membranes, and hemorrhage)⁴. ARDS is an important and costly public health problem associated with a short term mortality rate over 40%, and with long term disabilities, exercise limitations, and a reduced physical quality of life until 5 years after diagnosis in survivors⁵. Despite different treatments available, ARDS affects approximately 70 to 80 patients/100,000 habitants annually⁶. The application of MV in ARDS patients is complex due to many factors, however, the interaction between the patient and the ventilator has shown to play a major role in its success.

2. Understanding Patient-Ventilator Interaction

2.1 Synchrony between the patient and the ventilator

Once patients are undergoing MV, the quality of the interaction (temporally and quantitatively) between the patient and the ventilator is imperative for MV to be beneficial. Adequate synchrony at requires that: 1. Ventilator provides flow and

pressure as soon as patient effort begins; 2. The magnitude of the pressure and flow meets patient's respiratory demand; and 3. The ventilation assistance is terminated when patient effort ends. Thus, whenever any of these situations described above are not fulfilled, patient ventilator dyssynchrony (PVD) occurs. Consequently, PVD can be distinguished in two major categories: (1) dyssynchronies that occur because neural breath is not in phase with mechanical breath (timing dyssynchronies) and (2) dyssynchronies related to a discrepancy between the level of assist that the patient needs and the actual assist that the ventilator provides.

2.2 Mechanical ventilation modes

There are different modes of ventilation available and their choice is based on the clinician's preference, which depends on the patient's context and specific needs. Respiratory breaths on MV can be: 1. Fully controlled (patient does not actively contribute); 2. Partially supported or assisted (combination of patient effort and ventilator assistance occurs in the same cycle); and 3. Spontaneous (the inspiratory flow is entirely generated by the patient effort)³. Patient-ventilator dyssynchrony are often recognized in partially or spontaneous mode when the patient theoretically starts to participate. However, some dyssynchronies, such as reverse triggering, have been reported in controlled modes.

2.3 Pressures applied in the respiratory system

The equation of motion for the respiratory system constitutes the fundamental theory of respiratory mechanics. It characterizes mechanical forces and provides the mathematical foundation for measurements in clinical practice. During MV, both ventilator and respiratory muscles (depending on ventilatory mode and patient's condition) can apply pressures to the respiratory system. The sum of applied pressures is equal to the sum of two pressures opposing respiratory system inflation, the resistive

(P_{res}) and elastic (P_{el}) pressure of the respiratory system as follows (inertia is assumed to be negligible):

$$P_{vent} + P_{mus} = P_{el} + P_{res}$$

where P_{vent} is ventilator pressure; P_{mus} is muscle pressure.

During controlled or passive MV (without patient effort), the respiratory muscles do not contract, P_{mus} is 0 and the pressure needed to overcome the elastance and resistance of the respiratory system is entirely provided by the ventilator. Considering that P_{vent} is equal to airway pressure (P_{aw}), and P_{el} and P_{res} are compound by different factors, the equation is modified as follows:

$$P_{aw} = P_0 + (R \times Flow) + (Vt \times ERS)$$

where P_{aw} = airway pressure (at the airway opening), P_0 = initial alveolar pressure, R = resistance to flow, VT = tidal volume, and ERS = elastance of the respiratory system. Each term of this equation impacts the pressure applied to the airways.

The measurement of P_{aw} allows the description of the total respiratory system. However, to differentiate the mechanical properties of the lungs from those of the chest wall, measuring the pleural pressure (P_{pl}) is required. The pressure distending the lungs is the difference between P_{aw} and P_{pl} , which is called transpulmonary pressure (P_L): $P_L = P_{aw} - P_{pl}$

Unfortunately, assessment of P_{pl} in clinical setting is not feasible. Esophageal pressure (P_{eso}) is a valid surrogate for P_{pl} that has been shown to be a useful parameter to assess respiratory mechanics and inspiratory effort⁷. When respiratory muscles are active, its negative swing represents the pressure generated by the respiratory muscles needed to distend the chest wall⁸.

2.4 Importance of the respiratory drive and level of breathing effort

Respiratory drive is defined as the intensity of the neural output from the respiratory centers that control the magnitude of inspiratory effort⁹. In normal conditions the respiratory centers adapt breathing effort to the patient's needs. However, an inadequate respiratory drive under mechanical ventilation, either too high or too low, has recently been incriminated as a risk factor for both lung¹⁰ and diaphragmatic injury or myotrauma^{11,12}(see myotrauma details below). Thus, monitoring and controlling the drive to breathe might be important for clinical practice.

Several available techniques provide reliable measures of the intensity and timing of drive and the breathing effort including airway occlusion pressure during the first 100 milliseconds ($P_{0.1}$)¹³, pressure swing amplitudes of P_{eso} , gastric pressure (P_{ga}), and transdiaphragmatic pressure (P_{di}) and a variety of more sophisticated methods such as work of breathing¹⁴, tension time index¹⁵ and pressure time product (PTP)¹⁶.

Unlike the others, PTP is sensitive to the frequency and duration of contractions and it correlates well with energy expenditure during a broad range of inspiratory loads¹⁷. Moreover, the PTP is insensitive to changes in volume, meaning that it is also valid when effort does not result in volume generation, such as during isometric or eccentric contractions, usually observed in some PVD.

3. Reverse triggering dyssynchrony

3.1 Definition

Reverse triggering (RT) is a type of PVD where respiratory muscular contractions are triggered by the ventilator under different patterns of entrainment. RT was first described in sedated ARDS patients by Akoumianaki and colleagues, in 2013, who observed repetitive patient efforts occurring regularly within each mechanical inspiration (Figure 1). These inspiratory efforts were directly triggered by the mechanical insufflations and were observed during both pressure or volume controlled ventilation¹⁸.

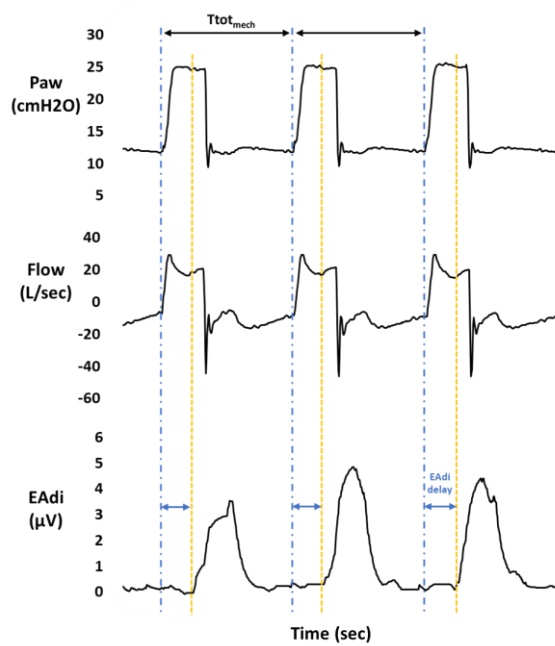


Figure 1. Reverse Triggering dyssynchrony. Patient effort and muscular contractions are assessed by electrical activity of the diaphragm (bottom). These diaphragmatic contractions begin (yellow dashed lines) systematically after the mechanical insufflations by the ventilator (blue dashed lines) causing a time delay between the machine insufflation and the patient effort (blue arrows).

3.2 How frequently does Reverse Triggering dyssynchrony occur?

The prevalence of PVD depends on different factors such as type of dyssynchrony, moment of assessment and method of detection¹⁹. Regarding RT, the evidence is scarce. In a French study, continuous recordings of airway pressure, flow, volume and P_{es0} were obtained in 21 moderate-to-severe ARDS patients. These patients were divided in 2 groups: patients using neuromuscular blockade (NMBA; $n=11$) and patients without NMBA ($n=10$). No RT was observed in patients receiving NMBA whereas the incidence of RT was 33% in the group without NMBA²⁰.

3.3 Pathophysiology

Reverse triggering is characterized by a regular and repeated activation of respiratory muscles after time-initiated ventilator cycles during controlled mechanical ventilation. It has also named entrainment or phase-locking phenomena. The term entrainment in respiratory physiology refers to the establishment of a fixed repetitive temporal relationship between the neural and mechanical respiratory cycles²¹. More in detail, the inspiratory efforts of the patient occur over a specific and repetitive phase of the ventilator cycle with a minimal variability of their neural respiratory time.

The entrainment ratio, which is the ratio of neural to ventilator breaths, is variable and can be interrupted by irregular patterns every 7–15 respiratory cycles²². Studies in humans have shown that the 1:1 ratio is the most frequent and stable entrainment pattern, mostly reported in heavily sedated patients ^{18,22}.

Importantly, as during RT the patient's inspiratory effort starts with a certain delay relative to the start of the machine's breath, the patient's inspiratory effort usually persists beyond the end of the machine's breath. Thus, if deep enough and long enough, the persistent effort could even produce a double cycling dyssynchrony (this is 2 consecutive inspirations without an expiration in between), and eventually lung injury because of larger lung volumes, or muscle injury because of eccentric contraction of the diaphragm (further details below).

3.4 Potential Mechanisms

The interaction between critical illness and respiratory entrainment is complex and not clearly understood. Entrainment appears to be produced mainly by the stretching of the slowly adapting receptors and a sustained activation of the vagally mediated Hering–Breuer reflex. Experiments in animals have shown that the abolition of the Hering–Breuer reflex by cooling or section of vagal nerves impedes entrainment^{23,24}. However, entrainment has also been reported in patients who underwent pulmonary transplant, where vagal afferents were resected²⁵.

Interestingly, a recent observation in two brain-dead patients demonstrated that passive ventilator insufflations may entrain respiratory muscles²⁶. In this context, the absence of respiratory drive from the brainstem suggests to think that respiratory muscle activation after ventilator insufflation may be mediated by various afferents, i.e. thoracic mechanoreceptors or passive thoracic movement by activation of respiratory muscles^{27,28}. Other hypotheses such as spinal reflexes or the presence of a spinal respiratory pattern generator could potentially be involved²⁶

3.5 Monitoring patient-ventilator dyssynchrony

To accurately detect PVD, patient's effort and ventilatory support must be assessed simultaneously. Assessment of patient's effort requires semi-invasive measurements of esophageal pressure and/or respiratory muscle electromyogram. However, these types of devices are not widely used in clinical practice. There are three main monitoring strategies to detect PVD: ventilator waveform analysis (visual inspection of flow and airway pressure), esophageal pressure and electrical activity of the diaphragm (EAdi). These signals can be analyzed either manually or automatically with the aid of a dedicated software.

Visual inspection of ventilator curves is the most used approach to analyze the presence of PVD. However, the ability of ICU physicians to detect dyssynchrony from ventilator curves can be poor and does not enable a simple and sensitive detection of dyssynchronies. In addition, this method does not allow to track waveforms continuously at the bedside and some types of dyssynchronies, such as RT, are not easily detected by the sole inspection of ventilator curves²⁹.

On the other hand, either P_{eso} or EAdi recordings may detect dyssynchrony by comparing the time occurrence of the changes in P_{eso} or EAdi with those of P_{aw} and flow-time waveforms in every ventilator cycle. These type of monitoring are considered the gold standard to detect inspiratory effort and both have been used to detect RT dyssynchrony¹⁸.

Due to several limitations from these methods to detect PVD, various dedicated software have been developed to continuously detect dyssynchronies in real time. These software are mainly based on changes of flow and pressure curves, or based on EAdi^{30,31}.

4. Understanding how patient- ventilator dyssynchrony might be harmful for the diaphragm

4.1 Myotrauma and Ventilation induced diaphragm dysfunction (VIDD)

The diaphragm is the most important muscle of inspiration. Its function therefore is critical for optimal breathing. Under normal conditions, the diaphragm acts like a piston within a cylindrical container, generating flow when its dome descends and displaces the abdominal contents beneath. The pressure generated across the dome between the thoracic and abdominal cavities is called the transdiaphragmatic pressure and is proportional to the tension developed within the muscle fibers. The magnitude of the pressure swings on either side of the diaphragm depends on the volume change induced by diaphragmatic contraction and the elastance of the thorax and abdomen³².

The term myotrauma is defined as various adverse patient–ventilator interactions leading to diaphragm atrophy and injury, resulting in a final common pathway of diaphragm weakness or loss of diaphragmatic force-generating capacity known as ventilator-induced diaphragm dysfunction (VIDD)¹¹. There is also strong evidence that other process including sepsis and/or other systemic infections are responsible for many cases of ICU-acquired diaphragm weakness. Several studies have shown that diaphragm dysfunction is highly prevalent in critically ill patients leading to serious complications. Demoule et al. reported that the prevalence of diaphragmatic dysfunction assessed by twitch tracheal pressure in response to bilateral magnetic phrenic nerve stimulation (P_{diTw}) is up to 64% of patients at the time of ICU admission³³.

Similarly, approximately 80% of patients in weaning phase and those requiring prolonged MV have been reported to present diaphragm dysfunction³²³⁴. In addition, Goligher et al. evaluated the diaphragm thickness and contractile activity by ultrasound in 107 mechanically ventilated patients. These authors found that over the first week of ventilation, diaphragm thickness decreased by more than 10% in 44% of patients and maximal thickening fraction (a measure of diaphragm function) was lower in patients with decreased diaphragm thickness compared with patients with unchanged thickness³⁵.

4.2 Diaphragm dysfunction and outcomes

Diaphragm dysfunction has been associated with poor outcomes and also proposed as a marker of illness severity. A recent study in 211 ventilated patients demonstrated that development of decreased diaphragm thickness was an independent factor associated with a lower daily probability of liberation from ventilation (HR 0.69, 95%CI 0.54-0.87), prolonged ICU admission and a higher risk of complications¹².

Additionally, Supinski et al. found that patients with severe diaphragm weakness ($P_{diTw} < 10$ cmH₂O) have markedly increased mortality (49%) compared to patients with $P_{diTw} \geq 10$ cmH₂O (7% mortality). Moreover, among patients who survived, patients with severe diaphragm weakness had longer duration of mechanical ventilation compared to patients with $P_{diTw} \geq 10$ cmH₂O (12.3 ± 1.7 v/s 5.5 ± 2.0 days, respectively)³⁶.

In another study by Medrinal et al. 124 patients underwent maximal inspiratory pressure evaluation (MIP; a measure of inspiratory muscles strength). These authors reported significant differences in mortality between patients with low and high MIP. One- year mortality was 31 % (95 % CI 0.21, 0.43) in the low MIP group and 7 % (95 % CI 0.02, 0.16) in the high MIP group³⁷.

4.3 Mechanisms of Myotrauma

Four types of myotrauma have been described:

4.3.1 Diaphragm disuse and atrophy

The deleterious effect of diaphragm disuse has been reported by animal experiments and clinical studies. Factors such as sedative drugs, neuromuscular blocking agents and mechanical ventilation per se have been involved in this process. For instance, Powers et al. showed that rats rapidly developed progressive diaphragm atrophy and loss of diaphragm force generating capacity during fully controlled mechanical ventilation mode³⁸. Besides, studies in patients undergoing prolonged mechanical ventilation have shown that diaphragm atrophy is developed^{39,40}. In this context, a landmark study by Levine et al. reported that mechanically ventilated brain-dead organ donors rapidly experience severe diaphragm atrophy. These authors found that the cross sectional area of slow and fast-twitch fibers decreased 57% and 53% respectively, as compared with control group⁴¹.

In terms of sedatives, propofol has shown to induce a dose-dependent decrease in the diaphragm's capacity to generate pressure and this has been correlated with the severity of diaphragm weakness^{42,43}.

The cellular mechanisms by which mechanical ventilation per se induces diaphragm atrophy and weakness are oxidative stress, activation of several proteolytic pathways (caspases, calpains, and the ubiquitin proteasomal system), and mitochondrial dysfunction⁴⁴.

4.3.2 Excessive loading

Conversely to muscle disuse, excessive loading or insufficient unloading of the respiratory muscles may result in diaphragm injury. These phenomena are

potentially present in mechanically ventilated patients with spontaneous breathing activity and PVD.

Different animal models have shown diaphragm injury after resistive loading (tracheal banding). In this case the diaphragm injury is characterized by susceptibility of myofibrillar complexes to calpain-mediated degradation^{45,46}. Jiang et al. evaluated in rabbits whether an acute episode of inspiratory resistive loading (IRL) can produce diaphragm injury. Histologic samples showed marked diaphragm injury characterized by fiber necrosis and profound influx of inflammatory cells⁴⁷.

Load-induced diaphragmatic injury has also been demonstrated in humans. Orozco-Levi et al. studied 18 patients with chronic obstructive pulmonary disease (COPD) and 11 healthy subjects showing that inspiratory loading can generate sarcomere disruption in the diaphragm. Inspiratory-loaded control subjects tended to show an 89% greater density and an 83% greater area fraction of sarcomere disruption compared with non-loaded control subjects. Similarly, patients with COPD showed a 38% greater density and a 32% greater fraction area of damage compared with non-loaded COPD⁴⁸.

4.3.3 Eccentric contractions

Eccentric contractions can be defined as a muscle activity that occurs when the force applied to the muscle exceeds the momentary force produced by the muscle itself and results in a lengthening action⁴⁹ or a muscle activation from a previously stretched position⁵⁰. According to these definitions, eccentric contractions of the diaphragm are present during exhalation, which is also called post inspiratory activity during normal breathing. In this case, a diaphragm contraction occurs while fibers are lengthening. Eccentric contraction of the diaphragm may occur during

several clinical situations capable of generating increases in intra-abdominal pressure and stretch the diaphragm before contraction.

It has been widely studied that forceful eccentric contractions can lead to muscle fiber injury and decreased ability to generate force on skeletal limb muscles ^{51,52}. However, the effects of eccentric contractions of the diaphragm have been scarcely studied.

In an animal model, Gea et al. evaluated the impact of eccentric contractions of the diaphragm on diaphragm injury. These authors found that diaphragmatic capacity to generate pressure decreased 67% immediately after the induction of eccentric contractions. Moreover, contractility of the diaphragm assessed by diaphragm displacement was 29% and 14% less in right and left hemidiaphragm, respectively, after eccentric contraction. Interestingly, these results were kept until 12 hours after induction of eccentric contraction and were associated with sarcomere muscle injury ⁵³.

In addition, contractile activity of the diaphragm during expiratory diaphragm lengthening was recently demonstrated in a pig model of acute hypoxemic respiratory failure. Pellegrini et al. found that these eccentric diaphragmatic contractions are able to delay and reduce the expiratory collapse and can increase lung aeration compared with mechanical ventilation with muscle paralysis and the absence of diaphragmatic activity⁵⁴.

Interestingly, although eccentric diaphragmatic contraction might be beneficial to the lung parenchyma and gas exchange⁵⁴, it could be detrimental to the muscle. The diaphragm muscle is particularly vulnerable to damage during MV and even more so in sepsis^{55,56}. Whether the diaphragm's eccentric muscle activity either in the context of synchronized breathing or during PVD is sufficiently strong to promote such damage is currently unknown.

4.3.4 Longitudinal atrophy

A more recent observation has emerged about how application of excessive positive end-expiratory pressure (PEEP) maintaining a shorter length of the diaphragm during MV may cause rapid sarcomere “dropout” resulting in longitudinal atrophy⁵⁷. This type of myotrauma may alter the optimal length-tension relationship of the muscle especially when PEEP is reduced or during a spontaneous breathing trial. The clinical significance of this mechanism remains to be elucidated.

4.4 Potential biomarkers of respiratory muscle injury

Several plasma markers of skeletal muscle injury have been extensively explored including myosin heavy chain, lactate dehydrogenase, myoglobin, carbonic anhydrase III, fatty acid binding protein, and creatine kinase. However, they are limited in their diagnostic sensitivity and specificity. Studies in animals and humans have shown that skeletal Troponin I (sTnI) might be used as a potential biomarker for respiratory muscle injury.

Simpson et al, found that rats breathing against an inspiratory resistive loading consistently developed hypercapnic ventilatory failure followed by diaphragmatic fatigue and blood release of the fast isoform of sTnI. This release of fast sTnI was consistent with load-induced injury of fast glycolytic fibres of inspiratory muscles, probably the diaphragm, suggesting that sTnI may be useful in detecting the role of injury in the development of respiratory muscle dysfunction⁵⁸. In the same line, Foster et al. showed that levels of sTnI in the serum of healthy patients, after a single 60 min of inspiratory threshold loading, were 24%, 27% and 24% increased at 1-hour (fast sTnI), at 3 days (fast sTnI), and at 4 days (slow sTnI), respectively ⁵⁹. Interestingly, other potential markers of respiratory muscle injury, such as a creatine kinase, did not show differences after inspiratory threshold loading, suggesting again that sTnI has superior sensitivity compared to other biomarkers of skeletal muscle injury.

Additionally, in the context of eccentric exercise, Chapman et al. have showed that eccentric contractions of skeletal muscles increase levels of fast sTnI and creatine kinase at day 4 after training in young men⁶⁰. Whether eccentric activation of respiratory muscles may provoke an increase in sTnI is unknown.

4.5 *How specifically reverse triggering may affect the diaphragm function?*

In the context of PVD, different mechanisms of diaphragmatic injury may occur (mainly excessive loading and eccentric contraction) depending on which type of dyssynchrony is present. In RT dyssynchrony, an inspiratory patient's effort is triggered by the ventilator within the inspiratory cycle and most of the times part of this patient's effort takes place in the expiratory phase. During the expiratory phase the inspiratory muscles (e.g. diaphragm) lengthen as lung volume decreases. Hence, activation of the inspiratory muscles at this time may result in muscle contraction during lengthening (eccentric contraction).

The impact of these eccentric contractions of the diaphragm on its function and structure could go in two opposite directions: on the one hand, this reflex mechanism could help to prevent diaphragm disuse and atrophy since greater forces are generated during eccentric contraction compared to other contraction types for a given angular velocity⁴⁹. In addition, it has been demonstrated that eccentric contractions require less motor unit activation and consume less oxygen and energy for a given muscle force than concentric contractions⁶¹.

On the other hand RT may be harmful for the diaphragm when contractions occur repeatedly during the expiratory phase concomitantly with lung volume decrease and inspiratory muscle lengthening (Figure 2.)^{53,62}. The potentially injurious effects of the eccentric contractions are due to a lack of homogeneity in sarcomeres stretching (asymmetric lengthening) triggering a cascade of events leading to more severe secondary damage such as loss of calcium homeostasis, possible inflammatory reaction and reactive oxygen species (ROS) production^{61,63}.

Some preliminary findings from Goligher et al. have shown that the rate of eccentric contractions was associated with the frequency of reverse triggering ($R^2=0.72$, $p<0.0001$) where 52% of reverse triggered breaths met criteria for eccentric contractions⁶².

Whether eccentric contractions are sufficiently frequent and severe to cause diaphragm injury and weakness in mechanically ventilated patients is unknown.

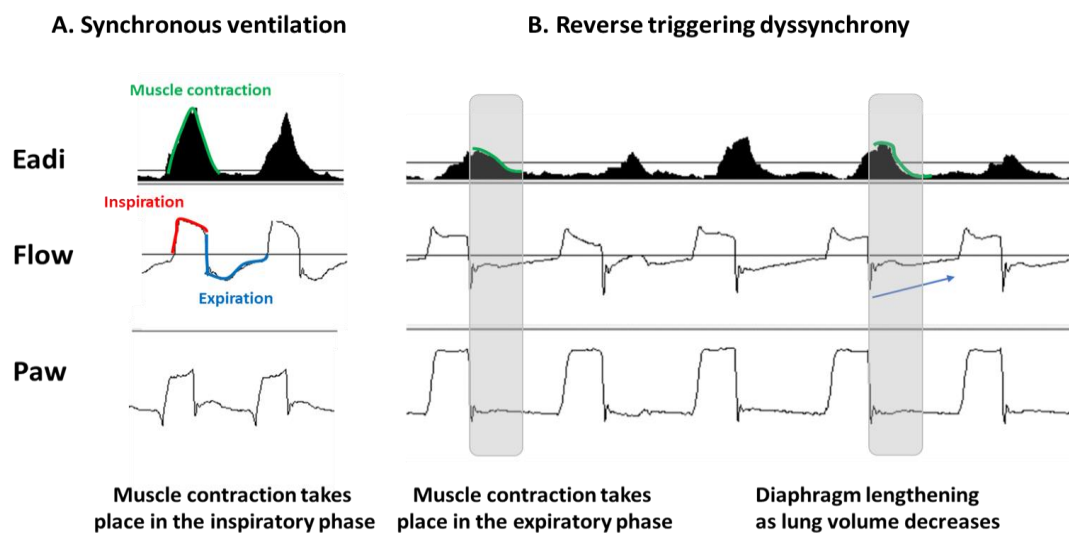


Figure 2. Reverse triggering leading to eccentric contraction of the diaphragm.

Patient effort and muscular contractions are shown with electrical activity of the diaphragm (upper black tracing). Left panel (A) shows that during synchronous ventilation muscle contractions (green line) occur mostly during inspiratory phase (red line). Right panel (B) shows that during reverse triggering dyssynchrony diaphragmatic contractions begin systematically after the mechanical insufflations by the ventilator and muscle activity takes place in the expiratory phase (eccentric contraction).

HYPOTHESIS

Reverse triggering dyssynchrony is a frequent phenomenon in patients under mechanical ventilation admitted to the Intensive Care Unit. Induction of reverse triggering in a porcine model of ARDS causes diaphragmatic injury, as reflected by functional and structural alterations.

GENERALS GOALS

To describe the incidence of reverse triggering dyssynchrony in mechanically ventilated patients admitted to the intensive care unit, and to evaluate the effects of reverse triggering on diaphragmatic function and structure in a porcine model of ARDS.

SPECIFIC GOALS

1. To describe the incidence of RT in recently intubated patients under assist-control ventilation in the ICU.
 - a. To develop an automatic method to detect RT based on the temporal relationship between pressure and flow waveforms and electrical activity of the diaphragm.
 - b. To determine the frequency of RT using the automatic method
 - c. To compare demographic and ventilatory variables in patients with high vs low rate of RT.

2. To establish and characterize a relevant porcine model of RT dyssynchrony during severe ARDS.
 - a. To reproduce a severe ARDS model and set a phrenic nerve stimulation
 - b. To establish a consistent approach to induce reverse triggering dyssynchrony in the severe ARDS model
 - c. To compare respiratory, cardiovascular, biochemical, sedation and lung injury data between ARDS pigs with RT and without RT (passive ventilation).

3. To evaluate the impact of RT dyssynchrony with different level of breathing effort on diaphragmatic structure and function in a porcine model of severe ARDS.
- a. To determine whether RT dyssynchrony with different levels of breathing effort has an impact on force generation capacity as compared with passive ventilation.
 - b. To determine whether RT dyssynchrony with different levels of breathing effort has an impact on diaphragm structure as compared with passive ventilation.
 - c. To compare levels of systemic markers of muscle damage between RT dyssynchrony with different levels of breathing effort and passive ventilation.

MATERIALS AND METHODS

1. Incidence of reverse triggering

1.1 Data collection and study design

This is an ancillary post-hoc study of an observational study (NCT02434016) conducted at St. Michael's Hospital in Toronto, Canada, to detect the timing of resumption of diaphragm activity after intubation. Patients were enrolled between June 2015 and August 2017, equipped and monitored with EAdi (NAVA catheter, Maquet) that was placed within 12 hours after endotracheal intubation and initiation of mechanical ventilation. EAdi catheter was positioned according to NEX formula and position carefully adjusted based on the ECG tracings (making sure the QRS amplitude decreased from top to bottom traces and checking for the disappearance of the P wave on the bottom tracing, indicating that the last electrode is below the diaphragm). This approach ensures a standardized placement and homogeneous EAdi electrical amplitude, as previously described^{64,65}. Patients were selected as being likely to remain under mechanical ventilation for at least 24 hours. Minute by minute trends in EAdi were recorded. A one-hour recording of P_{aw} , flow and EAdi tracings were obtained at 24 hours post-intubation in every patient. The Research Ethics Board approved the protocol and the participants or next-of-kin provided a written informed consent for enrollment (Research Ethics Board #15-073, St Michael's Hospital).

1.2 Derivation of the automated detection of reverse triggering

For the first ten consecutive patients in assist/control mode, a period of 200 breaths with recordings of P_{aw} , flow and EAdi was randomly selected, and visually reviewed for overall signal quality. Then, three independent trained reviewers visually assessed these tracings breath by breath and labeled each breath for the presence of reverse triggering: first, by analyzing airway pressure and flow waveforms only, and again (blind of the first assessment) also analyzing the same breaths with EAdi tracings. Briefly, based on previous work³¹, the presence of reverse triggering was first established by the presence of an EAdi

waveform starting after the beginning of a mandatory mechanical insufflation and reaching more than 1 microvolt (μV). Visual assessment with EAdi tracing was considered as the reference and the definitive presence of reverse triggering was considered when a breath was labelled the same among all three reviewers (gold standard). In addition, to estimate the gold standard uncertainty, a sensitivity analysis using different definitions was performed. Combinations for detecting each breath are as following:

- GS1 (Gold standard 1): Reverse triggering detected by at least one reviewer
- GS2 (Gold standard 2): Reverse triggering detected by at least two reviewers
- GS3 (Gold standard 3): Reverse triggering detected by the three reviewers.

In the primary analysis we wanted to describe the phenomenon of reverse triggering and tried to be as sensitive as possible using a threshold of $>1 \mu\text{V}$ to declare there was a RT. Selecting a higher EAdi threshold suggesting a stronger contraction, however, might better detect reverse triggering having a more clinically relevant impact, either on the diaphragm or on the lung. We thus also calculated the incidence of reverse triggering using a $>3 \mu\text{V}$ and a $>5 \mu\text{V}$ peak EAdi cut-off.

In order to calculate the incidence of reverse triggering, an algorithm was constructed to automatically detect reverse triggering, using the Neurosync software. Neurosync is an automatized and validated method based on the EAdi signal, which detects timing of EAdi activity and compare it to the ventilator timing (inspiratory and expiratory valves). The software has been designed to detect dyssynchrony ⁶⁶. To detect reverse triggering, we designed a simple algorithm consisting in a combination of four criteria coming from Neurosync output (Table 1): 1) Mandatory breath with no negative deflection in airway pressure (i.e., not triggered by the patient); 2) EAdi breath; 3) EAdi starting after the ventilator insufflation; and 4) EAdi $>1\mu\text{V}$. This algorithm was tested on a combined cohort; consisting of 10 patients on AC (2000 breaths) and 10 patients on pressure support

ventilation (2000 breaths); this latter group (triggered breaths) was used to rule out the presence of false positive detection.

Table 1. Definitions and criteria used for visual and automated detection of reverse triggering

Visual Inspection	
Criterion	Definition
Mandatory breath	No deflection in Paw curve at the initiation of the breath
Peak expiratory flow	Reduced expiratory peak flow compared with other breaths
Plateau pressure	Variation in plateau pressure compared with other breaths (volume control) in absence of airflow leak.
Flow and pressure	Drops in pressure and flow during ventilator inspiratory time (Pressure control)
EAdi peak	Peak EAdi >1 μ V
EAdi delay	EAdi onset after pressurization start
Automatic detection by Neurosync	
Criterion	Definition
Mandatory breath	Airway pressure drop less than 0.33 cmH ₂ O at the beginning of insufflation
EAdi breath	Sum of consecutive EAdi sample differences exceed the trigger level of 0.5uV and EAdi time integral > 0.5uV after cycling off at 70% of peak EAdi
EAdi delay	EAdi onset after pressurization start either during inspiratory or expiratory phase of respiratory cycle
EAdi peak	Peak EAdi >1 μ V Peak EAdi >3 μ V Peak EAdi >5 μ V
<i>For visual inspection, presence of at least EAdi, EAdi delay and Mandatory breath criteria were needed.</i>	
<i>For Neurosync, presence of all criteria was needed.</i>	
<i>Paw: Airway pressure; EAdi: Electrical activity of the diaphragm; μV: microvolts.</i>	

1.3 Validation of the automated detection of reverse triggering

We validated the constructed algorithm with two different approaches:

First, we wanted to be sure that the efforts labeled as reverse triggering always happened with a mandatory breath delivered by the ventilator, and not a patient-triggered breath; we used the expiratory time distribution to label a breath either machine or patient triggered (i.e., a machine triggered breath is preceded by a fixed, pre-set, expiratory time; see Annex 1) and compared it to our definition.

Second, a validation was performed on 1000 different additional breaths from five different ventilated patients on assist-control mode. Visual detection of RT by three reviewers was considered as the gold standard and done previously during the derivation phase. The algorithm sensitivity, specificity, positive predictive value (PPV) and negative predictive value (NPV) were calculated in the derivation and the validation cohorts.

1.4 Incidence of reverse triggering

After the algorithm had been developed and validated, for all patients on assist-control mode at the time of the recording, i.e. 24 h after intubation, we analyzed the complete 1-hour tracings. Incidence was analyzed as the number of cycles with this asynchrony over the total number of breaths for each patient and its distribution was calculated in the whole population as median and interquartile range and expressed in percentage of breaths. We also assessed the presence of different entrainment patterns: entrainment pattern was defined as the number of reverse triggered breaths (patient respiratory effort) within each ventilator breath. Thus, during 1:1 entrainment pattern, one reverse triggered breath is associated with one machine breath; during 1:2 pattern, one reverse triggered breath occurs every two machine breaths, and so on. Here, we defined that a 1:1 entrainment pattern occurred when reverse triggering was present over three or more consecutive breaths. A 1:2 entrainment pattern was identified when reverse triggering was present in each other mandatory breath for at least 6 events. Then, the cohort was divided in two

groups: one above the median rate and one equal or below to the median rate. In these two groups we looked for differences in demographic data, ventilatory parameters, sedation scores and medications used at the time of the recording.

Finally, because reverse triggering breaths were not all associated with a clear entrainment pattern, we performed a patient-level analysis of the 1st quintile of patients with the higher number of RT breaths in order to compare EAdi and phase angles of entrained and non-entrained RT events. The question was whether entrained or non-entrained breaths have the same characteristics. Phase angles were calculated as the phase delay between the onset of a mechanical breath and the onset of neural activity divided by the duration of a mechanical ventilation cycle (T_{tot}), and all multiplied by 360°: $[(\text{onset of pneumatic event} - \text{onset of neural event}) / (T_{tot})] * 360$.

1.5 Statistic analysis

No statistical power and sample size calculation were conducted prior to the study. As a secondary analysis of an observational study we aimed to include all patients based on our inclusion criteria. We arbitrary selected the first ten consecutive patients for derivation phase and five different patients for validation phase.

Descriptive statistics (frequencies, median, interquartile range (IQR) or mean and standard deviation) were used considering if variables had a normal or non-normal distribution assessed by the Shapiro-Wilk test. Inter-observer agreement was assessed by Fleiss Kappa statistic. Agreement is generally considered to be excellent if kappa is greater than 0.80, substantial if kappa ranges from 0.61 to 0.80, moderate if kappa ranges from 0.41 to 0.60, fair if kappa ranges from 0.21 to 0.40, and slight if kappa below 0.20 ⁶⁷. To calculate the diagnostic accuracy of the algorithm based on Neurosync, 2 × 2 tables, sensitivity, specificity, as well as positive and negative predictive value were calculated. Breaths were the unit of analysis and they were assumed to be independent. Sensitivity and specificity >80% were defined as acceptable. For comparison of demographic and ventilatory variables between patients above or below the reverse triggering median value, Chi-square test was

used for categorical variables and 2-sample *t*-test or U Mann-Whitney were used for continuous data. Outliers were defined as values below the 1st quartile (Q1) minus 1.5 times the IQR or above the 3rd quartile (Q3) plus 1.5 times the IQR. However, no action was needed since these values were clinically plausible. In addition, correlations between the amount of reverse triggering breaths and the percentage of breaths with entrainment, other ventilatory variables and sedation doses were calculated using Pearson's linear correlation coefficient r^2 . A two-sided p-value of <0.05 was considered statistically significant.

2. Development of a porcine model of reverse triggering during ARDS

2.1 ARDS model

Study design

We conducted an experimental study in a porcine animal model of severe acute respiratory distress syndrome followed either by passive ventilation, or by reverse triggering. The project was approved by the Animal Care Committee at Sick Kids, Toronto, Canada (animal use protocol # 46792).

Animal preparation and monitoring

Male or female Landrace pigs (35±5kg) received an intramuscular ketamine bolus of 5 ml (20mg/ml) for sedation followed by intravenous pentobarbital (55 mg/ml; 15-20 ml/h) for instrumentation and induction of lung injury. Once sedated, pigs were intubated with an endotracheal tube (I.D. 8 Fr) and connected to a mechanical ventilator. The femoral artery was cannulated with a 4 Fr catheter to monitor arterial blood pressure. An esophageal and gastric balloon catheter (Nutrivent; Sidam, Mirandola, Italy) and NAVA catheter was inserted to measure esophageal, gastric pressure and EAdi respectively, as previously described^{68,69}. Maintenance fluid was provided by a continuous intravenous infusion of

lactate Ringer's solution at 10 mL/kg/h. All animals were ventilated with Servo-I (Maquet) ventilator set on volume controlled ventilation mode with PEEP of 5 cmH₂O, tidal volume (VT) 10 ml/kg, and an I:E ratio 1:2. Respiratory rate (RR) was initially set at 30 breaths per minute, and adjusted thereafter to keep PaCO₂ between 35-45 mmHg. Inspired oxygen fraction was kept at 1.0 throughout the experiment.

Surgical placement of electrodes in the phrenic nerves

Phrenic nerve stimulation is crucial in our study in order to measure diaphragm function (force) at different frequencies of stimulation in a non-volitional dependent manner. First, we isolated both phrenic nerves through a surgical procedure. In brief, an anterior middle neck incision (10cm) was performed in order to localize the anterior scalenus muscle. Then, after cleaning and isolating 2-3 mm nerve's length, silicone electrodes with embedded platinum wire (Microprobes Nerve Cuff Electrodes) were placed surrounding the nerve (see Annex 2). These electrodes were attached to a pulse generator (AM-2200 Analog Stimulator) creating bipolar electrical current in the nerves to cause diaphragm contraction. We used PowerLab acquisition system (ADInstruments) to automatically program and control the stimulus.

Induction of lung injury

After instrumentation, experimental lung injury was induced by a 2-hit model. First, surfactant depletion and then injurious mechanical ventilation (ventilator-induced lung injury: VILI model). Surfactant depletion was achieved by repeated lung lavages with 30 mL/kg of normal saline (37°C) until PaO₂/FiO₂ ratio was below 150 mmHg for 10 minutes, with PEEP 5 cmH₂O and FiO₂ 1.0⁷⁰.

Then, animals were ventilated with an injurious strategy for 1 hour or until a 10% decrease in respiratory system compliance was observed. Injurious mechanical ventilation consisted in applying high airway pressures through pressure-controlled ventilation at FiO₂ 1.0, with a pre-set sliding scale of driving pressure and PEEP: 41 and 1, 39 and 3, 37 and 5, 37 and 7,

37 and 9, 37 and 11, 35 and 13, 33 and 15, and 31 and 17cmH₂O, respectively. This combination was adjusted every 15 minutes for 1 hour to maintain PaO₂/FiO₂ ratio between 55 and 65 mmHg.

2.2 Experimental protocol and study groups

After animal instrumentation and induction of lung injury, a stabilization period was kept for 20 minutes with the same ventilation parameters described above but anesthesia was modified to Ketamine (20mg/ml) 3 to 8 ml/h and Propofol (10mg/ml) 3-6 ml/h in order to prepare reverse triggering induction. Then, animals were allocated in two groups to receive either conventional mechanical ventilation without breathing effort (passive) or conventional mechanical ventilation plus reverse triggering dyssynchrony as follows:

-**Passive:** Animals received 3 hours of conventional mechanical ventilation set as : Volume controlled mode, VT= 10 ml/kg, PEEP = 8 cmH₂O, RR= 25-35 (adjusted to PaCO₂ <60 mmHg), I:E ratio = 1:2. These animals were used as controls and no breathing efforts were allowed (*i.e.* increasing sedation if necessary).

- **Reverse triggering:** Animals received 3 hours of conventional mechanical ventilation in volume-controlled mode, with PEEP 8 cmH₂O, but VT and RR were adjusted in order to induce reverse triggering (see below).

Ventilatory and hemodynamics variables and diaphragm function were assessed at baseline, 1, 2 and 3 hours after. Morphology and structure of the diaphragm was evaluated at the end of interventional phase (Figure 3).

Once the experiment was completed, animals were sacrificed with sedative overdose and 20ml of 19.1% KCL.

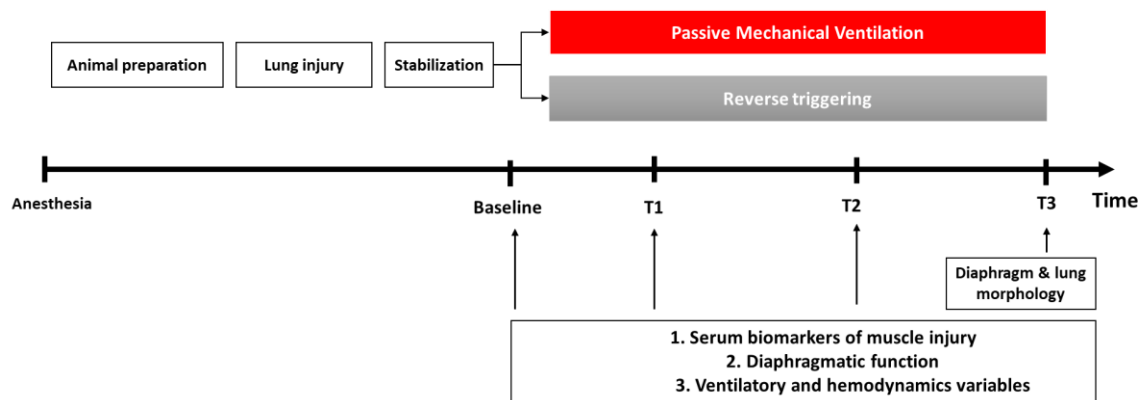


Figure 3. Study protocol and experimental groups

Sample size

Although we did not have reliable estimations of the impact of reverse triggering on diaphragmatic function, we estimated sample size based on a previous report of the observed changes of pressure generating capacity of the diaphragm after induction of eccentric contractions (proposed mechanisms for RT) in 6 ventilated dogs. In that study diaphragmatic contraction decreased by 60% after inducing eccentric contractions⁵³. Assuming a similar magnitude of the effect of RT in our model, we defined that 6 animals per group would be appropriate to demonstrate relevant changes in diaphragmatic function. In addition, after preliminary experiments, we observed that about 15% of animals died before completing the experiment so the final number of animals was set at 8 per group.

Finally, since our plan was to analyze the impact of different levels of breathing effort associated to RT dyssynchrony, on structure and function of the diaphragm, we pre-planned to analyze animals with RT dyssynchrony separating them in three subgroups: low, middle and high breathing effort, according to the pressure time product (PTP) observed during the 3 hour study period. Thus, a total of 32 pigs were studied, 8 of which were allocated to passive ventilation and 24 to reverse triggering.

2.3 Induction of reverse triggering dyssynchrony

According to reverse triggering definition, a muscle contraction is triggered by the passive lung insufflation. Fundamentally, reverse triggering induction was based on the ability of creating respiratory entrainment between the pig and the ventilator. In respiratory physiology, “respiratory entrainment” refers to the establishment of a fixed repetitive temporal relationship between the neural and mechanical respiratory cycles. Thus, in order to achieve this RT dyssynchrony we modified two main variables: 1. Dose of anesthesia to maintain a certain level of sedation and neural respiratory drive; and/or 2. Mechanical ventilator settings (ventilatory support) including respiratory rate, tidal volume, inspiratory time, and level of PEEP to modify respiratory afferences and at some point obtain this stage of respiratory entrainment. Stepwise changes were as follow: (1) decreasing VT and increasing RR; (2) decreasing dose of sedatives; (3) increasing PEEP. Increases or decreases in anesthesia depth were induced when pig neural rate goes greater than 60 or less than 20 breaths per minute, respectively.

2.4 Physiological measurements and sample collection

Ventilatory and hemodynamics variables

Mechanical ventilator setting including VT, RR, and PEEP level, were measured at baseline, 1, 2 and 3 hours of the study period. Peak airway pressure (P_{peak}) Plateau pressure (P_{plat}), Driving pressure (DP) and respiratory system compliance (C_{rs} ; calculated as $[VT/(P_{plat} - PEEP_{total})]$), were assessed under static conditions at baseline and at the end of the study period (3 hours).

Systemic hemodynamics, gas exchange parameters, and biochemical markers were also assessed hourly during the 3-hour study period.

Sedation

Anesthesia depth was titrated clinically and based on the bispectral index (BIS). The latter constitutes a numerical expression of the anesthetic depth ranging from 0–100, with 100 representing awake and zero representing isoelectric (or zero) brain activity⁷¹. In a clinical manner, we modified sedation in order to observe a certain level of respiratory effort in the animals allocated to RT and absence of respiratory effort in the passive group. Also, sedation level was modified based on the compressive toe pinch maneuver in order to ensure that level of sedation was adequate. We aimed to obtain BIS values between 45 and 60 (recommended for anesthetic maintenance during general anesthesia)⁷¹.

Alteration of the alveolar-capillary barrier

In order to estimate lung oedema, wet / dry weight ratio was determined. After euthanasia, a thoracotomy was performed and the whole accessory lung lobe was harvested and weighted immediately upon extraction and then dried for 24 hours in an oven at 120° C. A wet / dry weight ratio was then obtained and recorded.

Protein concentration in bronchoalveolar lavage (BAL) was measured as a surrogate marker of alveolar-capillary membrane permeability derangement. At the end of the experiment (hour 3) the right inferior lung lobe was harvested, and BAL performed. Plasma, serum and cell-free BAL samples were obtained by centrifugation of samples at 2000 g for 10 minutes. These samples were immediately frozen and kept at -80° C for total protein analysis. Total protein content in BAL was measured based on the Lowry method (Protein assay: Bio-Rad DC Protein assay kit), and a standard protein curve was obtained by diluting a stock solution of IgG.

2.5 Statistical analysis

In order to characterize the RT model, two experimental groups were considered in this analysis: passive (n=8) and RT (n=18). The subgroups in RT will be considered for the specific goal 3. Descriptive values were presented as means - standard deviation (SD) or median and interquartile range, as appropriate. For data measured along time comparisons were performed by 2-way (repeated-measures) analysis of variance (ANOVA) or Kruskal– Wallis test, as appropriate. Bonferroni adjustment for multiple comparisons was applied for post hoc analysis. For data measured at single time point comparisons between groups were performed by Student's *t*-test or Mann–Whitney U test, as appropriate. A *p* value < 0.05 was considered statistically significant. All statistical analyses were performed by R software version 3.3.2 (R project for Statistical Computing).

3. Measurements of function and structure of the diaphragm

3.1 Breathing effort and study groups

Pressure-Time-Product

Since the respiratory muscles exert their function by generating pressure, the breathing effort can be assessed by analysis of these pressures. A sophisticated and gold standard parameter to quantify breathing effort is the Pressure-Time-Product (PTP). The PTP is calculated as the time-integral of the P_{mus} ⁷²:

$$PTP = P \text{ (cmH}_2\text{O)} \times t(s) = \int P dt \text{ (cmH}_2\text{O*s)}$$

When P_{mus} is not available, the time integral of P_{eso} may also be calculated. PTP is commonly reported over a 1-minute interval as PTP_{min} .

Calculation of PTP_{eso}

As RT breaths occur after passive insufflation has already started, we could not use the flow criterion to determine the beginning nor the end of the breathing effort. We thus defined the respiratory cycle to calculate PTP_{eso} as follows. The start of the inspiratory effort was determined at the instant of the P_{eso} decay and the end of inspiration was determined to happen at the point of P_{eso} that elapsed 25% of time from its maximum deflection to return to baseline, as previously described (see Annex 3) . This assumes that the final part of the esophageal curve is simply due to chest wall relaxation.

We randomly selected a 5-minute tracing per each animal to calculate PTP as described above. This calculation was performed in a semi automatized manner using a designed algorithm to obtain PTP values (MATLAB), but also by visual inspection to check any abnormality in the calculation. The average value of PTP was then multiplied by respiratory rate to obtain PTP_{min} .

Study groups based on the PTP_{min}

Since the level of respiratory effort plays an important role in myotrauma development¹¹, we arbitrarily pre planned to analyze animals allocated to RT in terciles based on PTP_{min} . Thus, all results about diaphragm function and structure are analyzed based on 4 experimental groups:

- a. Passive ventilation: PTP_{min} equal to 0
- b. Reverse triggering with low effort: 1st tercile PTP_{min} value
- c. Reverse triggering with middle effort: 2nd tercile PTP_{min} value
- d. Reverse triggering with high effort: 3rd tercile PTP_{min} value

3.2 Diaphragm function

Function of the diaphragm (the ability to generate force) was determined measuring the Transdiaphragmatic pressure (P_{di}) which is defined as the difference between gastric and esophageal pressures in response to bilateral stimulation of the phrenic nerves. P_{di} was measured in two different ways: 1. P_{di} after a single twitch (P_{diTw}); and 2. P_{di} at different frequencies of stimulation and plotted as a force/frequency curve (F/F curve).

Based on pilot experiments, twitch stimulus was set as single pulse width of 0.015 sec and programmed during the expiratory phase of the respiratory cycle with 3 mA of intensity and repeated 3 times with 2 mechanical breaths between each stimulus. P_{diTw} was recorded hourly from baseline to 3 hours.

The F/F curve was performed at baseline and at the end of the experiment (3 hours). F/F curve characteristics were set as follows (Figure 4): 1. Five different stimulation frequencies are applied: 10,20,30,40 and 60 Hz; 2. Amplitude of 3 mA; 3. Pulse width of 0.0015 sec; 4. Duration of train of pulses: 1 second; 5. Time between stimuli: 30 seconds.

All F/F curves were performed after a lung recruitment maneuver (to standardize lung volume and thus diaphragm length) and at the same level of PEEP (8 cmH₂O). Besides, in order to avoid any spontaneous effort during the F/F curve, we increase respiratory rate achieving EtCO₂ ~ 35 mmHg, and a bolus of sedation (propofol 50-100 mg) was given.

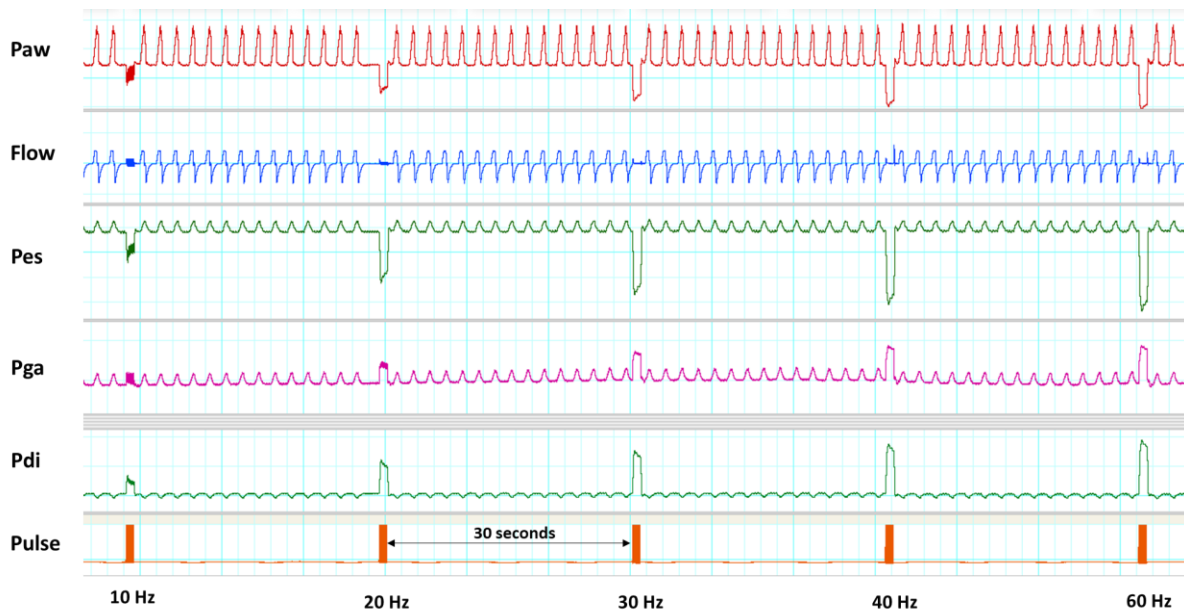


Figure 4. Example of force/frequency curve. Five different stimulation frequencies are applied to the phrenic nerves. The greater the frequency the greater the swings in P_{eso} and P_{ga} . Consequently, a higher P_{di} can be observed at higher frequencies. A plateau in P_{di} is observed around 40 Hz.

3.3 Diaphragm morphology

Biopsy sampling and histology

After euthanasia, muscle biopsies were harvested from the right costal diaphragm and snap-frozen in liquid nitrogen-cooled isopentane. Transverse serial frozen sections (8 μm thick) were stained with hematoxylin and eosin in order to measure cross-sectional area (CSA) and quantify abnormal fibers.

Quantification of abnormal fibers and CSA

A total of 5 randomly selected viewing fields per Hematoxylin & Eosin section were digitized and myofibers were categorized to determine the percentage of myofibers with abnormal

morphology. Abnormal morphology was defined using predetermined categories (Table 2), as previously described⁷³. To determine the myofiber CSA, selected viewing fields were loaded in Image J software for manually perimeter delimitation and automatic area calculation for each fiber. All muscle fiber analyses were performed blindly to the animal ID.

Table 2. Criteria for abnormal fibers of haematoxylin and eosin stained cross-sections of the diaphragm

Features	Definitions
Normal	
<i>Peripheral nucleus</i>	Nucleus situated within 2 mm of sarcolemma
<i>Normal cytoplasm</i>	Evenly textured, eosinophilic cytoplasm
<i>Normal size and shape</i>	Homogenous size, polygonal shape
Abnormal	
<i>Internal nucleus</i>	Minimum 2 mm of cytoplasm between nucleus and sarcolemma
<i>Abnormal cytoplasm</i>	Pale staining or basophilic cytoplasm; granular, whorled, vacuolated or disrupted texture; loss of sarcolemma integrity; lipofuscin accumulation; rounded, deeply eosinophilic fibre
<i>Abnormal size or shape</i>	Small fibre (,1/3 diameter of three largest fibres in the field), angulated fibre with concave edges, lobulated fibre

3.4 Biomarkers of muscle injury

We established a Western blot approach to detect porcine fast skeletal troponin I (fsTnI), based on previously described methods ⁷⁴, but modified to use non-reducing conditions to avoid interference from light chain IgG in plasma samples (see Annex 4 for specific details). Aliquots of plasma taken at baseline and at the end of the experiments were diluted with modified sample buffer (10 ul plasma + 90 ul buffer), heated for 10 min at 95°C, and briefly chilled on ice. Plasma proteins were size-fractionated on SDS-PAGE gels and transferred to PVDF membrane. After blocking overnight at 4°C using 5% non-fat dry milk/5% bovine serum albumin (BSA) in TBST buffer [20 mM Tris pH 7.5; 140 mM NaCl; 0.1% (wt vol⁻¹) Tween20], membranes were incubated 4 hr at room temperature with primary antibody recognizing Troponin I type 2 (NBP1-57842, 1:1000; Novus Biologicals, Oakville, ON, Canada) in 5% BSA/TBST. Secondary antibody (horseradish peroxidase-conjugated) was diluted 1:10,000 in blocking buffer and incubated for 1 h at room temperature. All washes were in TBST. Enhanced chemiluminescence detection reagents were used according to the manufacturer's recommendations (Pierce ECL Plus Western Blotting Substrate, Thermo Scientific, Rockford, IL)) to detect bound antibody. Signal intensity was quantified using Image Lab® software (Bio-Rad Laboratories, Mississauga, ON, Canada).

3.5 Statistical analysis

All statistical analyses were performed using R software version 3.3.2 (R project for Statistical Computing). Descriptive values were presented as means - standard deviation (SD) or median and interquartile range as appropriate. Comparison between 4 experimental groups, and changes along time or stimulation frequency, were performed by 2-way (repeated-measures) analysis of variance (ANOVA) or Kruskal– Wallis test, as appropriate. Tukey adjustment for multiple comparisons was applied for post hoc analysis. Changes in distribution of myofibers' cross-sectional area was performed by Kolmogorov-Smirnov test, and comparison between percentages of abnormal fibers was done using Chi-Square test. A p value < 0.05 was considered statistically significant.

RESULTS

1. Incidence of reverse triggering

1.1 Detection of Reverse Triggering

For the derivation phase using a total of 2000 breaths from 10 patients in assist-control mode, inter-rater agreement showed a Fleiss' kappa of 0.5 when only flow and airway pressure were used but increased to 0.84 when EAdi tracing was added. Diagnostic accuracy of the automatic method and sensitivity analysis with different definitions compared to our gold standard are shown in Table 3.

Table 3. Sensitivity analysis on 2000 breaths (n=10) in order to estimate variability of diagnostic value of proposed algorithm.

	Gold standard 1*	Gold standard 2**	Gold standard 3#
Incidence of reverse triggering	910/2000	854/2000	528/2000
Sensitivity (95%IC)	0.54 (0.51, 0.57)	0.56 (0.53, 0.59)	0.84 (0.80, 0.87)
Specificity (95%IC)	0.94 (0.92, 0.95)	0.93 (0.91, 0.95)	0.92 (0.91, 0.94)
Positive predictive value (95%IC)	0.88 (0.85, 0.91)	0.86 (0.83, 0.89)	0.79 (0.76, 0.83)
Negative predictive value (95%IC)	0.71 (0.68, 0.73)	0.74 (0.72, 0.76)	0.94 (0.93, 0.95)
Positive likelihood ratio (95%IC)	8.76 (6.89, 11.13)	8.12 (6.51, 10.13)	10.7 (8.95, 12.82)
Negative likelihood ratio (95%IC)	0.49 (0.46, 0.53)	0.47 (0.44, 0.51)	0.18 (0.15, 0.21)

Note: * Reverse triggering detected by at least one reviewer; **Reverse triggering detected by at least two reviewers; #Reverse triggering detected by the three reviewers. We used Gold standard 3 for validation phase.

1.2 Validation of the automated detection

Diagnostic accuracy of the algorithm for detection was sensitivity 0.86 (0.80 to 0.91), specificity 0.95 (0.93 to 0.96), PPV 0.74 (0.67 to 0.81), NPV 0.97 (0.96 to 0.98). The event rate was 15.4% in the validation cohort. The ratio of reverse breaths using expiratory time versus our automated algorithm (expiratory time method/automated algorithm) was 1.02, see Figure 5.

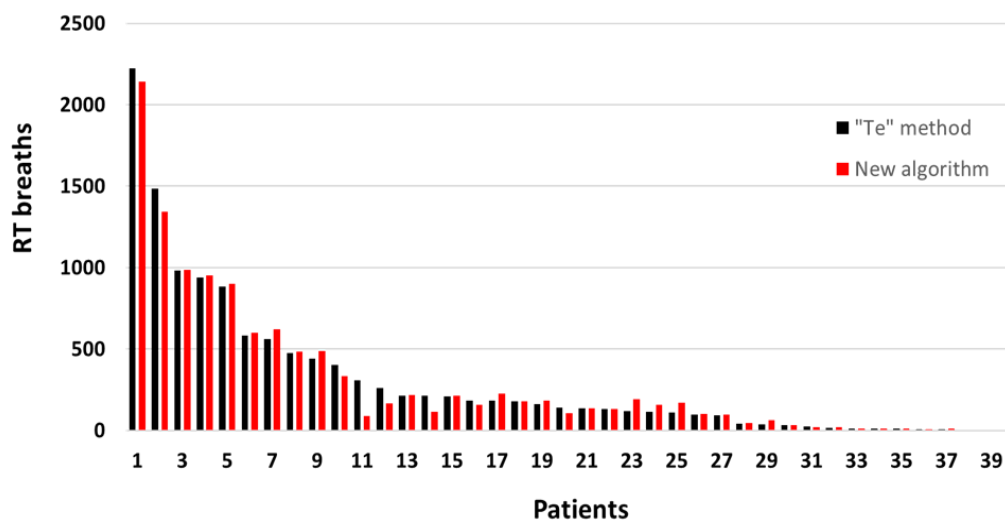


Figure 5. Comparison of reverse triggering incidence. Each bar represents one patient. Red bars show the frequency of RT using the new algorithm created. Black bars show the frequency of RT using the variation of expiratory time (Te method).

1.3 Incidence of reverse triggering

Reverse triggering above 1 μ V

Of the 75 patients included in the original observational study, 30 patients were under a partial mode of ventilation and were not used for the analysis; additionally, 6 patients were excluded for technical problems with the recording (See Figure 6).

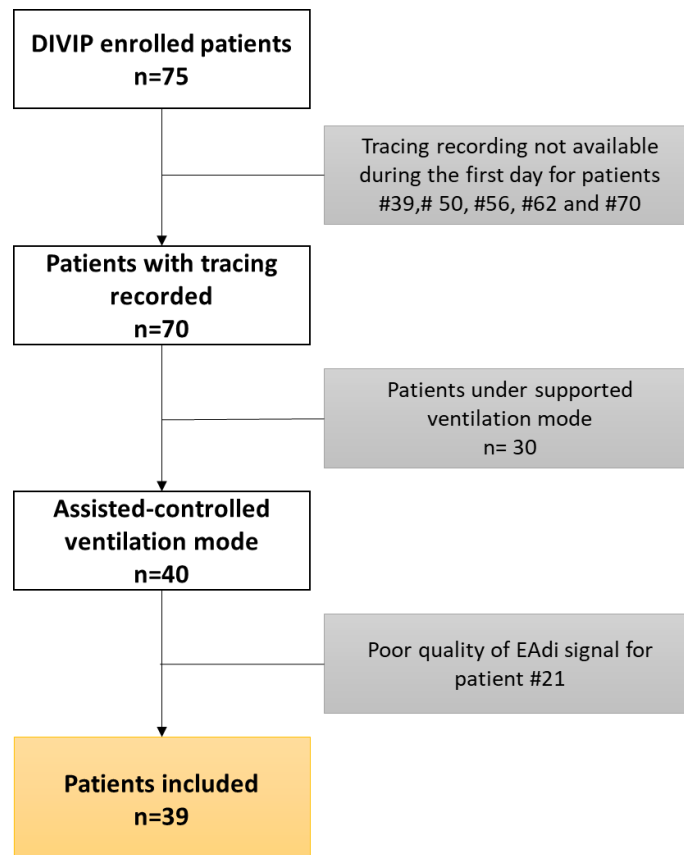


Figure 6. Flow diagram of the study population. Patients from the observational study “DIVIP” (diaphragm muscle inactivity in mechanically ventilated ICU patients) were included.

Finally, the 39 remaining patients ventilated in assist-control mode were all included in the present study to calculate the incidence of reverse triggering (Table 4). The tracings were

recorded at a median time (IQR) of 24 (21 to 26) hours after intubation: a total of 66,296 breaths with an average \pm SD breaths of 1699 ± 567 per patient were analyzed. Patients had a mean age of 57 y.o., an APACHE II of 21, and 22 out of 39 (56%) subjects had a primary pulmonary reason for intubation (Table 4). Regarding sedation, 32 patients (82%) were on a continuous infusion and 34 received any sedative during the recording (87%), with propofol being the most common used drug (continuously in 21 and bolus only in 2). Twenty-one patients were sedated with more than one continuous infusion (Table 4). The median Riker Sedation-Agitation Scale was 2, indicating 'very sedated' patients (Table 4). One patient was receiving neuromuscular blocking agents at the time of recording. No other patients had received neuromuscular blocking agents in the previous hours. Depth of paralysis was not recorded on the chart.

Table 4. Baseline patient characteristics

Variable	n=39
Age, y	57 \pm 17
Male, n (%)	23 (59)
BMI (IQR)	27 (23 to 34)
Number of breaths studied	1700 \pm 588
Time to recording after intubation, h	24 (21 to 26)
APACHE II	21 (18 to 29)
P/F ratio, mmHg	156 (107 to 282)

Table 4. Baseline patient characteristics (*continuation*)

Variable	n=39
Reason for intubation, n (%)	
Pulmonary	22 (56)
<i>Pneumonia</i>	8/22 (36)
<i>COPD</i>	5/22 (23)
<i>Chest trauma</i>	2/22 (9)
<i>ARF</i>	7/22 (32)
Non-pulmonary	17 (44)
<i>Sepsis</i>	3/17 (18)
<i>Seizures</i>	5/17 (29)
<i>Trauma</i>	5/17(29)
<i>Post-cardiac arrest</i>	3/17 (18)
<i>Stroke</i>	1/17 (6)
SAS score (sedation)	2 (1 to 3)
Continuous sedation, n (%)	32 (82)
Propofol	21 (65)
Midazolam	11 (34)
Both propofol and midazolam	4 (12)
Any opioid	21 (65)
Either propofol or midazolam plus opioid	17 (53)

Table 4. Baseline patient characteristics (*continuation*)

Variable	n=39
Sedatives during recording* (mg*kg IBW*h)	
Propofol	2.8 (0.9 to 4.4)
Midazolam	0.05 (0.03-0.12)
Equipotent Fentanyl	1.24 (0.80 to 2.63)
MV days	5 (2 to9)
ICU mortality, n (%)	11 (28)
Total number of patients	39

**All numeric variables are described in median (IQR) except for Age in mean \pm SD*

APACHE II: Acute Physiology And Chronic Health Evaluation II; P/F ratio: PaO₂/FIO₂;

COPD: Chronic obstructive pulmonary disease; ARF: Acute respiratory failure; here defined as a primary cause of intubation not led by any other pulmonary diagnosis;

*SAS: Riker Sedation-Agitation Scale (ranging from 1 to 7; with lower values indicating deeper sedation); *Sedatives doses only took into account those patients that*

received them. IBW: ideal body weight was calculated as $50 + 2.3(\text{height in inches} - 60)$ for men and $45.5 + 2.3(\text{height in inches} - 60)$ for women. Fentanyl equipotent

dose was calculated considering hydromorphone to be 20 times less potent. MV:

Mechanical ventilation; ICU: Intensive care Unit.

More than 90 % of patients had at least a few reverse triggered breaths detected using the threshold of 1 μ V and (17 out of 39 [44%]) of them had $\geq 10\%$ of reverse triggered breaths. The median rate for the whole group was 8% of the breaths (range 0.1 to 75%), see Figure 7A. No breaths with reverse triggering were observed for the patient who received neuromuscular blockade agents. The number per minute for each patient is presented in Figure 7B.

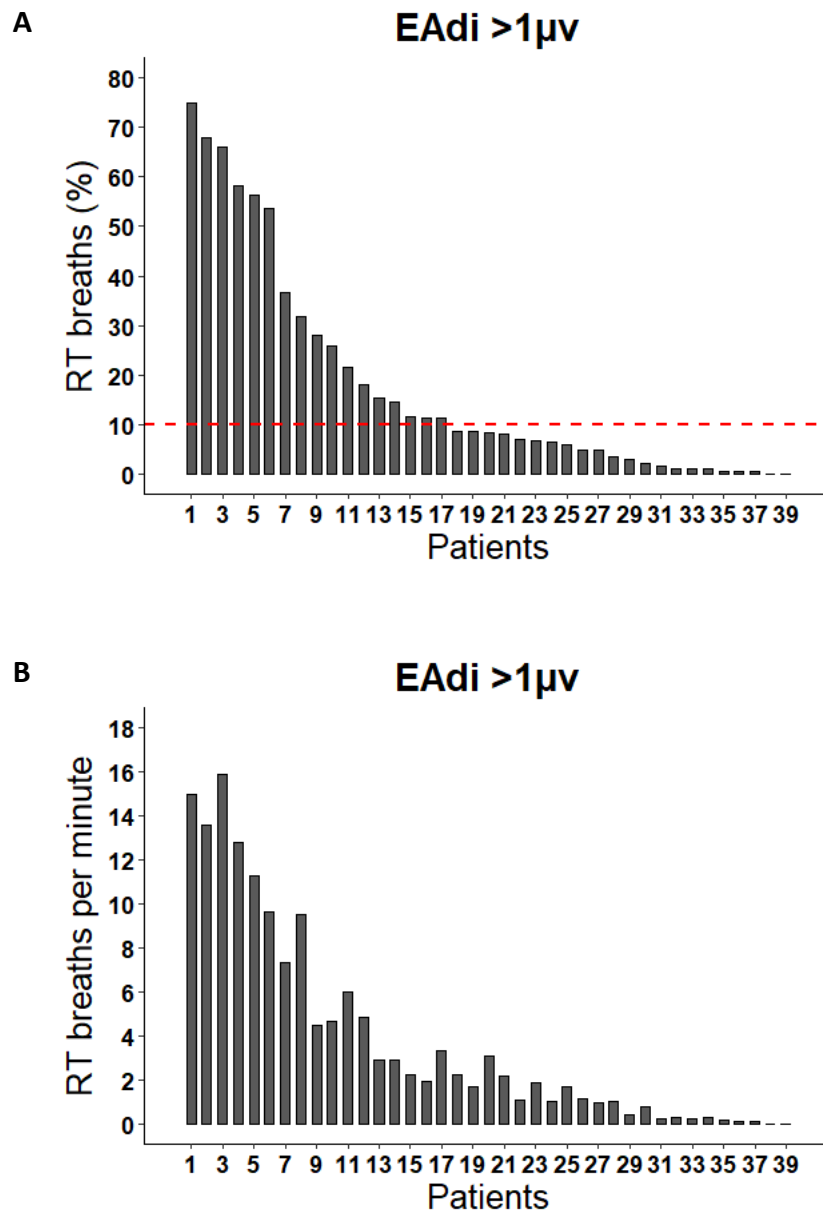
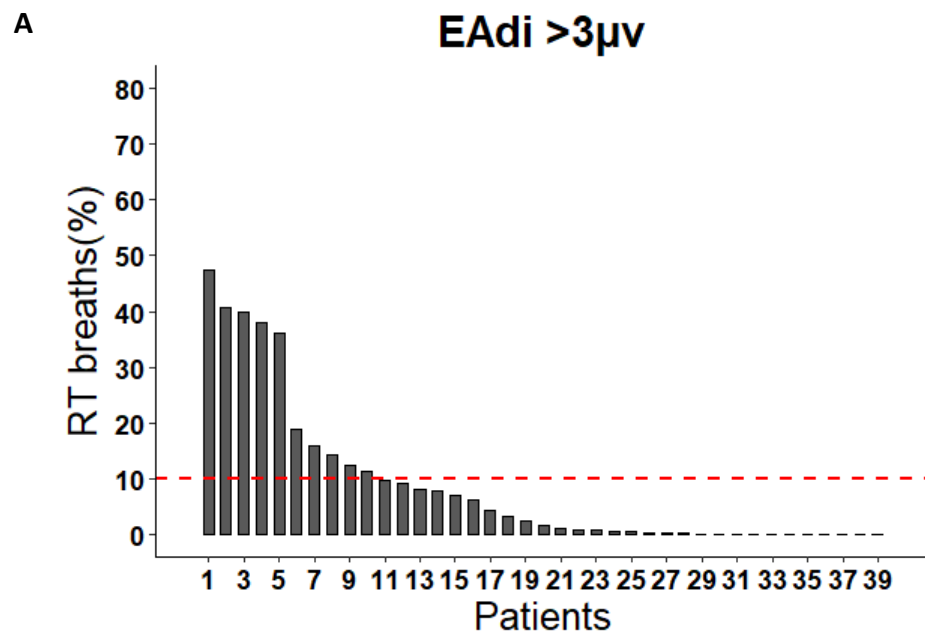


Figure 7. Incidence of reverse triggering using EAdi cut-off > 1 μ V. Each bar represents one patient. A. shows the percentage of RT breaths in each patient. B. shows the number of RT breaths per minute in each patient. Dashed red line shows 10% cut-off commonly used to categorized severe amount of dyssynchronies.

Incidence of reverse triggering with 3 and 5 μ V

When using a 3 μ V above baseline and 5 μ V above baseline EAdi threshold, the median value of reverse triggering was 2% (range 0 to 48%) and 0.1% (range 0 to 29%) respectively. The percent of patients with $\geq 10\%$ of reverse breaths was 26% (10 patients) using a 3 μ V and 13% (5 patients) using a 5 μ V EAdi threshold (Figure 8).



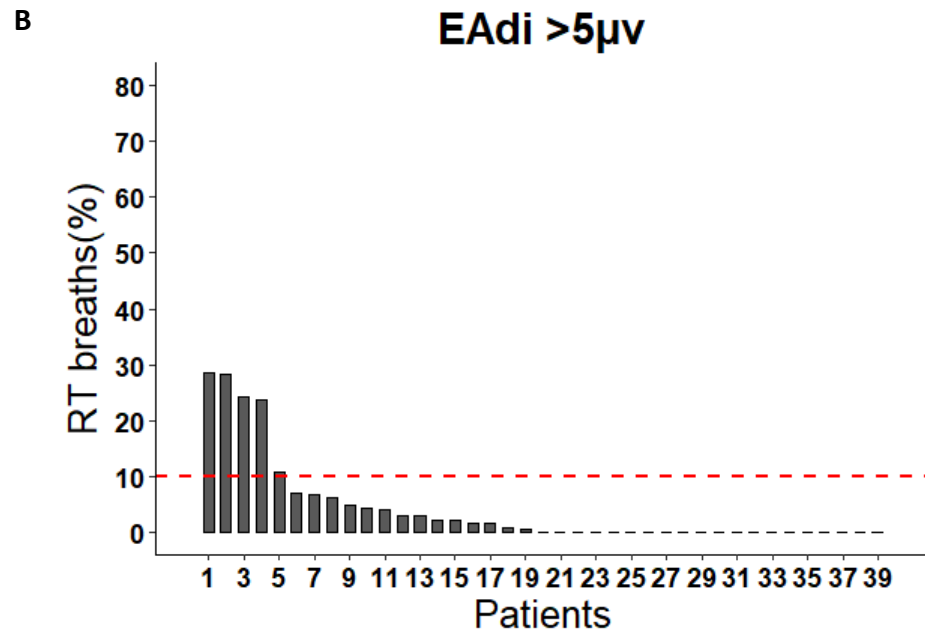


Figure 8. Incidence of Reverse triggering using EAdi cut-off >3 and >5 μ V. A. Percentage of RT using an EAdi cut-off greater than 3 μ V; B. Percentage of RT using an EAdi cut-off greater than 5 μ V. Each bar corresponds to a patient.

1.4 Entrainment and within subject analysis

A 1:1 and 1:2 entrainment pattern was identified in 69% and 62% of the patients over this one-hour recording, respectively: 77% of the subjects presented at least one of these two types of interactions. Overall, entrainment was present from 1% to 69% of all studied breaths. The correlation between the percentage of reverse breaths and the prevalence of 1:1 entrainment presented an r^2 coefficient of 0.73, ($p < 0.001$), see Figure 9.

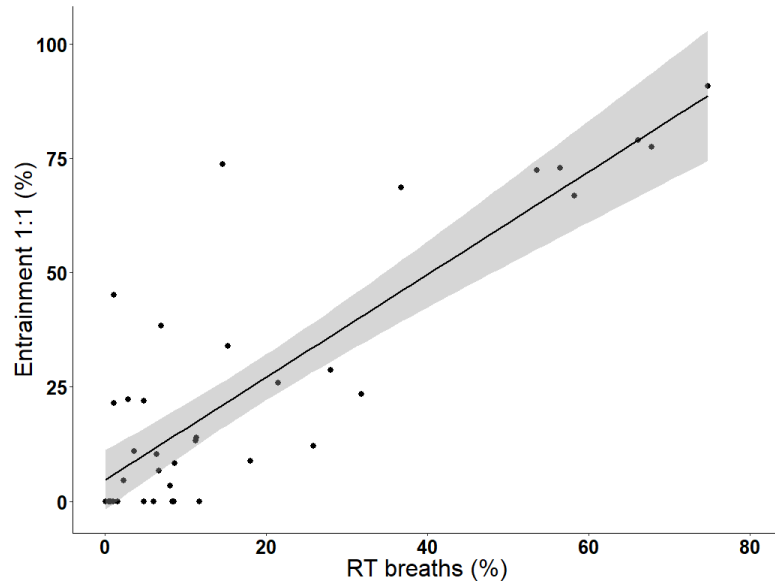


Figure 9. Correlation between amount of RT breaths and 1:1 entrainment. Entrainment was defined as 3 or more consecutive RT breaths. The higher the rate of RT per patient, the larger the percentage of 1:1 entrainment. Each point represents an individual patient.

Within-subject analysis

Patient-level analysis showed no differences (except for one patient) for both EAdi and phase angles when comparing entrained and non-entrained reverse-triggered breaths in the group of 8 patients displaying the most frequent RT (Table 5).

Table 5. Within-subject analysis of EAdi and phase angle in patients with a high incidence of entrainment (n=8)

	EAdi entrained	EAdi non-entrained	Angles entrainment	Angles non-entrainment
Patient 1; median (IQR)	3.4 (1.5)	3.4 (1.6)	48 (39)	37 (44)*
Patient 2; median (IQR)	3.8 (9.3)	8.7 (13.1)**	50 (27)	46 (40)+
Patient 3; median (IQR)	2 (0.6)	1.8 (0.8)+	36 (25)	40 (32)
Patient 4; median (IQR)	6.3 (2.1)	6.2 (2.0)	37 (57)	35 (55)
Patient 5; median (IQR)	4.1 (4.5)	4.1 (3.5)	11 (24)	9 (18)
Patient 6; median (IQR)	4.8 (4.8)	3.7 (3.6)**	100 (286)	82 (231) ‘
Patient 7; median (IQR)	2.4 (1.7)	2.3 (1.4)	47 (17)	47 (22)
Patient 8; median (IQR)	3.7 (2.4)	2.6 (1.5)**	104 (127)	121 (140)
All ; median (IQR)	3.5 (2.9)	3 (2.9)**	49 (42)	48 (50)

*EAdi is expressed in μV ; angles are expressed in $^{\circ}$; * $p=0.001$, ** $p<0.0001$, + $p=0.005$, ‘ $p=0.02$*

Note: Patients with RT and highest rate of entrainment (1st quartile) were selected.

1.5 Factors associated with a high incidence of reverse triggering

Table 6 shows the characteristics and ventilatory parameters of patients with higher than the median rate of RT, compared to those with equal or below the median rate. There was no difference in baseline characteristics and ventilatory parameters, except for the baseline PaO₂/FIO₂ ratio which was higher in the group with more reverse triggering (200 vs 124 mmHg; $p=0.020$) and set respiratory rate which was lower in the group of patients with more reverse triggering (20 vs 28 breaths per minute; $p=0.041$). Sedation scores showed most patients were deeply sedated in both groups (Table 4). Use of propofol, midazolam and either fentanyl or hydromorphone did not differ between groups. However, propofol dosage was higher in those patients displaying more reverse triggering (Table 6). The group with higher incidence had more frequent patient-triggered breaths during the one-hour

recording (12% vs 1%, $p<0.001$) and 24h after the recording they were more likely to be ventilated in a supported mode (pressure support or Neurally Adjusted Ventilator Assist (NAVA) or extubated (68% vs 35%, $p=0.039$). For both the 3 and 5 μV EAdi threshold, 68% and 63% of patients above the median rate (2% and 0.1% respectively) were either extubated or switched to supported mode 24h after ($p=0.039$ and $p=0.153$, respectively). The rate of double cycling was very low (median 0%, IQR 0 to 0.11%; 0 breaths per hour; IQR 0 to 2) and not different between groups.

Table 6. Outcomes, demographic and respiratory variables grouped by prevalence of RT

Variable	High RT (> 8%) n=19	Low RT (≤ 8%) n=20
Age, y	53 ±17	62 ±16
Male, n (%)	10(53)	13(65)
Number of breaths studied	1601 ± 601	1794 ± 567
Time to recording from intubation, h	26 (21-28)	24 (22-26)
APACHE II	20 (16-27)	24 (21-30)
Pulmonary cause of intubation, n (%)	9(47)	13(65)
SAS	2 (1-3)	2 (1-3)
MV, days	5 (2-9)	6 (4-10)
Switch to a partial support mode or extubation the next day, n (%)	13 (68)	7 (35)*
PF ratio, mmHg	200 (148-353)	124 (96-229)**
Respiratory rate, bpm	20 (19-26)	28 (21-30)
TV PBW, ml	6.8 ± 1.3	6.5 ± 1
PEEP, cmH2O	8 (5-11)	9 (6-12)
Median Peak EAdi, µV	1.7 (0.8-4.3)	0.7 (0.7-0.8)***
Patient-triggered breaths over the 1-hour recording, %	12 (8-26)	1 (0-3)***
Double Cycling, %	0 (0-0.4)	0 (0-0.0)

All numeric variables are presented as median (IQR) except for age, number of breaths studied and TV PBW; which are expressed as a mean ±SD

** p=0.02, *p=0.04, *** p<0.0001

APACHE II: Acute Physiology And Chronic Health Evaluation II; SAS: Riker Sedation-Agitation Scale (ranging from 1 to 7; with lower values indicating deeper sedation); MV: Mechanical ventilation; P/F ratio: pO₂/FIO₂; TV PBW: Tidal volume predicted body weight; PEEP: Positive end-expiratory Pressure; EAdi: Electrical activity of the diaphragm.

2. Porcine model of reverse triggering during ARDS

2.1 *ARDS model*

We were able to reproduce an established model of acute lung injury. Induction of lung injury required a median [IQR] of 3 [2,4] lung lavages to reach a PaO₂/FiO₂ ratio lower than 150 mmHg. Then, after a variable period of injurious ventilation or second hit (from 15 minutes to 1 hour in order to achieve 10% decrease in respiratory system compliance), animals developed severe hypoxemia (~100 mmHg) and increased airway pressures, all of them in line with clinical manifestations of ARDS. In addition, this model was characterized by high lung recruitment, evidenced by a significant increase in O₂ after a recruitment maneuver prior to baseline assessments (see Table 6 below).

2.2 *Development of the reverse triggering model*

Induction of RT was performed as previously described in methods. Right after stabilization period (20 min), induction of RT was attempted by modifying ventilator parameters. Our strategy consisted mainly in continuously changing mechanical ventilator settings, especially respiratory rate and tidal volume. To induce RT, we always set the ventilator rate 1 to 5 breaths/min above the neural rate. For instance, if a pig was breathing at 30 breaths per minute (neural rate) for any given level of sedation, we set a machine rate between 31 to 36 breaths per minute.

Among all pigs allocated to RT (n=24), 6 animals died at some point before completing the experiment. One of them died due to pneumothorax during lung injury induction. Other two died while trying to induce RT, whereas 3 out of 6 died at 30, 45 and 120 minutes after starting RT due to hypotension and severe hypoxemia.

So 18 of the 24 animals allocated to RT completed the study period. Reverse triggering was induced successfully in all of them, however different patterns and features were observed.

The time required to observe the first breaths with reverse triggering after ventilatory modifications ranged from 2 to 30 min and this was considered the starting point of the 3-hour study period.

In addition, different entrainment patterns were observed. Entrainment 1:1 was the most frequent pattern, occurring at least at some point of the experiment in 83% of animals. Pattern 1:2 was observed in 10 animals (56%) whereas other infrequent patterns such as 1:3, 1:4, 3:1 and 2:1 were also observed in 4 out of 18 animals. Seven animals presented a fix and repetitive unique pattern (1:1), all other animals showed constant changes of the entrainment pattern. Breathing effort was also variable between animals and sometimes within the animals. The median (min-max) PTP_{breath} and PTP_{min} was 5.3 (1.4 -19) cmH₂O and 181 (36 – 819) cmH₂O*s/min, respectively.

Since pigs and humans can adapt their neural drive to either avoid or enhance a respiratory entrainment status, a continuous supervision to adjust ventilatory parameters and/or anesthesia depth was required to keep the model with ongoing RT. Despite this limitation we were able to sustain RT dyssynchrony for around 80% to 90% of the 3-hour study period.

Figure 10 shows a representative tracing of RT in our animal model. Diaphragm contractions are represented by negative deflections in the P_{eso} and are initiated after passive insufflations (dashed black lines). In this case, a 1:1 pattern (RT in every breath) is observed. Noteworthy, respiratory efforts are long enough to extend into the expiratory phase and create changes in the shape of the expiratory flow (blue tracing), which is crucial to test our hypothesis that eccentric contractions (diaphragm lengthening) may induce diaphragm injury.

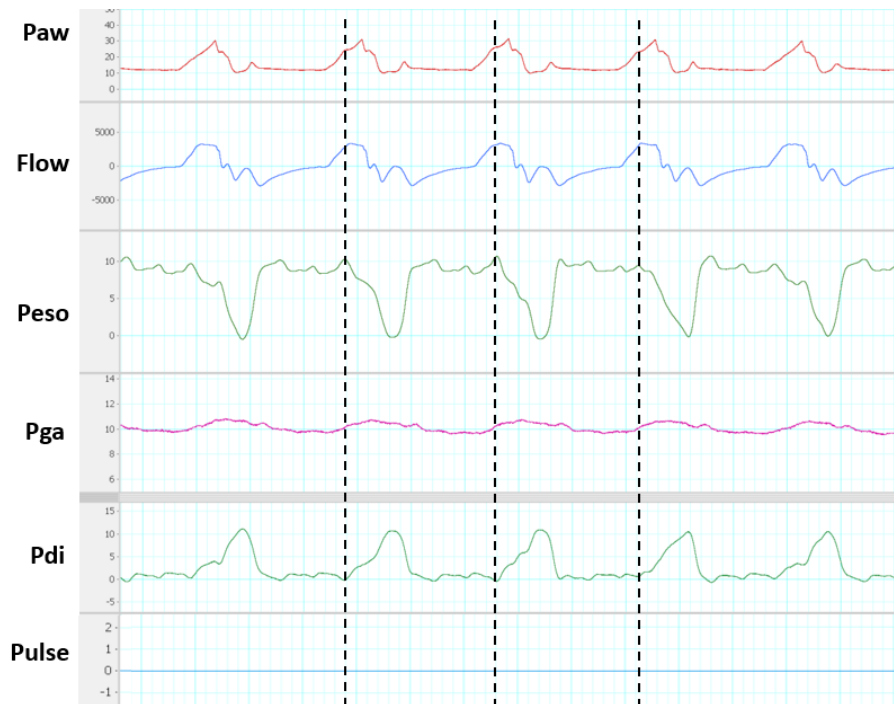


Figure 10. Representative tracing of one animal with reverse triggering dyssynchrony.

2.3 Characteristics of the reverse triggering model

As defined in methods section, all animals allocated to RT who completed the study period (n=18) were analyzed as a single group for the purpose of characterizing the model, and the pre-defined subgroup analysis was used only for specific goal 3.

2.3.1 Respiratory and cardiovascular variables

Following a stabilization period and lung recruitment maneuver (volume control 6ml/kg and stepwise increasing PEEP to 15, 20 and 25 cmH₂O for 1 min each), baseline measurements were performed, and no difference was observed in ventilatory variables between passive and RT groups. Table 6 shows different respiratory variables over time. Tidal volume was the same at the beginning of the experiment, however RT group had significantly lower VT than passive group thereafter at 1 and 2 hours. RT group also had statistically significant

higher RR, than passive group at 1 and 2 hours. Variables such as PaO₂ and PEEP did not differ between groups but a significant decreased was observed in O₂ at 1 and 2 hours. There was no difference in PaCO₂ throughout the experiment in both groups.

Table 6. Ventilatory variables in RT and passive ventilation

Variable	Group	Baseline	Hour 1	Hour 2	Hour 3	Analysis of variance		
		(mean ± SD)	(mean ± SD)	(mean ± SD)	(mean ± SD)	Group	Time	Group*Time
PaO ₂ , mmHg	Passive	341 ± 114	140 ± 52* [^]	135 ± 45* [^]	239 ± 139	0.033	<0.001	0.924
	RT	384 ± 130	206 ± 128*	216 ± 131*	275 ± 148			
PaCO ₂ , mmHg	Passive	52.9 ± 6.8	55.7 ± 7.3	54.3 ± 7.4	58.3 ± 8.6	0.754	0.067	0.280
	RT	50.1 ± 7.6	59 ± 9.9	56.8 ± 11.5	52.1 ± 10			
RR, bpm	Passive	31.8 ± 2.1	33.6 ± 2.6	34.1 ± 2.7	33 ± 2.39	<0.001	<0.001	<0.001
	RT	31.1 ± 1.3	45.6 ± 6.1* ^{&#}	47.5 ± 7.5* ^{&#}	31.2 ± 1.7			
VT, ml/kg	Passive	10 ± 0	9.8 ± 0.4	9.7 ± 0.6	9.9 ± 0.2	<0.001	<0.001	<0.001
	RT	10 ± 0	7.5 ± 1.2 * ^{&#}	7.0 ± 1.1 * ^{&#}	10 ± 0			
PEEP, cmH ₂ O	Passive	8 ± 0	8.4 ± 0.7	8.5 ± 0.9	8 ± 0	0.207	<0.001	0.658
	RT	8 ± 0	8.8 ± 1.2	8.9 ± 1.3 *	8 ± 0			

Note: Statistical analysis was performed using two-factorial repeated measures analysis of variance (ANOVA).

p < 0.05 was considered statistically significant.

**p < 0.05 against baseline; & p < 0.05 against Hour 3; # p < 0.05 against passive; ^ p < 0.05 against RT baseline*

In terms of respiratory mechanics there were no changes in respiratory system compliance nor in airway pressures over time (intra group analysis), and no differences between groups either at baseline or after 3 hours (see Table 7).

Table 7. Respiratory mechanics (static conditions) in RT and passive group

Variable	Group	Baseline	Hour 3	<i>p-value</i>		
		(mean \pm SD)	(mean \pm SD)	Intra-group	Inter-group (baseline)	Inter-group (3h)
Crs, ml/cmH2O	<i>Passive</i>	16.9 \pm 1.9	16.7 \pm 3.6	0.906	0.073	0.217
	<i>RT</i>	18.7 \pm 2.7	19 \pm 5.4	0.775	-	-
Pplat, cmH2O	<i>Passive</i>	31 \pm 3.6	31.4 \pm 5.8	0.694	0.298	0.414
	<i>RT</i>	28.8 \pm 3.6	29.4 \pm 4.9	0.722	-	-
Ppeak, cmH2O	<i>Passive</i>	43.4 \pm 7.6	45.8 \pm 11	0.456	0.285	0.286
	<i>RT</i>	40 \pm 6.2	40.9 \pm 8.1	0.640	-	-
Driving pressure, cmH2O	<i>Passive</i>	21.5 \pm 3.2	22.4 \pm 5.5	0.642	0.335	0.399
	<i>RT</i>	20.1 \pm 3.7	20.4 \pm 4.8	0.750	-	-

Note: Statistical analysis was performed using pairwise t-test for intra group and two sample t-test for intergroup at baseline and 3 hours. P-value <0.05 was considered statistically significant.

Analysis of hemodynamic and metabolic variables did not show any difference between groups when comparing different experimental times. Compared to baseline, intragroup analysis showed that HR presented a significant increase at hour 1, hour 2 and hour 3 in both passive and RT groups. Also, a significant drop was observed in pH at 3 hours in both experimental groups. Additionally, intra-group analysis revealed that mean arterial pressure remained unchanged throughout the study period, both in passive and RT groups (Table 8).

Table 8. Hemodynamic and metabolic variables in RT and passive ventilation

Variable	Group	Baseline	Hour 1	Hour 2	Hour 3	Analysis of variance		
		(mean ± SD)	(mean ± SD)	(mean ± SD)	(mean ± SD)	Group	Time	Group*Time
pH	<i>Passive</i>	7.14 ± 0.02	7.09 ± 0.04	7.07 ± 0.04	7.05 ± 0.1*	0.062	<0.001	0.064
	<i>RT</i>	7.15 ± 0.04	7.09 ± 0.03*	7.09 ± 0.06*	7.12 ± 0.1*			
HR, lpm	<i>Passive</i>	147 ± 36	194 ± 20 *	196 ± 28*	192 ± 24*	0.093	<0.001	0.953
	<i>RT</i>	137 ± 26	186 ± 27*	188 ± 31*	176 ± 29*			
MAP, mmHg	<i>Passive</i>	76.2 ± 13	61.4 ± 13^	61.4 ± 14^	63 ± 11	<0.001	0.088	0.423
	<i>RT</i>	80.3 ± 12	75.6 ± 16	79.8 ± 18	73 ± 14			

Note: Statistical analysis was performed using two-factorial repeated measures analysis of variance (ANOVA).

P-value <0.05 was considered statistically significant.

**p<0.05 against baseline; & p<0.05 against Hour 3; # p<0.05 against passive; ^ p<0.05 against RT baseline*

2.2.2 Sedation level

After animal instrumentation and induction of lung injury, we changed the anesthesia during the stabilization period to Ketamine and Propofol until the end of the experiment. When comparing passive vs RT, no difference was found in cumulative doses of both ketamine and propofol with p-value=0.435 and 0.433, respectively; see Figure 11.

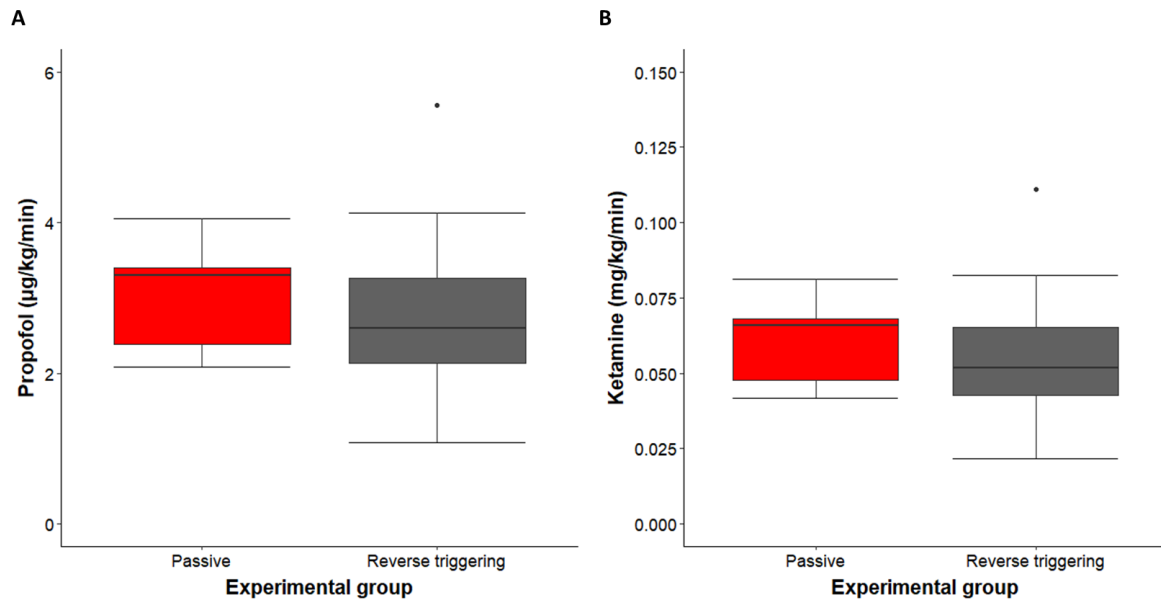


Figure 11. Cumulative doses of sedatives in passive and RT group. A. Amount of propofol doses. B. Amount of ketamine doses. Red boxes represent passive group and gray boxes represent RT group.

BIS index average values ranged from 59.5 to 57.7 in RT group and from 54.5 to 53.2 in passive group. No significant differences were found in BIS values neither over time in the intragroup analysis (p-value= 0.685), nor between groups at any time point (p-value=0.096), see Figure 12.

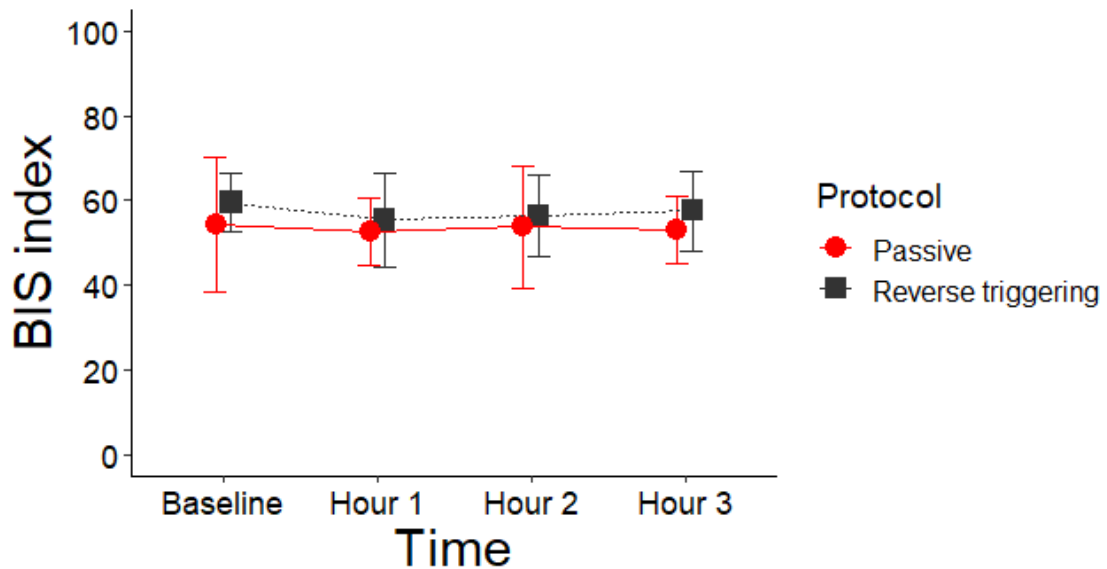


Figure 12. Anesthesia depth in passive and RT group. Graph shows BIS index values over time in both groups (redpoints for passive, black squares for RT)

2.2.3 Alteration of the alveolar-capillary barrier

Lung wet-dry weight ratio.

High values of accumulated lung water, consistent with some degree of alteration of the alveolar-capillary barrier in pigs as demonstrated in other studies^{75,76}, were found in both groups (8.9 ± 0.6 and 8.3 ± 1 for passive and RT respectively; [p -value=0.051]), see Figure 13.

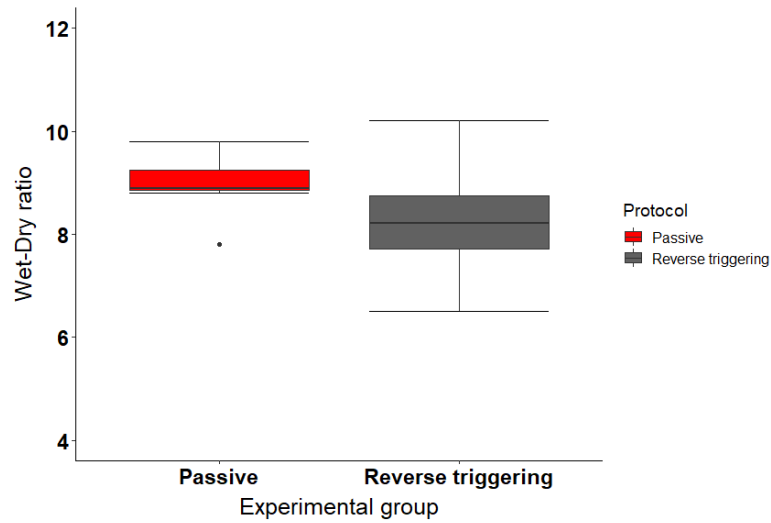


Figure 13. Wet-dry weight ratio in passive and RT group

BAL protein concentration.

Figure 14 shows the amount of BAL total protein content in both experimental groups where no statistical difference was observed (p -value= 0.311).

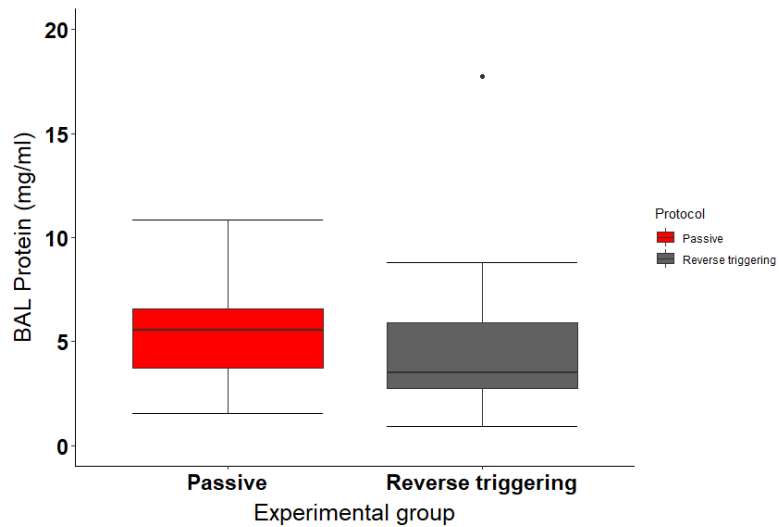


Figure 14. BAL protein total content in passive and RT group

3. Impact of reverse triggering on diaphragm function and structure

3.1 *Pressure time product and study groups*

As previously described, a pre-planned analysis of PTP_{min} was conducted in order to split the RT group in 3 subgroups according to the intensity of breathing effort, and thus analyze the impact of RT with different levels of breathing effort on the diaphragm function and structure.

Figure 15 shows individual PTP_{min} values for each animal. PTP_{min} terciles were calculated. Average \pm SD (min-max) PTP_{min} for RT low_effort, RT middle_effort and RT high_effort were 85 ± 42 (36-135), 177 ± 25 (135-207) and 404 ± 211 (248-819) $cmH_2O \cdot s/min$, respectively. Then, including animals from passive group (PTP_{min} equal to 0), a total of 4 experimental groups were established.

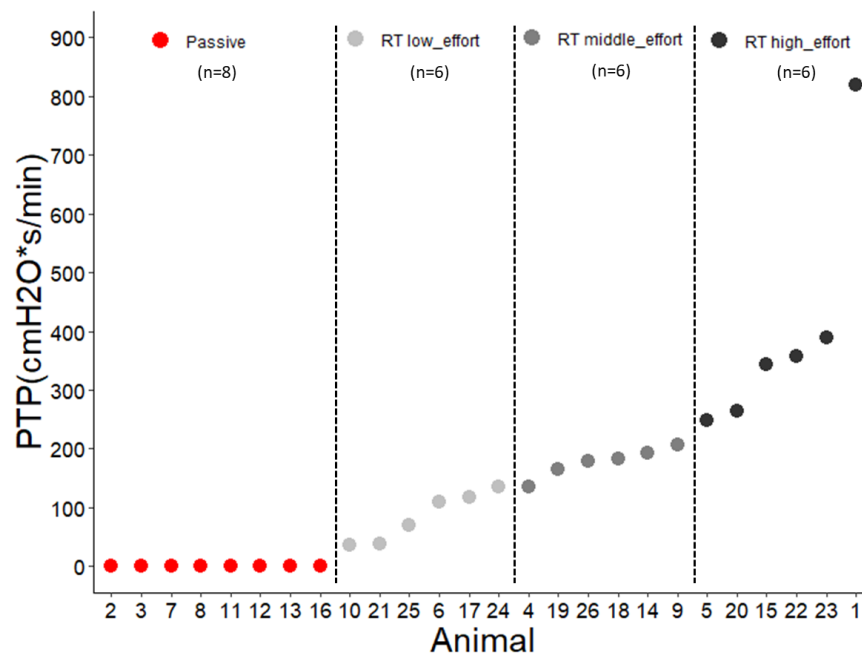


Figure 15. PTP_{min} values and experimental groups. Individual animal values of PTP_{min} are represented by different points. Animals were divided in 4 experimental groups according to PTP.

3.2 Diaphragm force generating capacity

P_{di} absolutes values

Evolution of the P_{diTw} values over time are presented in Figure 16. Intragroup analysis showed that P_{diTw} did not change over time in any of the experimental groups (p-value over time=0.834, p-value for interaction=0.921). However, animals which presented RT with low level of breathing effort presented a higher P_{diTw} values than the other groups (p-value between groups<0.001).

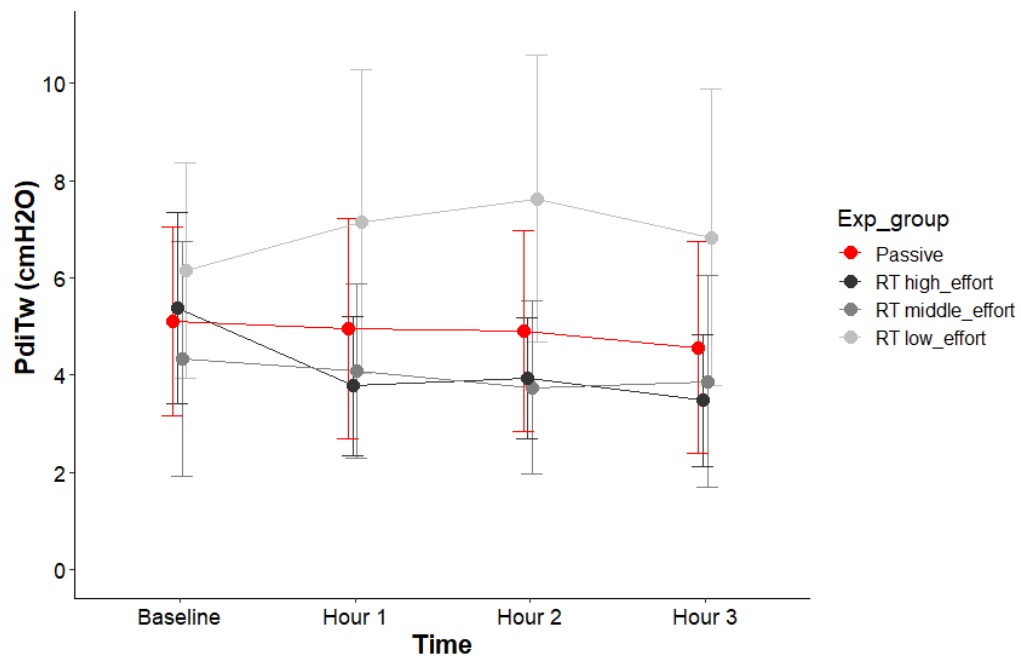


Figure 16. Transdiaphragmatic twitch pressure (P_{diTw}). P_{diTw} calculated as the difference between P_{ga} and P_{eso} after single twitch at different time points for each experimental group.

Force frequency curves of all experimental groups are presented in Figure 17. No statistically significant difference was found between P_{di} obtained at baseline and P_{di} obtained at 3 hours in any experimental group (P-value= 0.558 in passive; P-value= 0.679 in RT low_effort; P-value= 0.517 in RT middle_effort; P-value= 0.215 in RT high_effort).

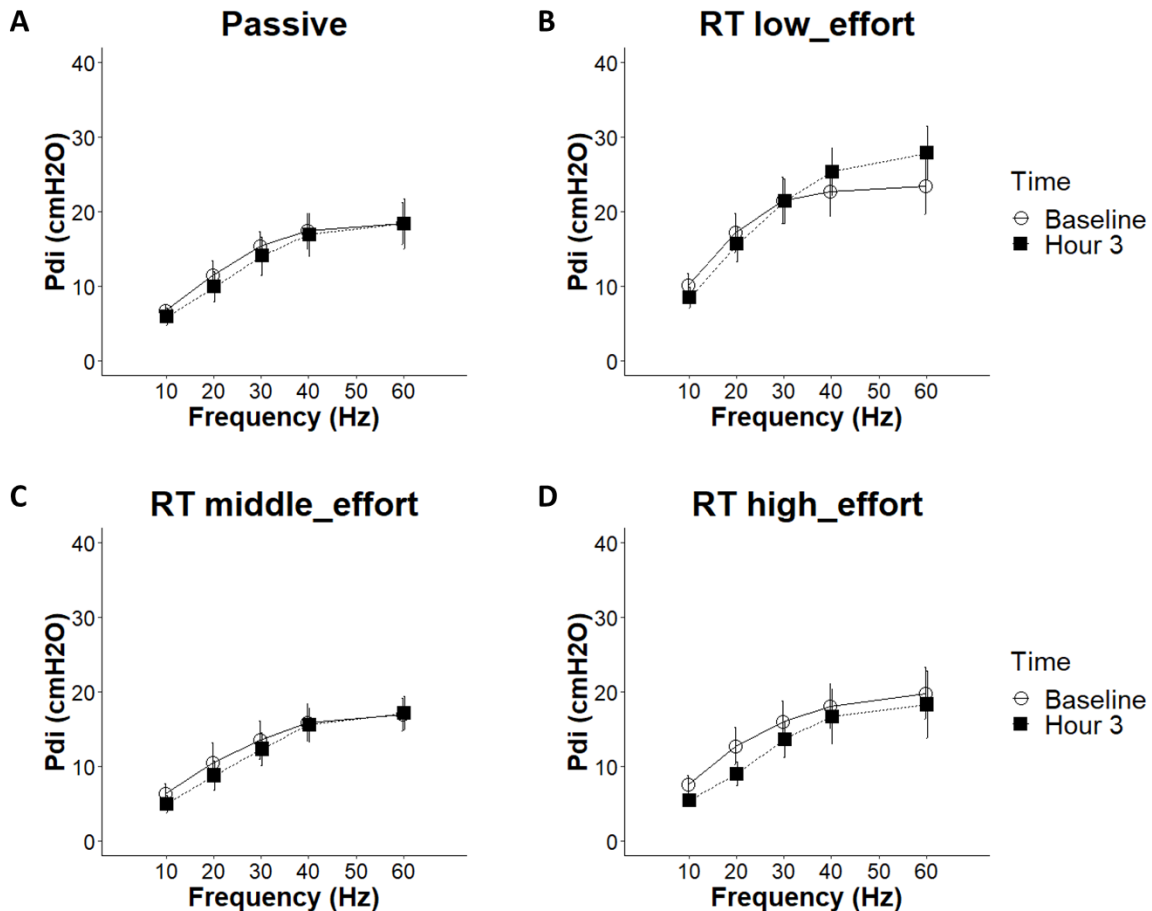


Figure 17. Force/frequency curves. Transdiaphragmatic pressure (P_{di}) was calculated as the difference between P_{ga} and P_{eso} after different stimulation frequencies at baseline (white

circle) and after 3 hours (black square) in each group. (A) passive; (B) RT with low effort; (C) RT with middle effort; (D) RT with high effort.

P_{di} normalized to baseline

Due to the high variability of the absolute values of P_{di} observed between different animals already at baseline, we also analyzed P_{di} data normalized to the baseline value of each animal. Therefore, P_{diTw} ratio was calculated as P_{diTw} values obtained at hours 1, 2 and 3 over P_{diTw} at baseline, whereas P_{di} ratio (Force/frequency curve) was calculated as the actual P_{di} value obtained with different frequencies at hour 3, over the corresponding values at baseline.

Figure 18 shows P_{diTw} ratio over time in all groups. At 3 hours, animals from RT high_effort group presented a larger decrease in force (34%) as compared with animals with RT middle and low effort which presented a decrease in force of 7% (p-value=0.034), and increase in force of 10% (p-value<0.001), respectively. In addition, the RT low_effort group had significantly higher P_{diTw} ratio than the passive group (p-value=0.005).

P_{diTw} did not change when comparing all groups at different experimental time points (p-value over time=0.523), nor was there any interaction between group and time (p-value=0.995).

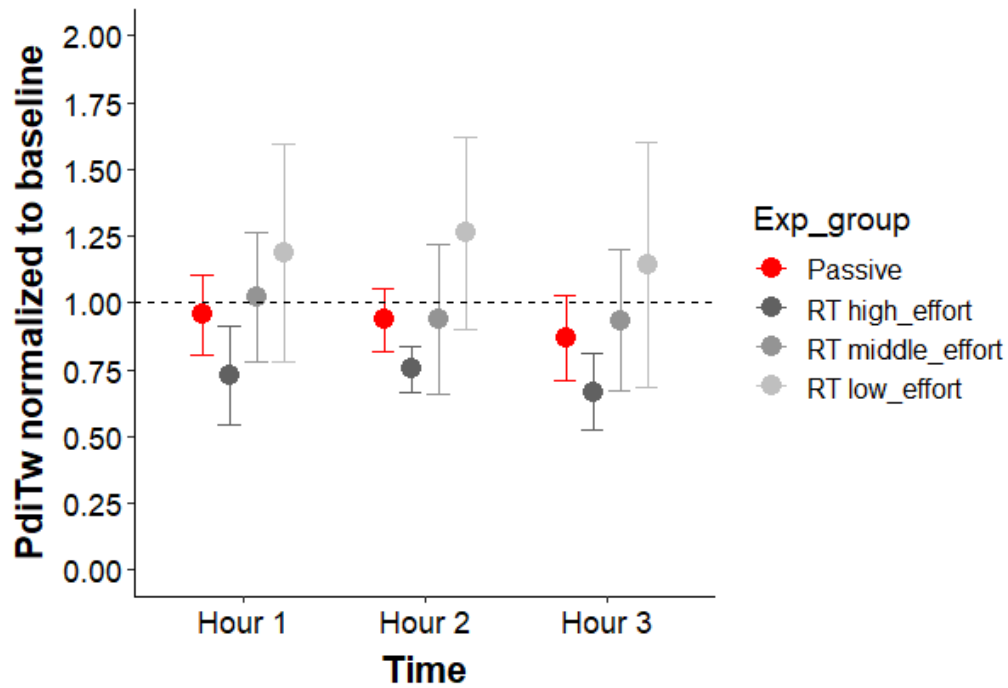


Figure 18. Transdiaphragmatic twitch pressure (P_{diTw}) normalized to baseline. P_{diTw} ratio calculated as $P_{diTw} / P_{diTw \text{ baseline}}$ at different time points in each experimental group. Dashed black line (P_{diTw} ratio of 1) represents no change in force compared to baseline.

Regarding P_{di} ratio assessed after 3 hours of experiment, a significant increase in P_{di} ratio was observed from lower (10-20-30Hz) to higher (40-60Hz) stimulation frequencies (p-value= 0.006), see Figure 19. In addition, a significant difference in the P_{di} ratio between experimental groups (p-value= 0.025) was found. For instance, at 60Hz of stimulation (tetanus contraction), the force generating capacity in the RT high_effort group was significantly lower than the RT low_effort group (p-value=0.043), decreasing by 10% in the former, while the latter showed a 23% increase in force, as compared with baseline. No interaction between stimulation frequency and experimental group was observed.

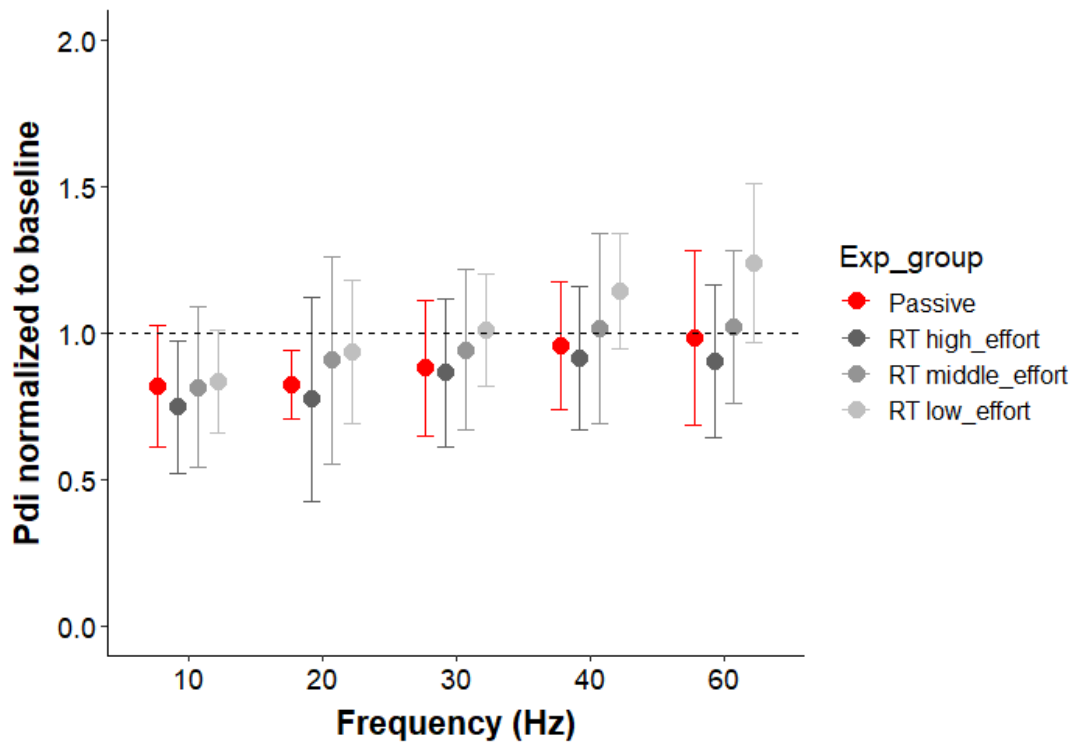


Figure 19. Transdiaphragmatic pressure (P_{di}) normalized to baseline. P_{di} ratio calculated as P_{di} obtained at 3 hours over P_{di} at baseline after different frequencies of stimulation in each experimental group. Dashed black line (P_{di} ratio of 1) represents no change in force.

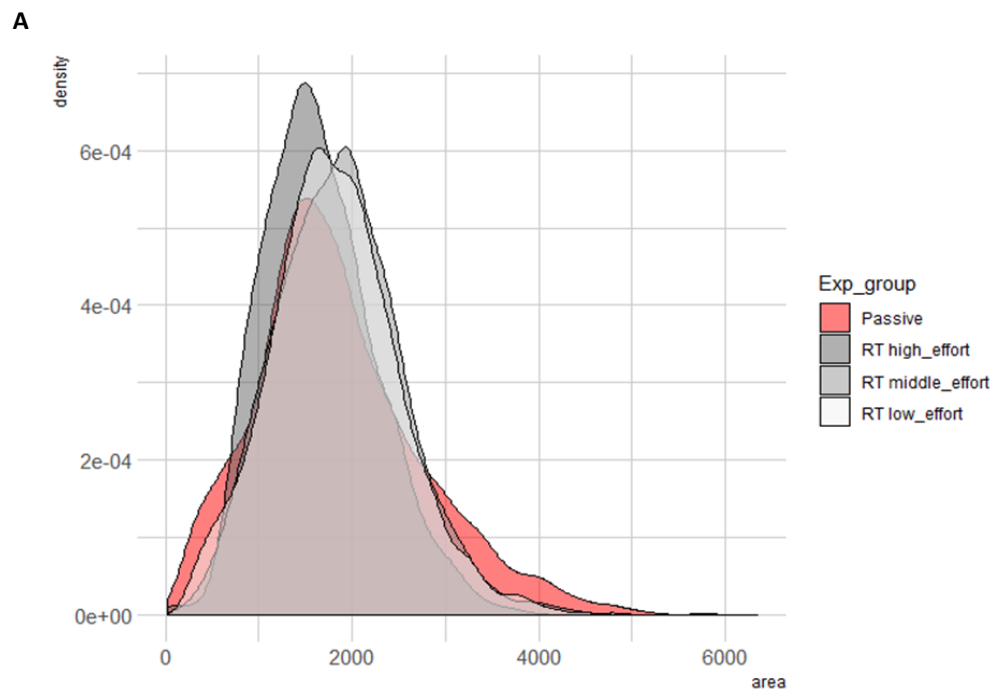
3.3 Histological evidence of diaphragm injury

Cross sectional area (CSA) of diaphragm fibers

A total of 16,734 fibers were analyzed. No difference was found in the amount of analyzed fibers per animal between experimental groups with an average \pm SD of 743 ± 134 in passive, 773 ± 112 in RT low_effort, 766 ± 123 in RT middle_effort and 756 ± 121 in RT high_effort.

Cumulative distributions and density for myofiber CSA were significantly different between groups (Kolmogorov-Smirnov test p -value <0.001), see Figure 20A.

A significant difference was found in the mean CSA when comparing groups (p -value <0.001). The mean diaphragm myofiber CSA for the RT high_effort group ($1,650 \pm 605 \mu\text{m}^2$) was significantly lower than CSA from passive ($1,859 \pm 911 \mu\text{m}^2$; p -value <0.001), RT_middle effort s ($1,864 \pm 683 \mu\text{m}^2$; p -value <0.001) and RT low effort groups ($1,824 \pm 699 \mu\text{m}^2$; p -value <0.001), see Figure 20B.



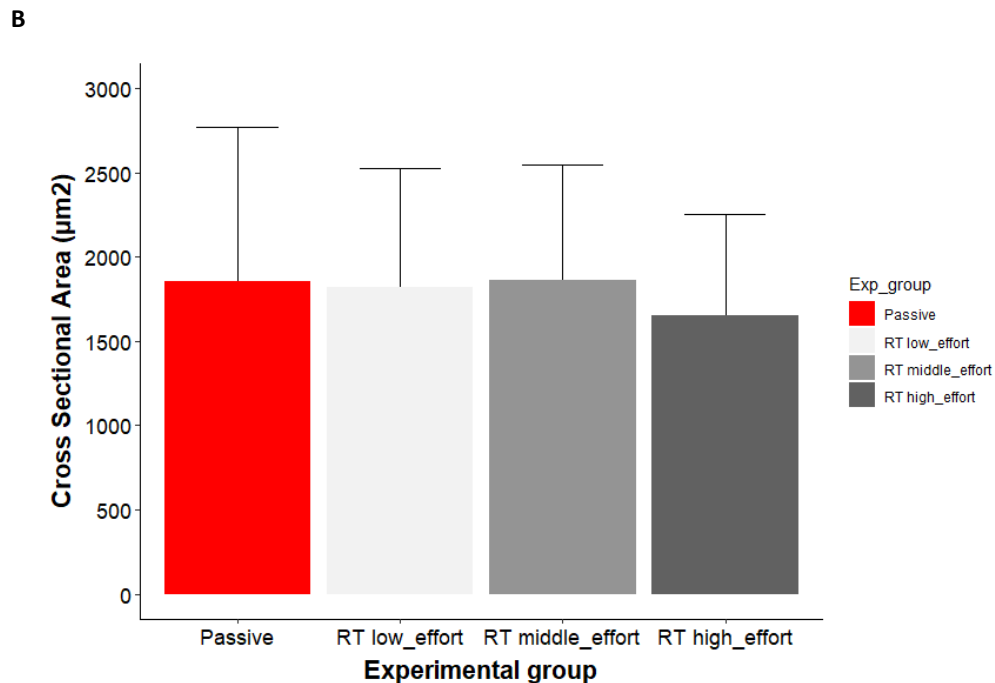
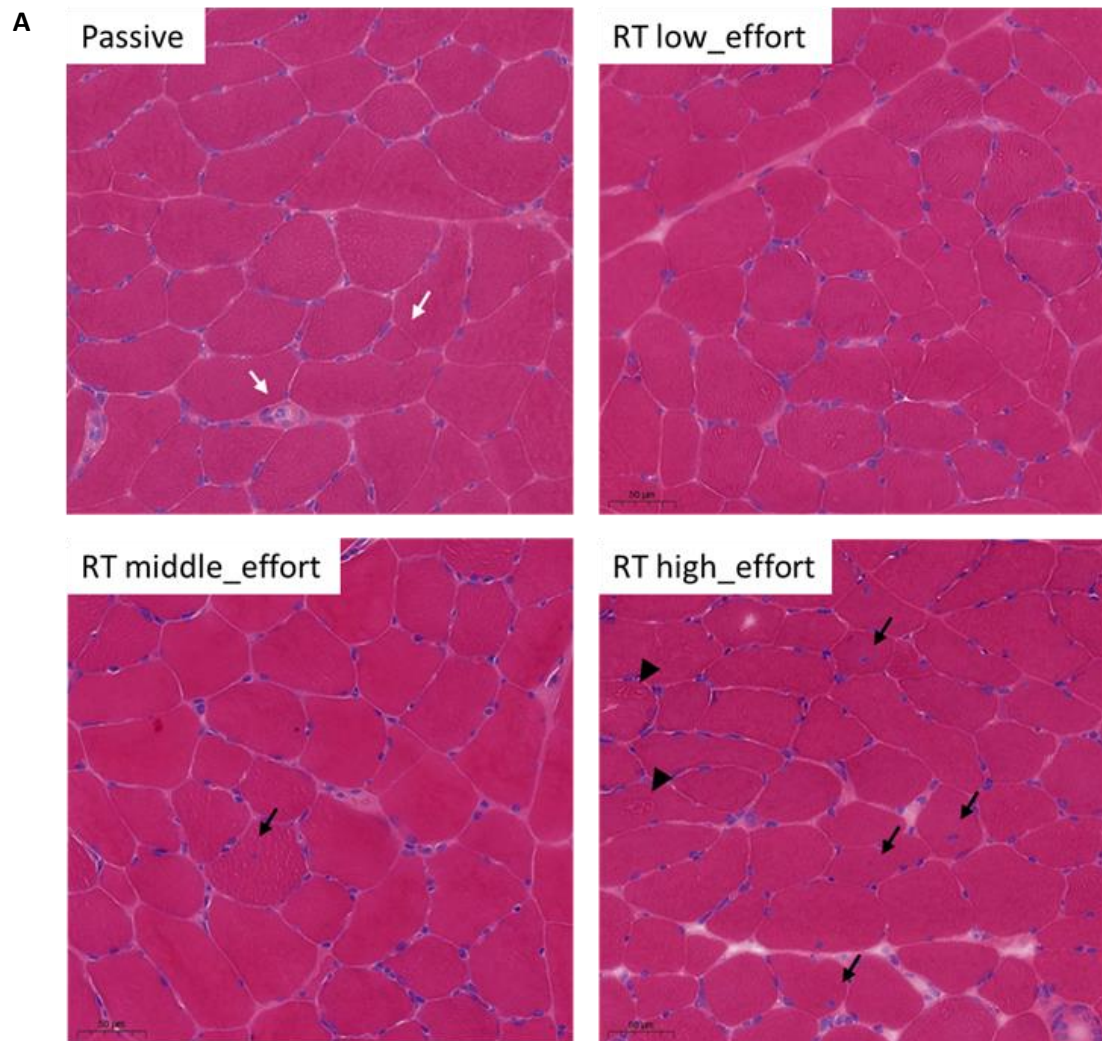


Figure 20. Myofiber cross-sectional area of diaphragm muscle. (A) Cumulative distribution of diaphragm CSA in each group. (B) Average and standard deviation CSA of diaphragm myofibers in each experimental group. Passive (red); RT with high effort (dark grey); RT with middle effort (light grey); RT with low effort (grey)

Abnormal myofibers

Hematoxylin & Eosin staining revealed a variety of abnormalities that were present in both passive and RT groups. No difference was found in the total number of abnormal diaphragm myofibers between groups. When comparing different subcategories of abnormal fibers, the percentage of fibers with abnormal size or shape (smaller size) was significantly higher in the passive group as compared with the RT high_effort group (27.8 versus 14.7%; p -value=0.044). Common observations of abnormal cytoplasm were absent cytoplasm centrally or peripherally; and nonhomogeneous cytoplasm with distinct regions of peripheral basophilia and central or peripheral eosinophilia. The percentage of internally

nucleated myofibers and myofibers with abnormal cytoplasm were not significantly different between groups (Fig 21).



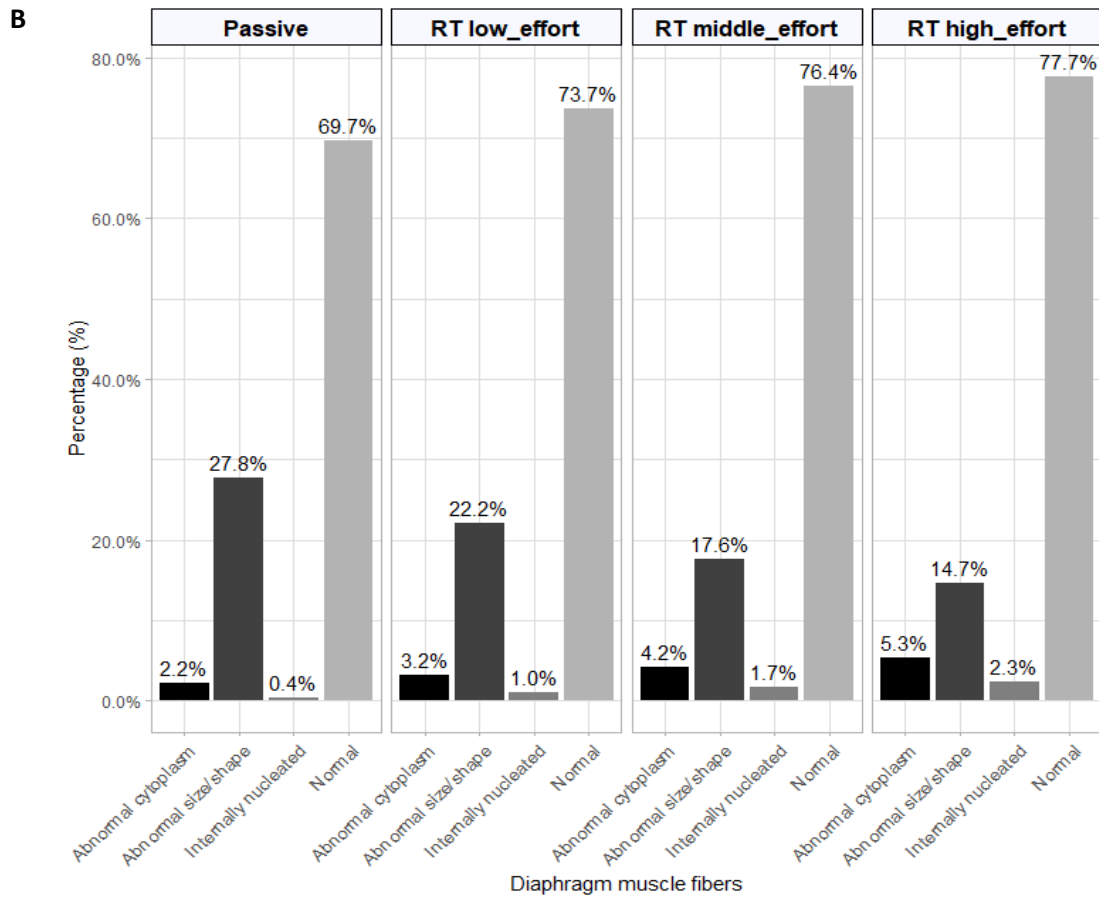


Figure 21. Histologic assessment of diaphragm fibers. (A) Representative images of diaphragm histology for each experimental group (hematoxylin & eosin, scale bar= 50µm). Images from passive group presented cumulative distributions of nucleus and smaller CSA of fibers (white arrows). RT with middle and high effort groups presented internally nucleated fibers (black arrows). RT with high effort group showed abnormal cytoplasm (black arrowheads). (B) Quantitative analysis of the amount of normal and abnormal myofibers.

3.4 Serum samples of skeletal troponin I

Similar to diaphragm force, absolute values of serum troponin I were highly variable at baseline. Therefore, a ratio between troponin I obtained at 3 hours over troponin I obtained

at baseline was calculated. Figure 22 shows the sTnI_3hours/sTnI_baseline ratio in all experimental groups. Although an increase of sTnI was observed after 3 hours in all animals from RT high effort group (ratio>1), no statistically significant difference was found when comparing against other groups (p -value= 0.380), see Figure 22.

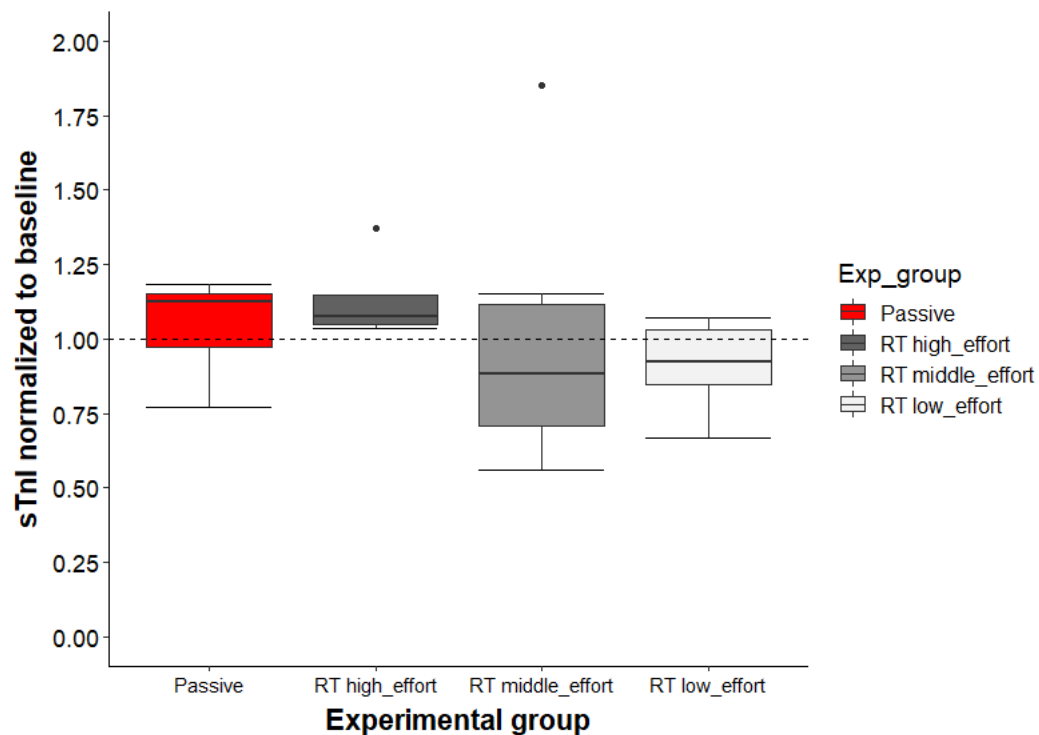


Figure 22. Relative change of Fast skeletal troponin I as a marker of diaphragm injury. Troponin I ratio calculated as serum sTnI obtained at 3 hours over serum sTnI at baseline, in each group. Dashed black line (sTnI ratio of 1) represents no change in sTnI.

DISCUSSION

1. Incidence of reverse triggering

An automatized method to detect reverse triggering based on the airway pressure and the EAdi waveforms proved to be feasible and with a good diagnostic accuracy. Using this method, we found, using the most sensitive threshold, that 44% of patients under assist-control ventilation 24h after intubation had $\geq 10\%$ of their breaths presenting reverse triggering whereas the median rate per patient was 8%, with a wide variability among subjects (range 0.1-75%). This variability could not be explained by patient demographics, cause of intubation, disease severity or depth or type of sedation.

The presence of reverse triggering dyssynchrony in ICU patients was recently reported by Akoumianaki et al ¹⁸ to be present in eight out of eight patients with ARDS studied at time of deep sedation. In the present study, we report the incidence in a larger group of mechanically ventilated patients, all requiring mechanical ventilation and sedation for critical illness. Our study population comprised mostly medical patients including a wide array of admission diagnosis with more than 50% of patients having a pulmonary cause of admission but not necessarily ARDS.

In terms of detection, monitoring P_{eso} or EAdi were used in the original work ¹⁸ whereas other authors have described how flow and airway pressure curves might look in reverse triggered breaths ⁷⁷. To evaluate the incidence in our tracings, we needed to develop an automatic method of detection. The assessment performed by the three reviewers showed a good agreement when using EAdi associated with ventilator waveforms. Given the time consuming task of visually analyzing ventilator waveforms, and also that dyssynchrony might occur in clusters ⁷⁸, dedicated software seems necessary ^{31,66,79}. Our algorithm using Neurosync showed a good sensitivity (0.86) with excellent specificity (0.95) to automatically detect breaths with reverse triggering and allowed us to calculate the incidence of this phenomenon at 24 hours after intubation. The algorithm was further validated by checking

that all breaths labeled with reverse triggering were identified as being mandatory breaths and not patient-triggered breaths.

The high incidence of reverse triggering reported in this study (44% of patients $\geq 10\%$ reverse triggering) suggests that this is a very frequent phenomenon in deeply sedated mechanically ventilated ICU patients. This high frequency of reverse triggering may justify exploring further the potential consequences on the lung and the diaphragm. In a recent study by de Haro et al.⁸⁰ 34% of the breaths with double cycling were caused by this interaction. Goligher et al. showed that 52% of breaths with reverse triggering caused eccentric contractions of the diaphragm⁸¹. Conversely, in our study we did not find an increased double cycling rate in patients with higher reverse triggering rates; likely because many diaphragmatic contractions were not strong enough to trigger the ventilator. Overall, double cycling was uncommon in our cohort (median $<0.5\%$) representing a lower incidence than published reports from patients with ARDS^{82,83}; suggesting that patients enrolled in this study presented with an overall low respiratory drive. An observational study aiming to investigate the relationship between asynchronies and patient-centered outcomes in ARDS or acute respiratory failure is currently ongoing (BEARDS study, NCT03447288) and will hopefully provide more insight about this phenomenon.

In this study, reverse breaths were often associated with a 1:1 entrainment phenomenon, for up to three or more consecutive breaths. The entrainment phenomenon or respiratory phase locking has been previously described in sedated patients as well as in healthy individuals and patients after lung transplantation^{18,22,25}. The mechanisms generating entrainment are poorly understood and could be multiple, including stretching of the slowly adapting receptors and a sustained activation of the vagally mediated Hering–Breuer reflex^{22,25,84}. Graves et al. showed that the temporal relationship between mechanical inflation and patient effort was highly dependent of the ventilator-to-patient neural rate ratio. In that study, only when patients' intrinsic neural rate was close to the ventilator set rate, a stable 1:1 pattern would ensue. In our study, ventilator set rate was lower in patients

presenting with more reverse triggering, which could be explained by a ventilator-to-patient neural rate ratio closer to 1.

Additionally, while most reverse-triggered breaths had an entrainment pattern, others were isolated or irregular without clear entrainment. Modifications in drive with the use of sedation can have dramatic effects on the appearance of respiratory-phase locking²² and different brain states might change the range of ventilator-to-patient neural rate ratios to result in entrainment⁸⁵. But one could question whether reverse triggering without entrainment could represent artifacts or random activity of the patients. Thus, we compared reverse-triggered breaths with or without entrainment. We found similar EAdi amplitude and similar phase angles between these two types of breaths (Table 5), suggesting that these isolated reverse-triggered breaths were still related to the same mechanism.

Many of our patients were deeply sedated at the time of the recording and it seemed that reverse triggering was especially frequent in patients who later resumed spontaneous activity. It is worth to mention that patients with more reverse-triggered breaths who were under a propofol infusion were receiving higher doses than the individuals sedated with propofol who displayed less reverse triggering. Given the nature of our study, we can only speculate whether this was related to clinicians increasing sedative doses to blunt patient drive or to higher doses of sedation enabling the appearance of reverse triggering. In our study, the group of patients with a higher incidence of reverse triggering also presented with more patient-triggered breaths and showed a higher probability of either being ventilated on a partial mode or extubated the day after the initial recording. These data, in line with Graves²², suggest that it may represent the point where patient's drive is starting to recover, and it could be interpreted as a phenomenon susceptible to happen during a transition phase from deep sedation to patient triggered breaths.

This study has important strengths. We created an automatic method to detect reverse triggering with a high sensitivity and tested the model during supported modes and, hence,

present an algorithm with an excellent specificity. Finally, we performed an internal validation of our model confirming the accuracy of the algorithm and we provide the first results on the incidence of this phenomenon.

Detection of reverse triggering based on EAdi is feasible with a good diagnostic accuracy. It is very frequent early after intubation, but the incidence depends on the amplitude of the detected EAdi.

2. Reverse triggering model

Diaphragm dysfunction is highly prevalent in ICU patients and associated with worse outcomes including longer duration of MV. More mechanistic and physiologic studies are needed to understand how different forms of myotrauma affect the diaphragm in ICU patients. Particularly, we were interested in eccentric myotrauma, a type of patient ventilator interaction occurring during reverse triggering and other types of dyssynchrony. Thus, in order to study this phenomenon and its potential consequences on diaphragm muscle, we established an experimental model in which pigs were first subjected to an acute lung injury, and then reverse triggering dyssynchrony (eccentric myotrauma) was induced in a physiologic manner by modifying ventilator settings and level of sedation. Noteworthy, our approach to induce reverse triggering was not only feasible, but consistently reproducible in all animals, although with different presentations.

The creation of RT dyssynchrony on top of an ARDS model was successfully achieved. However, 6 animals assigned to the RT group died before completing the study period mainly due to severe hypoxemia and hypotension. This early mortality may be explained by the injurious effect of breathing efforts on lung injury, especially in severe ARDS.

Different mechanisms could explain how RT may be injurious for the lungs. First, superimposing a spontaneous effort onto a ventilator breath has an additive effect on the distending transpulmonary pressure and therefore on the resulting VT. Second, the

patient's inspiratory effort may persist beyond the end of the machine's breath. Thus, the patient's inspiratory muscles are still active at the beginning of expiration. If deep and long enough, the persistent effort could produce a fall in airway pressure that can lead to breath stacking⁸², which is the occurrence of two consecutive inspirations without an expiration in between, resulting in a greater VT delivered (the sum of the two consecutive tidal volumes). Recent data in ARDS patients showed that breath stacking exhibits tidal volumes of at least 11 ml/kg predicted body weight⁸⁶, almost 2-fold greater than what now is accepted as protective ventilation. Third, during RT breaths a pendelluft phenomena may occur which consist in the exchange of air from one lung region to another without causing a significant change in overall VT. However, since an exchange of air from nondependent to dependent zones occurs, a rapid tissue deformation results in tidal recruitment and local overstretch of the involved dependent region, as well as rapid deflation (followed by reinflation) of the corresponding nondependent region⁸⁷. Yoshida et al. have shown that pendelluft occurs in RT. These authors calculated that exchange of air from nondependent to dependent lung is causing a local overstretch up to 2-fold compared to that observed in the same region during passive controlled ventilation at the same VT⁸⁸. Further studies aiming to understand the impact of RT on lung injury are needed in order to avoid deaths and improve our model.

Induction of RT was mainly achieved by diminishing VT and increasing RR to in pigs that had certain amount of respiratory drive. Interestingly, these "RT settings" are very similar if not identical to what clinicians apply to ventilate ARDS patients in a protective way. Since the lungs of ARDS patients are functionally smaller than normal, and are heterogeneously aerated, mechanical ventilation itself can also aggravate the pre-existing damage, leading to what is known as ventilator induced lung injury, or VILI^{89,90}. To date, all interventions found to improve survival in multicenter trials in ARDS such as lower tidal volumes^{91,92}, prone positioning⁹³, and, most controversially, neuromuscular blockade⁹⁴ are thought to exert their effect by preventing VILI. Lower tidal volumes directly mitigate overdistension of the aerated baby lung, decreasing plasma membrane wounding and rupture, disruption

of cell junctions, and detachment of basement membranes^{95–97}. Lower tidal volumes also attenuate shear strain from spatial mechanical heterogeneity by limiting the magnitude of shear deformation with each inspiratory cycle. Finally, lower tidal volumes may attenuate atelectrauma by decreasing likelihood of tidal recruitment with each inspiratory cycle. Nowadays, due to all its potential benefits, use of low tidal volumes (~6 ml/kg of ideal body weight) is thus considered the ventilatory standard for patients with ARDS. Data from the largest epidemiological study worldwide about ARDS patients including 50 countries, the LUNG SAFE study, has shown that the average tidal volume set is 7.4 ml/kg in patients with moderate and severe ARDS⁶. Here, in our model we modified the tidal volume from 10 ml/kg (passive group) to ~7 ml/kg (RT group) matching almost perfectly the current lung protective ventilation strategy. Interestingly, the first observation about reverse triggering in ARDS patients was described in 2013, thirteen years after the seminal studies about tidal volume reduction, at a time in which an increasing proportion of patients were already being ventilated with low tidal volumes. Whether RT is caused by current lung protective ventilation strategy or is just a marker of severity remains unknown.

In terms of model performance, apart from lower tidal volume and higher RR when comparing with passive ventilation, the RT group did not show differences in respiratory mechanics at baseline nor after 3 hours of experiment. Similarly, CO₂ did not change over time and was not different among groups, a key result since decrease in diaphragmatic function has been associated to high levels of CO₂^{98,99}. In addition, although not statistically significant, higher O₂ and MAP were observed in the RT group. These results are due to increasing aeration of the dependent lung¹⁰⁰, as well as increased lung perfusion¹⁰¹, causing therefore, a reduction on intrapulmonary shunt and improved gas exchange. Also, beside increasing preload, negative pleural swings during spontaneous efforts are transmitted to the pulmonary capillary system¹⁰² reducing right ventricular afterload.

Regarding lung injury, no differences were found between groups on alterations of alveolar capillary barrier, assessed by BAL total protein and Wet to dry ratio. However, despite

having low tidal volume and a more lung protective mechanical ventilation in the RT group, mean values reported in wet to dry ratio were 8.29 for RT and 9.95 for passive, consistent with lung injury in pigs^{75,76}. These results suggest that both passive ventilation with 10ml/kg (known as injurious) and RT with ~7 ml/kg, cause a similar degree of lung injury, probably due to loss of lung protection when breathing efforts are occurring. Further experiments designed to study the impact of RT on lung injury are needed.

In terms of sedation, we did not observe differences between groups in cumulative doses (e.g. propofol and ketamine), nor in sedation depth (BIS index). BIS index values were kept under 60 throughout the experiment suggesting adequate sedation but no deep hypnosis. Unlike the original description of RT where this phenomenon was observed in deeply sedated patients, our model was developed based on the hypothesis that respiratory entrainment tends to occur during a phase of transition between deep and light sedation²². Since causal mechanisms for RT are poorly understood, we could not induce RT in deeply sedated animals (original description in patients) where no inspiratory effort would be detected, and the occurrence of RT would turn unpredictable. In contrast, we modified level of sedation to achieve certain level of respiratory drive (confirmed by decrease in P_{aw} and P_{es} during an expiratory hold) but always reassuring a BIS level below 60 and no movement in response to a toe pinch maneuver.

Reverse triggering is also named as entrainment and this phenomenon occurs in patterns. In the first study including 8 patients, Akoumianaki et al. showed that reverse triggered breaths were characterized by a stable entrainment pattern described as 1:1, 1:2 and 1:3 being 1:1 the most dominant. Conversely, Bourenne et al. observed an unstable entrainment pattern in 3 patients who presented reverse triggered breaths, with 1:2 and 1:3 being the most frequent ones. In our model, reverse triggering resulted in different and variable entrainment patterns as well as different levels of respiratory efforts. In line with the first study, the 1:1 was the most frequent and stable pattern in our study (83%). However, patterns described as 1:4, 3:1 and 2:1 were also observed in 4 out of 18 animals.

The larger variability in entrainment patterns observed in our study may be due to the fact that it was performed in animals, that we studied a larger number of individuals, and that we analyzed a longer period (i.e. 3 h vs 60 min and 6–27 min).

The establishment of this RT model has valuable strengths. To our knowledge, this is the first animal model mimicking RT dyssynchrony observed in clinical ARDS. The high similarity with clinical practice in terms of entrainment variability makes this model even more powerful and attractive. We think this new model constitutes a starting point to better understand RT.

In conclusion, we have established a feasible and reproducible model of RT dyssynchrony in pigs with ARDS, mainly by reducing tidal volume and increasing RR while adjusting sedation to keep certain amount of respiratory drive. RT is rather a complex phenomenon, with several phenotypes characterized by different combinations of entrainment pattern and breathing effort.

3. Impact of RT on function and structure of the diaphragm

After the establishment of our RT model, we evaluated the impact of RT on function and structure of the diaphragm as well as serum troponin I as a biomarker of diaphragmatic injury. For this analysis, animals with RT were divided as previously planned in 3 subgroups according to the level of breathing effort.

The central findings of this analysis are that presence of RT dyssynchrony affects diaphragm function in different ways depending on the level of breathing effort. Animals with RT and high breathing effort exhibit decreased diaphragm force whereas animals with RT and low breathing effort increase diaphragmatic force, as compared with animals with passive ventilation. We also found that animals with RT and high breathing effort had a lower cross-sectional area of diaphragm myofibers as well as smaller amount of atrophic fibers as

compared to passive group, however, no significant differences were found in troponin I between experimental groups.

The magnitude of decrease or increase in force was dependent on the stimulation frequency (F/F curve) and also on the experimental time assessed (P_{diTw}). These results suggest that RT dyssynchrony may have two opposite effects on diaphragm function depending on the breathing effort developed during RT breaths, and therefore a careful assessment and interpretation should be done when RT is observed.

The importance of breathing effort on diaphragm function/structure as well as on outcomes has been directly and indirectly demonstrated in clinical and experimental studies. Goligher et al. prospectively included 191 ventilated patients to assess whether changes in the thickness of the diaphragm, as assessed by ultrasound, were associated with adverse outcomes, including prolonged mechanical ventilation, reintubation, and death. Among patients, 44% had >10% decrease in thickness whilst 24% had an increase in diaphragm thickness during the first 3 days of mechanical ventilation. The authors also demonstrated that the change in diaphragm thickness varied with the level of breathing effort as assessed by muscle-thickening fraction or diaphragm electrical activity¹⁰³. High levels of thickening fraction (high inspiratory effort) were associated with an unexpected rapid rise in diaphragm thickness during mechanical ventilation. This increase in thickness was associated with impaired diaphragm function and prolonged mechanical ventilation. Similarly, we observed in our study that force generating capacity was significantly lower at 3 h in those animals with high breathing effort (10% lower in P_{di} ratio and 34% lower in P_{diTw}) as compared with baseline. These changes in force were not observed in animals which presented middle or low effort, nor in animals with passive ventilation (no breathing effort).

Different studies support the idea that high breathing efforts may induce diaphragm muscle fiber injury, resulting in an inflammatory response and fiber swelling. In experimental studies, resistive loading imposed on breathing has been shown to induce diaphragm injury

characterized by susceptibility of myofibrillar complexes to calpain-mediated degradation, fiber necrosis and profound influx of inflammatory cells^{45–47}. Load-induced diaphragmatic injury has also been demonstrated in humans. Orozco-Levi et al. studied 18 patients with COPD and 11 healthy subjects showing that inspiratory loading can generate sarcomere disruption in the diaphragm⁴⁸. Hooijman et al. demonstrated elevated number of inflammatory cells in diaphragm fibers of critically ill non-septic patients, suggesting that this does not reflect systemic inflammation but rather a local inflammatory response, possibly elicited by diaphragm injury¹⁰⁴.

The evidence described above is clear in supporting the deleterious effects of high breathing effort on diaphragm function and structure. However, there is almost no evidence supporting that patient-ventilator dyssynchrony can contribute to diaphragm injury, and only general approaches have been done to explore this hypothesis. Shimatani et al. studied the impact of different MV strategies including controlled MV, pressure support and NAVA on diaphragm injury. In this study, several types of dyssynchronies were measured in order to calculate the asynchrony index (number of asynchronous events over total analyzed breaths). The authors found a strong correlation between the asynchrony index and sarcomere disruptions (coefficient 0.834, $p < 0.001$)¹⁰⁵. To our knowledge, our study constitutes the first experimental evidence showing that a specific type of dyssynchrony (reverse triggering) may affect diaphragm function.

In reverse triggering, because the diaphragm is contracting as it lengthens (i.e., eccentric loading), muscle injury may result. Eccentric loading has shown to be more injurious compared to concentric loading¹⁰⁶. Acute weakness of the diaphragm because of eccentric loading has been demonstrated experimentally. Gea et al. found that diaphragmatic capacity to generate pressure decreased 67% immediately after the induction of eccentric contractions. Interestingly, these results persisted until 12 hours after induction of eccentric contraction and were associated with sarcomere muscle injury⁵³. In our study, the

combination of RT and high inspiratory effort was associated to impaired diaphragmatic function. However, whether RT per se may cause this effect is unknown.

Quantitative histologic analysis of CSA of diaphragm muscle fibers showed that animals with RT and high breathing effort had lower CSA than animals from passive group, and the animals from the groups RT with middle or low breathing effort. Since positive relationships between muscle force production and CSA have been shown, and since muscle CSA has been proposed as a major predictor of force production¹⁰⁷, the impaired diaphragm function found in animals with RT and high breathing effort might be explained by their lower CSA. Nonetheless, other studies examining force and CSA have reported inconsistent findings, suggesting that other factors such as type of muscle fiber, neural adaptation, fascicle length and pennation angles, may be important in the force generating process^{108,109}. Although not assessed in this study, changes in specific types of muscle fiber might also explain our results. In comparison with Type I slow twitch fibers, Type II fast twitch fibers have greater size and produce greater force. Whether RT with high effort caused a specific reduction in the amount of type II fibers is unknown.

Injurious effect of over assistance myotrauma (null or very low breathing effort) has also been well documented. A landmark study conducted in brain-dead organ donors demonstrated marked diaphragm atrophy after 18-69 h of controlled mechanical ventilation⁴¹ and this effect was related to the duration of MV¹¹⁰. Diaphragm inactivity triggers proteolytic pathways that result in myofibrillar atrophy and mitochondrial dysfunction leading to contractile dysfunction¹¹¹. In our study, the passive group showed no differences in force generating capacity of the diaphragm over time, however, the duration of our experiment (3h) might be not long enough to find differences in diaphragm function. Despite no changes in diaphragm function and total amount of abnormal fibers between groups, histologic analysis of different subcategories showed an increased percentage of fibers with abnormal size and shape (small size) in the passive group as compared with RT groups, confirming that inactivity may be detrimental for the muscle.

In contrary, animals which presented RT and low breathing effort showed a significant increase in diaphragm force after 3 hours, suggesting that certain level of diaphragm activity even in a dyssynchronous manner may be protective. Both experimental and clinical studies suggest that atrophy can be mitigated by maintaining some level of inspiratory effort during mechanical ventilation^{35,112}. For instance, adaptive support ventilation targeting a low-normal level of work of breathing successfully prevented diaphragm atrophy and weakness as compared with controlled mechanical ventilation in a porcine model¹¹². Sassoon et al. also reported attenuation of diaphragmatic muscle force loss in rabbits maintained on assist controlled ventilation¹¹³. Alternatively but similarly, phrenic stimulation has also shown decreased diaphragm atrophy, and it seems that relatively low levels of muscle activity are sufficient to prevent mitochondrial dysfunction^{114,115}. In the same line, histologic analysis of abnormal fibers in our study showed a decreasing trend in the amount of atrophic diaphragm fibers while breathing effort was increasing (27.8 % in passive and 14.7% in RT with high effort), supporting the idea that some level of effort is needed to prevent muscle atrophy.

Also, apart from some level of breathing effort, specific features of reverse triggered breaths (eccentric muscle contractions) might be interacting on strength gaining. For example, the metabolic demand of generating force during eccentric activity is greatly reduced compared to generation of similar force during muscle shortening (concentric contractions)¹¹⁶. Moreover, for the same velocity of contraction, muscle force generation in eccentric contractions can be up to 20-40% greater than concentric muscle activity¹¹⁷. Taken together, it seems that the presence of RT (eccentric activity) with some level of effort might be favorable for the diaphragm in ventilated patients. In addition, results from the clinical study about the incidence of RT (first objective of this thesis) showed that the group of patients with a higher incidence of reverse-triggering also presented with more patient-triggered breaths and showed a higher probability of either being ventilated on a partial mode or extubated the day after the initial recording. Interestingly, the median (IQR) peak EAdi of these patients was 1.7 μ V (0.8 to 4.3), a rather low effort, favoring a potential

protective role of this type of RT. Further clinical studies are needed to determine whether RT with low breathing effort may impact clinical outcomes.

Despite differences in force, in terms of CSA we observed no differences in fiber size between animals with RT and low effort and those from the passive group. The experimental time might have been insufficient to disclose structural changes. Other explanation may be that the pattern of muscle growth induced by eccentric loading has been shown substantially different from that induced by concentric loading^{117,118}. Eccentric contractions have shown to promote muscle growth through addition of sarcomeres in series, while concentric contraction training seems to mainly promote addition of sarcomeres in parallel^{119,120}. Thus, it is possible that the eccentric activity exerted by reverse triggering may not result in higher CSA.

The importance of inspiratory effort has been widely demonstrated and its mediating role in the relationship between ventilator settings and changes in the diaphragm has been recently proven¹¹. The existing evidence along with our results, suggest that maintaining a safe level of inspiratory effort could be a promising strategy to protect the diaphragm from myotrauma.

Is there an optimal breathing effort? It seems reasonable that the optimal level of respiratory muscle effort might be that of healthy individuals breathing at rest, equivalent to a respiratory muscle pressure swing of 5–10 cmH₂O and PTP_{min} of 50–150 cmH₂O*s/min^{8,16,121–123}. Although no reference values are known for pigs, animals in our study from low effort group had a mean PTP_{min} of 85±42 cmH₂O*s/min, supporting the idea that certain amount but not excessive level of breathing effort, is ideally required. Other values such as diaphragm electrical activity of 8% of maximum value¹²⁴ and inspiratory thickening fraction >40% may also have a role in preventing myotrauma¹⁰³.

Regarding the effect of RT on serum skeletal troponin I, our study did not show any difference between experimental groups when sTnI ratio (sTnI at 3 hours/ sTnI baseline) was compared. Individual data was highly variable showing both increases and decreases

of sTnI at 3 hours in comparison with baseline value. In contrast, Foster et al. showed significant increases in sTnI about 24% at 1 hour and 27% after 3 days of a single 60 min bout of inspiratory threshold loading using ~70% of maximal inspiratory pressure⁵⁹. Several factors including different species, training load and type of contraction (eccentric vs concentric) may explain these different results.

4. Conclusion, limitations and future projections

In this thesis we have developed an automatized method to detect reverse triggering dyssynchrony based on the airway pressure and the EAdi waveforms with a good diagnostic accuracy. In addition, using this method, we found that RT dyssynchrony is a very frequent phenomenon occurring in most patients regardless of their diagnosis. We demonstrated that 24h after intubation 44% of patients under assist-control ventilation had $\geq 10\%$ of their breaths presenting reverse triggering, whereas the median rate per patient was 8%, with a wide variability among subjects. We also observed that the group of patients with a higher incidence of reverse-triggering also presented with more patient-triggered breaths and showed a higher probability of either being ventilated on a partial mode, or extubated, the day after the initial recording, suggesting that RT may constitute a phenomenon characteristic of the transition from deep sedation to awakening, in which the respiratory center is preparing to regain its function.

In order to study the effects of RT we developed a large animal model. First, we reproduced a porcine animal model of severe ARDS and we succeeded to induce reverse triggering by modifying ventilator settings and level of sedation to a more protective ventilation strategy with low tidal volume and high RR. The ARDS model mimics the essential characteristics of the pathology, including the presence of severe hypoxemia that is non-responsive to oxygen therapy alone, abnormal pulmonary mechanics with a decrease in respiratory system compliance. On the other hand, RT was characterized by a variety of entrainment patterns and different levels of breathing effort evidencing its complexity but at the same

time simulating a real clinical scenario. To our knowledge this is the first animal model of reverse triggering dyssynchrony.

In addition, we have provided advanced insights in the knowledge regarding the potential effect of RT on diaphragm function and structure, and therefore eccentric myotrauma. In our study, assessment of diaphragm function revealed an increase in force generation capacity of the diaphragm in those animals who had low breathing effort associated to reverse triggered breaths whereas in contrast, a decrease in diaphragm force was observed in animals which presented high levels of breathing effort. This result was also accompanied by a lower myofiber CSA and lower amount of small size myofibers as compared with passive group. Taken together, these results support the idea that the level of breathing effort is crucial in the eccentric myotrauma development.

This thesis has limitations. Our clinical study corresponds to a single center study and we only assessed one-hour recording at 24 hours. Second, we assessed diaphragm electromyography with a NAVA catheter that uses a filtered EMG instead of the raw signal. This may delay the apparent EAdi onset and result in misleading classification. The latter forced us to create an additional step in our algorithm, which assessed the presence of an airway drop to detect patient-triggered breaths and avoid false positives. Third, we arbitrarily divided the cohort into two groups based on the median rate since the rather small number of subjects precluded a multiple regression analysis.

The creation of a RT model and the evaluation of its impact on diaphragm structure and function also has limitations. First, we were unable to control some specific characteristics inherent to RT, such as magnitude of contraction, starting delay and entrainment pattern (1:1 or 1:2, etc.), which reinforces the complexity of this phenomenon. It would have been desirable to obtain a more consistent and stable pattern of RT but with our current understanding of this phenomenon we were unable to control these variables. Second, the number of animals per group was small, making extrapolations to larger populations difficult and potentially masking down possible differences between groups. Nonetheless,

we were able to observe important differences in force generating capacity between groups. Third, the duration of our experiment was perhaps too short to observe the full development of diaphragm dysfunction. Fourth, we arbitrarily decided to divide the RT group in terciles based on the level of breathing effort during reverse triggered breaths since no reference values have been reported in pigs. Finally, we are not totally certain whether the results observed in diaphragm function are due to RT or level of breathing effort since we did not include a control group with synchronous ventilation. Notwithstanding, comparison between specific breathing effort ranges would have required the same level of breathing effort to isolate the RT effect, an impossible fact due to animal variability.

To conclude, it is encouraging that from this thesis further research might emerge. Since we have demonstrated that RT constitutes a frequent phenomenon in ICU patients, additional studies should confirm this and also assess potential association with outcomes. In fact, an observational study aiming to investigate the relationship between asynchronies and patient-centered outcomes in ARDS or acute respiratory failure is currently ongoing (BEARDS study, NCT03447288) and will hopefully provide more insight about this phenomenon. In addition, studies exploring potential lung and diaphragm consequences in patients should be conducted. As far as I am concerned, The MYOTRAUMA study (NCT03108118), is currently ongoing and will be the first clinical study exploring dyssynchronies and diaphragm injury.

The creation of our RT model will provide a new opportunity to evaluate more details about eccentric myotrauma including involved cellular pathways. Additionally, careful experiments using this model may also help to understand potential mechanisms of respiratory entrainment. Finally, since RT is associated to different phenomena such as pendelluft, double cycling, or high lung stretch due to superimposed pressure, the presence of RT might be injurious for the lung. Our model may be used to determine the effect of RT on lung injury.

ABBREVIATIONS

ARDS: Acute respiratory distress syndrome

ANOVA: Analysis of Variance

ARF: Acute respiratory failure

APACHE II: Acute Physiology and Chronic Health Evaluation II

BIS: Bispectral index

BAL: Bronchoalveolar lavage

BMI: Body mass index

COPD: Chronic Obstructive Pulmonary Disease

CSA: Cross Sectional Area

C_{rs} : Respiratory system compliance

DP: Driving pressure

EAdi: Electrical activity of the diaphragm

ERS: Elastance of the respiratory system

ECG: Electrocardiogram

EtCO₂: End tidal CO₂

FiO₂: Fraction of inspired oxygen

fsTnI: Fast skeletal troponin I

F/F curve: Force frequency curve

HR: Heart rate

ICU: Intensive care unit

IQR: Inter quartile range

IBW: Ideal body weight

IRL: Inspiratory resistive loading

MAP: Mean arterial pressure

MV: Mechanical ventilation

MIP: Maximal inspiratory pressure

NMBA: Neuromuscular blockade

NAVA: Neurally adjusted ventilatory assist

NEX: Distance from the bridge of the Nose to the Earlobe and then to the Xiphoid process

NPV: Negative predictive value

PVD: Patient- Ventilator dyssynchrony

PaCO₂: Arterial pressure of carbon dioxide

PO₂: Partial pressure of oxygen

P_{res}: Resistive pressure

P_{el}: Elastic pressure

PEEP: Positive end expiratory pressure

P_{vent}: Ventilator pressure

P_{mus}: Muscle pressure

P_{aw}: Airway pressure

P_{ga}: Gastric pressure

P_{plat}: Plateau pressure

P_{pl}: Pleural pressure

P_{peak}: Peak pressure

P_L : Transpulmonary pressure

P_{eso} : Esophageal pressure

P_{di} : Transdiaphragmatic pressure

PTP: Pressure time product

PTP_{min} : Pressure time product in a minute

P_{diTw} : Twitch transdiaphragmatic pressure

PPV: Positive predictive value

RT: Reverse triggering

RR: Respiratory Rate

ROS: reactive oxygen species

SAS: Riker Sedation-Agitation Scale

sTnI: Skeletal troponin I

SD: standard deviation

T_{tot} : Total duration of a mechanical ventilation cycle

VT: Tidal Volume

VIDD: Ventilator Induced Diaphragm Dysfunction

VILI: Ventilator Induced Lung Injury

REFERENCES

1. Wunsch H, Linde-Zwirble WT, Angus DC, Hartman ME, Milbrandt EB, Kahn JM. The epidemiology of mechanical ventilation use in the United States. *Crit Care Med*. 2010;38(10):1947-1953. doi:10.1097/CCM.0b013e3181ef4460.
2. Retamal J, Castillo J, Bugedo G, Bruhn A. Encuesta sobre humidificación de la vía aérea en unidades de cuidados intensivos de adultos de Chile. 2012:1425-1430.
3. Pham T, Brochard LJ, Slutsky AS. Mechanical Ventilation: State of the Art. *Mayo Clin Proc*. 2017;92(9):1382-1400. doi:10.1016/j.mayocp.2017.05.004.
4. Definition TB. Acute Respiratory Distress Syndrome. *Jama*. 2012;307(23). doi:10.1001/jama.2012.5669.
5. Herridge MS, Tansey CM, Matté A, et al. Functional Disability 5 Years after Acute Respiratory Distress Syndrome. *N Engl J Med*. 2011;364(14):1293-1304. doi:10.1056/NEJMoa1011802.
6. Bellani G, Laffey JG, Pham T, et al. Epidemiology, Patterns of Care, and Mortality for Patients With Acute Respiratory Distress Syndrome in Intensive Care Units in 50 Countries. *Jama*. 2016;315(8):788-. doi:10.1001/jama.2016.0291.
7. Yoshida T, Brochard L. Ten tips to facilitate understanding and clinical use of esophageal pressure manometry. *Intensive Care Med*. 2017;1-3. doi:10.1007/s00134-017-4906-x.
8. Mauri T, Yoshida T, Bellani G, et al. Esophageal and transpulmonary pressure in the clinical setting: meaning, usefulness and perspectives. *Intensive Care Med*. 2016;42(9):1360-1373. doi:10.1007/s00134-016-4400-x.
9. Vaporidi K, Akoumianaki E, Telias I, Goligher EC, Brochard L, Georgopoulos D. Respiratory drive in critically ill patients pathophysiology and clinical implications. *Am J Respir Crit Care Med*. 2020;201(1):20-32. doi:10.1164/rccm.201903-0596SO.
10. Brochard L, Slutsky A, Pesenti A. Mechanical ventilation to minimize progression of lung injury in acute respiratory failure. *Am J Respir Crit Care Med*. 2017;195(4):438-442. doi:10.1164/rccm.201605-1081CP.
11. Goligher EC, Brochard LJ, Reid WD, et al. Diaphragmatic myotrauma: a mediator of prolonged ventilation and poor patient outcomes in acute respiratory failure. *Lancet Respir Med*. 2018;2600(18):1-9. doi:10.1016/S2213-2600(18)30366-7.
12. Goligher EC, Dres M, Fan E, et al. Mechanical Ventilation-induced Diaphragm Atrophy Strongly Impacts Clinical Outcomes. *Am J Respir Crit Care Med*. 2017;(August):rccm.201703-0536OC. doi:10.1164/rccm.201703-0536OC.
13. Telias I, Damiani F, Brochard L. The airway occlusion pressure (P 0.1) to monitor respiratory drive during mechanical ventilation: increasing awareness of a not-so-new problem. *Intensive Care Med*. 2018;44(9):1532-1535. doi:10.1007/s00134-018-5045-8.
14. Mancebo J, Isabey D, Lorino H, Lofaso F, Lemaire F, Brochard L. Comparative effects of

- pressure support ventilation and intermittent positive pressure breathing (IPPB) in non-intubated healthy subjects. *Eur Respir J*. 1995;8(11):1901-1909. doi:10.1183/09031936.95.08111901.
15. Field S, Sanci S, Grassino A. Respiratory muscle oxygen consumption estimated by the diaphragm pressure-time index. *J Appl Physiol Respir Environ Exerc Physiol*. 1984;57(1):44-51. doi:10.1152/jappl.1984.57.1.44.
 16. Brochard L, Martin GS, Blanch L, et al. Clinical review: Respiratory monitoring in the ICU - a consensus of 16. *Crit Care*. 2012;16(2). doi:10.1186/cc11146.
 17. Collett PW, Perry C, Engel L a. Pressure-time product, flow, and oxygen cost of resistive breathing in humans. *J Appl Physiol*. 1985;58(4):1263-1272.
 18. Akoumianaki E, Lyazidi A, Rey N, et al. Mechanical ventilation-induced reverse-triggered breaths: A frequently unrecognized form of neuromechanical coupling. *Chest*. 2013;143(4):927-938. doi:10.1378/chest.12-1817.
 19. Rolland-Debord C, Bureau C, Poitou T, et al. Prevalence and Prognosis Impact of Patient–Ventilator Asynchrony in Early Phase of Weaning According to Two Detection Methods. *Anesthesiology*. 2017;(Xxx):1. doi:10.1097/ALN.0000000000001886.
 20. Bourenne J, Guervilly C, Mechat M, et al. Variability of reverse triggering in deeply sedated ARDS patients. *Intensive Care Med*. 2019;45(5):725-726. doi:10.1007/s00134-018-5500-6.
 21. D G. Effects of Mechanical ventilation on control of breathing . In: Tobin MJ, ed. *Principles and Practice of Mechanical Ventilation* . New. ; 2006:715-728.
 22. Graves C, Glass L, Laporta D, Meloche R, Grassino A. Respiratory phase locking during mechanical ventilation in anesthetized human subjects. *Am J Physiol*. 1986;250(5 Pt 2):R902-R909. <http://www.ncbi.nlm.nih.gov/pubmed/3706575>.
 23. Petrillo GA, Glass L, Trippenbach T. Phase locking of the respiratory rhythm in cats to a mechanical ventilator. *Can J Physiol Pharmacol*. 1983;61(6):599-607. http://www.ncbi.nlm.nih.gov/entrez/query.fcgi?cmd=Retrieve&db=PubMed&dopt=Citation&list_uids=6576843.
 24. Vibert J, Caille D, Segundo JP. Respiratory Oscillator Entrainment by Periodic Vagal Afferentes: An Experimental Test of a Model. *Biol Cybern*. 1981;41:119-130.
 25. Simon PM, Habel AM, Daubenspeck JA, Leiter JC. Vagal feedback in the entrainment of respiration to mechanical ventilation in sleeping humans. *J Appl Physiol*. 2000;89(2):760-769. <http://hinarilogin.research4life.org/uniquesigap.physiology.org/uniquesig0/content/89/2/760.abstract>.
 26. Delisle S, Charbonney E, Albert M, et al. Patient–Ventilator Asynchrony due to Reverse Triggering Occurring in Brain-Dead Patients: Clinical Implications and Physiological Meaning. *Am J Respir Crit Care Med*. 2016;194(9):1166-1168. doi:10.1164/rccm.201603-0483LE.
 27. Mitrouska I, Bshouty Z, Younes M, Georgopoulos D. Effects of pulmonary and intercostal denervation on the response of breathing frequency to varying inspiratory flow. *Eur Respir*

- J. 1998;11(4):895-900. doi:10.1183/09031936.98.11040895.
28. Shannon R. Reflexes from Respiratory Muscles and Costovertebral Joints. *Handb Physiol.* 1986;341-447. doi:10.1002/cphy.cp030213.
 29. Dres M, Rittayamai N, Brochard L. Monitoring patient-ventilator asynchrony. *Curr Opin Crit Care.* 2016;22(3):246-253. doi:10.1097/MCC.0000000000000307.
 30. Chao DC, Scheinhorn DJ, Stearn-Hassenpflug M. Patient-ventilator trigger asynchrony in prolonged mechanical ventilation. *Chest.* 1997;112(6):1592-1599. doi:10.1378/chest.112.6.1592.
 31. Blanch L, Sales B, Montanya J, et al. Validation of the Better Care?? system to detect ineffective efforts during expiration in mechanically ventilated patients: A pilot study. *Intensive Care Med.* 2012;38(5):772-780. doi:10.1007/s00134-012-2493-4.
 32. Dres M, Goligher EC, Heunks LMA, Brochard LJ. Critical illness-associated diaphragm weakness. *Intensive Care Med.* 2017;43(10):1441-1452. doi:10.1007/s00134-017-4928-4.
 33. Demoule A, Jung B, Prodanovic H, et al. Diaphragm Dysfunction on Admission to the Intensive Care Unit. Prevalence, Risk Factors, and Prognostic Impact—A Prospective Study. *Am J Respir Crit Care Med.* 2013;188(2):213-219. doi:10.1164/rccm.201209-1668OC.
 34. Jung B, Moury PH, Mahul M, et al. Diaphragmatic dysfunction in patients with ICU-acquired weakness and its impact on extubation failure. *Intensive Care Med.* 2016;42(5):853-861. doi:10.1007/s00134-015-4125-2.
 35. Goligher EC, Fan E, Herridge MS, et al. Evolution of diaphragm thickness during mechanical ventilation: Impact of inspiratory effort. *Am J Respir Crit Care Med.* 2015;192(9):1080-1088. doi:10.1164/rccm.201503-0620OC.
 36. Supinski GS, Ann Callahan L. Diaphragm weakness in mechanically ventilated critically ill patients. *Crit Care.* 2013;17(3):R120. doi:10.1186/cc12792.
 37. Medrinal C, Prieur G, Frenoy É, et al. Respiratory weakness after mechanical ventilation is associated with one-year mortality - a prospective study. *Crit Care.* 2016;20(1):231. doi:10.1186/s13054-016-1418-y.
 38. Powers SK, Shanely RA, Coombes JS, et al. Mechanical ventilation results in progressive contractile dysfunction in the diaphragm. *J Appl Physiol.* 2002;92:1851-1858. doi:10.1152/japplphysiol.00881.2001.
 39. Knisely AS, Leal SM, Singer DB. Abnormalities of in neonates with diaphragmatic muscle ventilated lungs. 1988.
 40. Hussain SNA, Cornachione AS, Guichon C, et al. Prolonged controlled mechanical ventilation in humans triggers myofibrillar contractile dysfunction and myofilament protein loss in the diaphragm. *Thorax.* 2016;71(5):436-445. doi:10.1136/thoraxjnl-2015-207559.
 41. Levine S, Nguyen T, Taylor N, et al. Rapid Disuse Atrophy of Diaphragm Fibers in Mechanically Ventilated Humans. *N Engl J Med.* 2008;358(13):1327-1335. doi:10.1056/NEJMoa070447.

42. Hermans G, Agten A, Testelmans D, Decramer M, Gayan-Ramirez G. Increased duration of mechanical ventilation is associated with decreased diaphragmatic force: a prospective observational study. *Crit Care*. 2010;14(4):R127. doi:10.1186/cc9094.
43. Shaw I, Mills G, Turnbull D. The effect of propofol on airway pressures generated by magnetic stimulation of the phrenic nerves. *Intensive Care Med*. 2002;28(7):891-897. doi:10.1007/s00134-002-1347-x.
44. Powers SK, Wiggs MP, Sollanek KJ, Smuder AJ. Ventilator-induced diaphragm dysfunction: cause and effect. *AJP Regul Integr Comp Physiol*. 2013;305(5):R464-R477. doi:10.1152/ajpregu.00231.2013.
45. Reid WD, Belcastro AN. Time course of diaphragm injury and calpain activity during resistive loading. *Am J Respir Crit Care Med*. 2000;162(5):1801-1806. doi:10.1164/ajrccm.162.5.9906033.
46. Reid WD, Belcastro AN. Chronic resistive loading induces diaphragm injury and ventilatory failure in the hamster. *Respir Physiol*. 1999;118(2-3):203-218. doi:10.1016/S0034-5687(99)00089-4.
47. JIANG T-X, REID WD, BELCASTRO A, ROAD JD. Load Dependence of Secondary Diaphragm Inflammation and Injury after Acute Inspiratory Loading. *Am J Respir Crit Care Med*. 1998;157(1):230-236. doi:10.1164/ajrccm.157.1.9702051.
48. Orozco-levi M, Lloreta J, Minguella J, Serrano S, Broquetas JM. Injury of the Human Diaphragm Associated with. *Crit Care Med*. 2001;(Imim). doi:10.1164/rccm.2011150.
49. Douglas J, Pearson S, Ross A, McGuigan M. Eccentric Exercise: Physiological Characteristics and Acute Responses. *Sport Med*. 2017;47(4):663-675. doi:10.1007/s40279-016-0624-8.
50. Faulkner JA. Terminology for contractions of muscles during shortening, while isometric, and during lengthening. *J Appl Physiol*. 2003;95(2):455-459. doi:10.1152/japplphysiol.00280.2003.
51. Dueweke JJ, Awan TM, Mendias CL. Article Title: Regeneration of Skeletal Muscle Following Eccentric Injury Regeneration of skeletal muscle following eccentric injury. *Mendias CL J Sport Rehabil*. 2016. doi:10.1123/jsr.2016-0107.
52. Lieber RL, Shah S, Fridén J. Cytoskeletal disruption after eccentric contraction-induced muscle injury. *Clin Orthop Relat Res*. 2002;(403):S90-S99. doi:10.1097/01.blo.0000031310.06353.9f.
53. Gea J, Zhu E, Gáldiz JB, et al. Consecuencias de las contracciones excéntricas del diafragma sobre su función. *Arch Bronconeumol*. 2009;45(2):68-74. doi:10.1016/j.arbres.2008.04.003.
54. Pellegrini M, Hedenstierna G, Roneus A, Segelsjö M, Larsson A, Perchiazzi G. The diaphragm acts as a brake during expiration to prevent lung collapse. *Am J Respir Crit Care Med*. 2017;195(12):1608-1616. doi:10.1164/rccm.201605-0992OC.
55. Ebihara S, Hussain SNA, Danialou G, Cho WK, Gottfried SB, Petrof BJ. Mechanical ventilation protects against diaphragm injury in sepsis: Interaction of oxidative and mechanical stresses.

- Am J Respir Crit Care Med.* 2002;165(2):221-228. doi:10.1164/rccm.2108041.
56. Laghi F, Tobin MJ. Disorders of the respiratory muscles. *Am J Respir Crit Care Med.* 2003;168(1):10-48. doi:10.1164/rccm.2206020.
 57. Lindqvist J, Van Den Berg M, Van Der Pijl R, et al. Positive end-expiratory pressure ventilation induces longitudinal atrophy in diaphragm fibers. *Am J Respir Crit Care Med.* 2018;198(4):472-485. doi:10.1164/rccm.201709-1917OC.
 58. Simpson JA, Van Eyk J, Iscoe S. Respiratory muscle injury, fatigue and serum skeletal troponin I in rat. *J Physiol.* 2004;554(3):891-903. doi:10.1113/jphysiol.2003.051318.
 59. Foster GE, Nakano J, Sheel AW, Simpson JA, Road JD, Reid WD. Serum skeletal troponin I following inspiratory threshold loading in healthy young and middle-aged men. *Eur J Appl Physiol.* 2012;112(10):3547-3558. doi:10.1007/s00421-012-2337-5.
 60. Chapman DW, Simpson JA, Iscoe S, Robins T, Nosaka K. Changes in serum fast and slow skeletal troponin I concentration following maximal eccentric contractions. *J Sci Med Sport.* 2013;16(1):82-85. doi:10.1016/j.jsams.2012.05.006.
 61. Hody S, Croisier JL, Bury T, Rogister B, Leprince P. Eccentric muscle contractions: Risks and benefits. *Front Physiol.* 2019;10(MAY):1-18. doi:10.3389/fphys.2019.00536.
 62. Goligher EC, Urrea C, Vorona SL, et al. Diaphragm Inactivity And Eccentric Contractile Activity Are Common And Impair Diaphragm Function During Mechanical Ventilation. *Am J Respir Crit Care Med.* (D105):3-4.
 63. Morgan DL. New insights into the behavior of muscle during active lengthening. *Biophys J.* 1990;57(2):209-221. doi:10.1016/S0006-3495(90)82524-8.
 64. Barwing J, Ambold M, Linden N, Quintel M, Moerer O. Evaluation of the catheter positioning for neurally adjusted ventilatory assist. *Intensive Care Med.* 2009;35(10):1809-1814. doi:10.1007/s00134-009-1587-0.
 65. Sinderby CA, Beck J. Neurally Adjusted Ventilatory Assist. In: Tobin MJ, ed. *Mechanical Ventilation 3rd Edition*. New York; 2013:351-375.
 66. Sinderby C, Liu S, Colombo D, et al. An automated and standardized neural index to quantify patient-ventilator interaction. *Crit Care.* 2013;17(5):R239. doi:10.1186/cc13063.
 67. Landis JR, Koch GG. The measurement of observer agreement for categorical data. *Biometrics.* 1977;33(1):159-174.
 68. Baydur A, Behrakis PK, Zin WA, Jaeger M, Milic-Emili J. A Simple Method for Assessing the Validity of the Esophageal Balloon Technique1–2. *Am Rev Respir Dis.* 2015:5-8. doi:10.1164/arrd.1982.126.5.788.
 69. Sinderby C, Navalesi P, Beck J, et al. Neural control of mechanical ventilation in respiratory failure. *Nat Med.* 1999;5(12):1433-1436. doi:10.1038/71012.
 70. Lachmann B, Robertson B, Vogel J. In Vivo Lung Lavage as an Experimental Model of the Respiratory Distress Syndrome. *Acta Anaesthesiol Scand.* 1980;24(3):231-236.

doi:10.1111/j.1399-6576.1980.tb01541.x.

71. Johansen JW. Update on bispectral index monitoring. *Best Pract Res Clin Anaesthesiol.* 2006;20(1):81-99. doi:10.1016/j.bpa.2005.08.004.
72. ATS/ERS Statement on Respiratory Muscle Testing. *Am J Respir Crit Care Med.* 2002;166(4):518-624. doi:10.1164/rccm.166.4.518.
73. Scott A. Increased injury and intramuscular collagen of the diaphragm in COPD: autopsy observations. *Eur Respir J.* 2006;27(1):51-59. doi:10.1183/09031936.06.00143004.
74. Simpson JA, Labugger R, Collier C, Brison RJ, Iscoe S, Van Eyk JE. Fast and slow skeletal troponin I in serum from patients with various skeletal muscle disorders: A pilot study. *Clin Chem.* 2005;51(6):966-972. doi:10.1373/clinchem.2004.042671.
75. Araos J, Alegría L, García P, et al. Extracorporeal membrane oxygenation improves survival in a novel 24-hour pig model of severe acute respiratory distress syndrome. *Am J Transl Res.* 2016;8(6):2826-2837.
76. Yoshida T, Engelberts D, Otulakowski G, et al. Continuous negative abdominal pressure reduces ventilator-induced lung injury in a porcine model. *Anesthesiology.* 2018;129(1):163-172. doi:10.1097/ALN.0000000000002236.
77. Murias G, de Haro C, Blanch L. Does this ventilated patient have asynchronies? Recognizing reverse triggering and entrainment at the bedside. *Intensive Care Med.* 2016;42(6):1058-1061. doi:10.1007/s00134-015-4177-3.
78. Vaporidi K, Babalis D, Chytas A, et al. Clusters of ineffective efforts during mechanical ventilation: impact on outcome. *Intensive Care Med.* 2017;43(2):184-191. doi:10.1007/s00134-016-4593-z.
79. Sottile PD, Albers D, Higgins C, Mckeehan J, Moss MM. The Association Between Ventilator Dyssynchrony, Delivered Tidal Volume, and Sedation Using a Novel Automated Ventilator Dyssynchrony Detection Algorithm*. *Crit Care Med.* 2018;46(2):e151-e157. doi:10.1097/CCM.0000000000002849.
80. de Haro C, López-Aguilar J, Magrans R, et al. Double Cycling During Mechanical Ventilation. *Crit Care Med.* 2018;54:1. doi:10.1097/CCM.0000000000003256.
81. Goligher EC. Diaphragm Activity and Function During Mechanical Ventilation. 2016.
82. Pohlman MC, McCallister KE, Schweickert WD, et al. Excessive tidal volume from breath stacking during lung-protective ventilation for acute lung injury*. *Crit Care Med.* 2008;36(11):3019-3023. doi:10.1097/CCM.0b013e31818b308b.
83. Beitler JR, Sands SA, Loring SH, et al. Quantifying unintended exposure to high tidal volumes from breath stacking dyssynchrony in ARDS: the BREATHE Criteria HHS Public Access. *Intensive Care Med.* 2016;42(9):1427-1436. doi:10.1007/s00134-016-4423-3.
84. Muzzin S, Trippenbach T, Baconnier P, Benchetrit G. Entrainment of the respiratory rhythm by periodic lung inflation during vagal cooling. *Respir Physiol.* 1989;75(2):157-172.

doi:10.1016/0034-5687(89)90060-1.

85. Simon PM, Zurob AS, Wies WM, et al. Entrainment of respiration in humans by periodic lung inflations: Effect of state and CO₂. *Am J Respir Crit Care Med*. 1999;160(3):950-960. doi:10.1164/ajrccm.160.3.9712057.
86. Beitler JR, Sands SA, Loring SH, et al. Quantifying unintended exposure to high tidal volumes from breath stacking dyssynchrony in ARDS: the BREATHE criteria. *Intensive Care Med*. 2016;42(9):1427-1436. doi:10.1007/s00134-016-4423-3.
87. Yoshida T, Torsani V, Gomes S, et al. Spontaneous effort causes occult pendelluft during mechanical ventilation. *Am J Respir Crit Care Med*. 2013;188(12):1420-1427. doi:10.1164/rccm.201303-0539OC.
88. Yoshida T, Nakamura MAM, Morais C, Amato MBP, Kavanagh BP. REVERSE TRIGGERING CAUSES AN INJURIOUS INFLATION PATTERN DURING MECHANICAL VENTILATION. *Am J Respir Crit Care Med*. 2018;in press.
89. Gattinoni L, Marini JJ, Pesenti A, Quintel M, Mancebo J, Brochard L. The “baby lung” became an adult. *Intensive Care Med*. 2016;42(5):663-673. doi:10.1007/s00134-015-4200-8.
90. Gattinoni L, Carlesso E, Cadringer P, Valenza F, Vagginelli F, Chiumello D. Physical and biological triggers of ventilator-induced lung injury and its prevention. 2003:15-25. doi:10.1183/09031936.03.00021303.
91. Amato MBP, Barbas CSV, Medeiros DM, et al. Effect of a Protective-Ventilation Strategy on Mortality in the Acute Respiratory Distress Syndrome. *N Engl J Med*. 1998;338(6):347-354. doi:10.1056/NEJM199802053380602.
92. Acute Respiratory Distress Syndrome Network. Ventilation with Lower Tidal Volumes as Compared with Traditional Tidal Volumes for Acute Lung Injury and the Acute Respiratory Distress Syndrome. *N Engl J Med*. 2000;342(18):1301-1308. doi:10.1056/NEJM200005043421801.
93. Guérin C, Reignier J, Richard J-C, et al. Prone Positioning in Severe Acute Respiratory Distress Syndrome. *N Engl J Med*. 2013;368(23):2159-2168. doi:10.1056/NEJMoa1214103.
94. Papazian L, Forel J-M, Gacouin A, et al. Neuromuscular Blockers in Early Acute Respiratory Distress Syndrome. *N Engl J Med*. 2010;363(12):1107-1116. doi:10.1056/NEJMoa1005372.
95. Oeckler RA, Lee WY, Park MG, et al. Determinants of plasma membrane wounding by deforming stress. *Am J Physiol - Lung Cell Mol Physiol*. 2010;299(6). doi:10.1152/ajplung.00217.2010.
96. Vlahakis NE, Schroeder MA, Pagano RE, Hubmayr RD. Role of deformation-induced lipid trafficking in the prevention of plasma membrane stress failure. *Am J Respir Crit Care Med*. 2002;166(9):1282-1289. doi:10.1164/rccm.200203-207OC.
97. Vlahakis NE, Hubmayr RD. Cellular stress failure in ventilator-injured lungs. *Am J Respir Crit Care Med*. 2005;171(12):1328-1342. doi:10.1164/rccm.200408-1036SO.

98. Schnader JY, Juan G, Howell JS. Arterial CO₂ partial pressure affects diaphragmatic function. *J Appl Physiol*. 1985;58(3):823-829. doi:10.1152/jappl.1985.58.3.823.
99. Georgopoulos D, Mitrouska I, Webster K, Bshouty Z, Younes M. Effects of inspiratory muscle unloading on the response of respiratory motor output to CO₂. *Am J Respir Crit Care Med*. 1997;155(6):2000-2009. doi:10.1164/ajrccm.155.6.9196108.
100. Wrigge H, Zinserling J, Neumann P, et al. Spontaneous breathing improves lung aeration in oleic acid-induced lung injury. *Anesthesiology*. 2003;99(2):376-384. doi:10.1097/00000542-200308000-00019.
101. Neumann P, Wrigge H, Zinserling J, et al. Spontaneous breathing affects the spatial ventilation and perfusion distribution during mechanical ventilatory support. *Crit Care Med*. 2005;33(5):1090-1095. doi:10.1097/01.CCM.0000163226.34868.0A.
102. Pinsky MR. Cardiopulmonary interactions: Physiologic basis and clinical applications. *Ann Am Thorac Soc*. 2018;15(3):S45-S48. doi:10.1513/AnnalsATS.201704-339FR.
103. Goligher EC, Dres M, Fan E, et al. Mechanical ventilation-induced diaphragm atrophy strongly impacts clinical outcomes. *Am J Respir Crit Care Med*. 2018;197(2):204-213. doi:10.1164/rccm.201703-0536OC.
104. Hooijman PE, Beishuizen A, Witt CC, et al. Diaphragm muscle fiber weakness and ubiquitin-proteasome activation in critically ill patients. *Am J Respir Crit Care Med*. 2015;191(10):1126-1138. doi:10.1164/rccm.201412-2214OC.
105. Shimatani T, Shime N, Nakamura T, Ohshimo S, Hotz J, Khemani RG. Neurally adjusted ventilatory assist mitigates ventilator-induced diaphragm injury in rabbits. *Respir Res*. 2019;20(1):1-10. doi:10.1186/s12931-019-1265-x.
106. Proske U, Morgan DL. Muscle damage from eccentric exercise: mechanism, mechanical signs, adaptation and clinical applications. *J Physiol*. 2001;537(2):333-345. doi:10.1111/j.1469-7793.2001.00333.x.
107. Moss BM, Refsnes PE, Abildgaard A, Nicolaysen K, Jensen J. Effects of maximal effort strength training with different loads on dynamic strength, cross-sectional area, load-power and load-velocity relationships. *Eur J Appl Physiol Occup Physiol*. 1997;75(3):193-199. doi:10.1007/s004210050147.
108. Castro MJ, McCann DJ, Shaffrath JD, Adams WC. Peak torque per unit cross-sectional area differs between strength-trained and untrained young adults. *Med Sci Sports Exerc*. 1995;27(3):397-403. doi:10.1249/00005768-199503000-00016.
109. Brechue WF, Abe T. The role of FFM accumulation and skeletal muscle architecture in powerlifting performance. *Eur J Appl Physiol*. 2002;86(4):327-336. doi:10.1007/s00421-001-0543-7.
110. Jaber S, Petrof BJ, Jung B, et al. Rapidly progressive diaphragmatic weakness and injury during mechanical ventilation in humans. *Am J Respir Crit Care Med*. 2011;183(3):364-371. doi:10.1164/rccm.201004-0670OC.

111. Levine S, Biswas C, Dierov J, et al. Increased proteolysis, myosin depletion, and atrophic AKT-FOXO signaling in human diaphragm disuse. *Am J Respir Crit Care Med*. 2011;183(4):483-490. doi:10.1164/rccm.200910-1487OC.
112. Jung B, Constantin JM, Rossel N, et al. Adaptive support ventilation prevents ventilator-induced diaphragmatic dysfunction in piglet: An in vivo and in vitro study. *Anesthesiology*. 2010;112(6):1435-1443. doi:10.1097/ALN.0b013e3181d7b036.
113. Sassoon CSH, Zhu E, Caiozzo VJ. Assist-control mechanical ventilation attenuates ventilator-induced diaphragmatic dysfunction. *Am J Respir Crit Care Med*. 2004;170(6):626-632. doi:10.1164/rccm.200401-042OC.
114. Masmoudi H, Coirault C, Demoule A, et al. Can phrenic stimulation protect the diaphragm from mechanical ventilation-induced damage? *Eur Respir J*. 2013;42(1):280-283. doi:10.1183/09031936.00045613.
115. Martin AD, Joseph AM, Beaver TM, et al. Effect of intermittent phrenic nerve stimulation during cardiothoracic surgery on mitochondrial respiration in the human diaphragm. *Crit Care Med*. 2014;42(2):1-9. doi:10.1097/CCM.0b013e3182a63fdf.
116. Bassett DR. Scientific contributions of A. V. Hill: exercise physiology pioneer. *J Appl Physiol*. 2002;93(5):1567-1582. doi:10.1152/jappphysiol.01246.2001.
117. Franchi M V., Atherton PJ, Reeves ND, et al. Architectural, functional and molecular responses to concentric and eccentric loading in human skeletal muscle. *Acta Physiol*. 2014;210(3):642-654. doi:10.1111/apha.12225.
118. Narici M, Franchi M, Maganaris C. Muscle structural assembly and functional consequences. *J Exp Biol*. 2016;219(2):276-284. doi:10.1242/jeb.128017.
119. Franchi M V., Wilkinson DJ, Quinlan JL, et al. Early structural remodeling and deuterium oxide-derived protein metabolic responses to eccentric and concentric loading in human skeletal muscle. *Physiol Rep*. 2015;3(11):1-11. doi:10.14814/phy2.12593.
120. Reeves ND, Maganaris CN, Longo S, Narici M V. Differential adaptations to eccentric versus conventional resistance training in older humans. *Exp Physiol*. 2009;94(7):825-833. doi:10.1113/expphysiol.2009.046599.
121. Carteaux G, Mancebo J, Mercat A, et al. Bedside adjustment of proportional assist ventilation to target a predefined range of respiratory effort. *Crit Care Med*. 2013;41(9):2125-2132. doi:10.1097/CCM.0b013e31828a42e5.
122. Sassoon CSH, Light RW, Lodia R, Sieck GC, Mahutte CK. Pressure-time product during continuous positive airway pressure, pressure support ventilation, and T-piece during weaning from mechanical ventilation. *Am Rev Respir Dis*. 1991;143(3 Pt 1):469-475. doi:10.1164/ajrccm/143.3.469.
123. Jubran A, Tobin MJ. Pathophysiologic basis of acute respiratory distress in patients who fail a trial of weaning from mechanical ventilation. *Am J Respir Crit Care Med*. 1997;155(3):906-915. doi:10.1164/ajrccm.155.3.9117025.

124. Sinderby C, Beck J, Spahija J, Weinberg J, Grassino A. Voluntary activation of the human diaphragm in health and disease. *J Appl Physiol.* 1998;85(6):2146-2158. doi:10.1152/jappl.1998.85.6.2146.

ANNEXES

Annex 1. Reverse triggering detection based on expiratory time (Te).

When a ventilator is set to a control mode (pressure or volume), we assume (by definition) that the Maximum Expiratory time (Max-Te) must be determined by the set respiratory rate and percentage of inspiratory pause. Thus, Max-Te was determined using all breaths where no EAdi was found. Then, to determine if a breath was either a machine or patient triggered, we analyzed the “Te” duration using the Max-Te as a reference. If the “Te” of the previous breath was \geq (“Max-Te” – 0.0165 seconds) (Neurosync samples every 16 milliseconds), the current breath must be mandatory and initiated by the ventilator. In contrast, if the “Te” of the previous breath was $<$ to “Max-Te” – 0.0165 seconds, the current breath was labeled as patient triggered (See Figure).

Detection of reverse triggering using expiratory time method was determined according to the following criteria: 1. Machine triggered breath (when previous “Te” was \geq to Max-Te); 2. EAdi delay (EAdi starting after the pneumatic event); 3. EAdi breath (when the sum of consecutive EAdi sample differences exceed the trigger level of 0.5uV and EAdi time integral $>$ 0.5uV after cycling off at 70% of peak EAdi); and 4. Peak EAdi $> 1\mu\text{V}$.

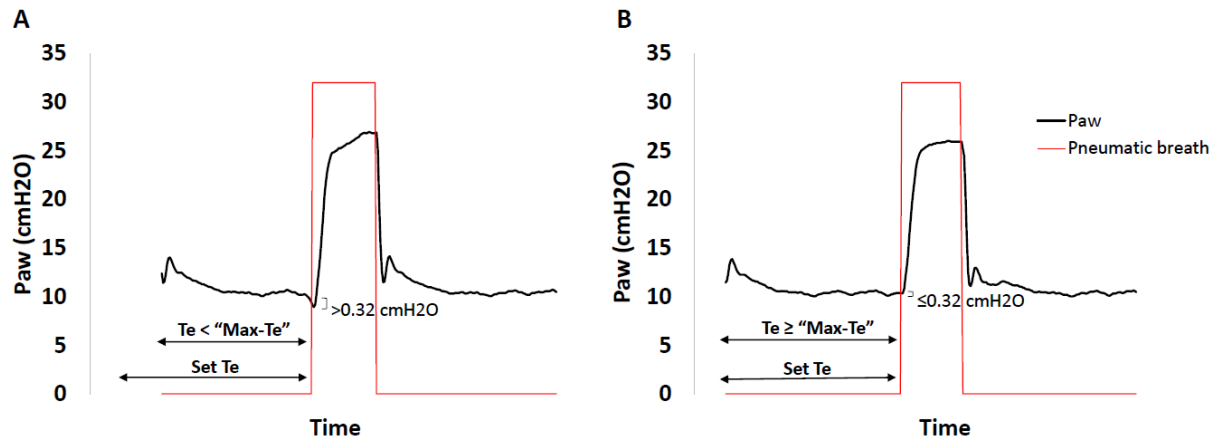
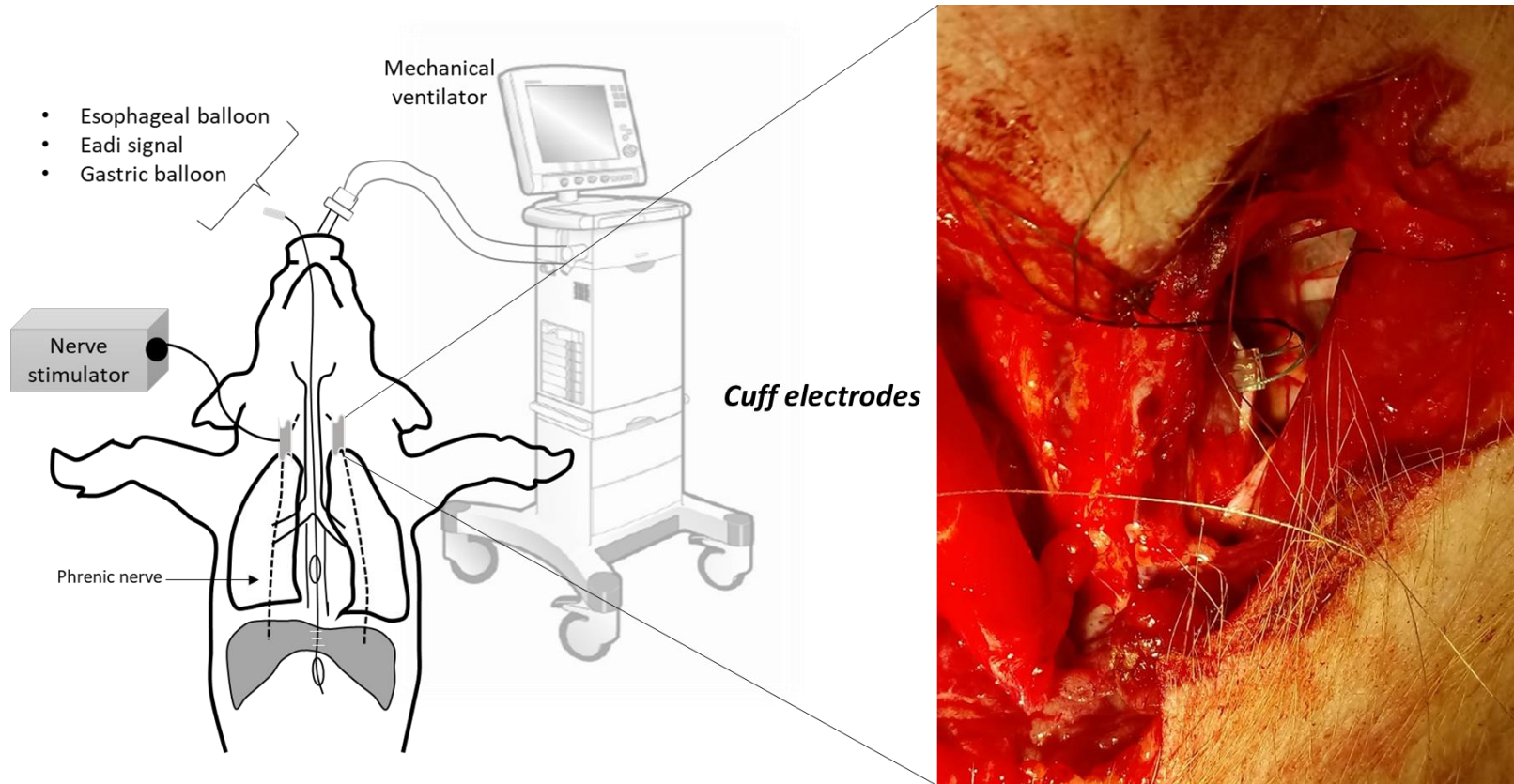
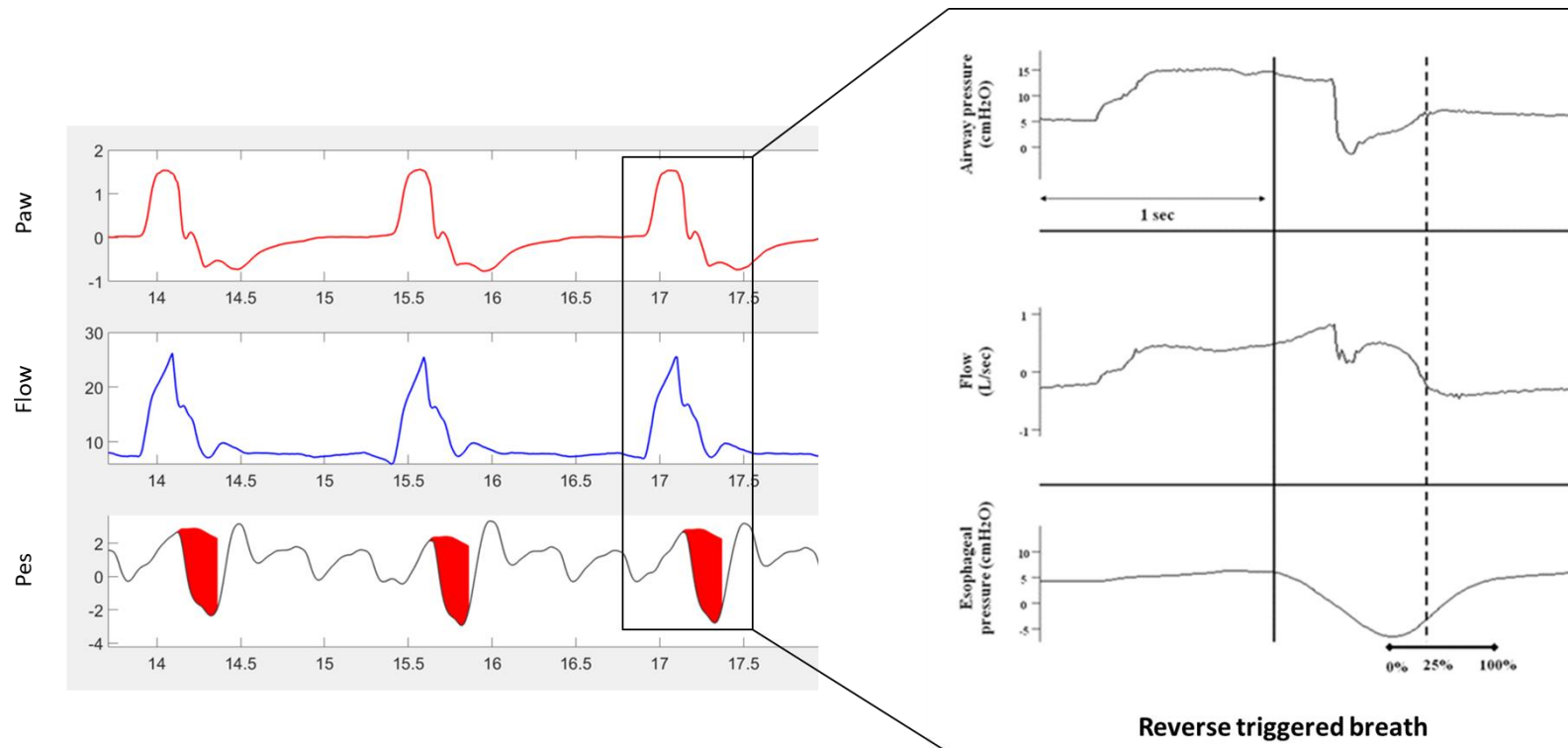


Figure. Definition of patient or machine triggered breath by Neurosync or expiratory time method. **A.** Representative tracing of a patient triggered breath where preceding Te is less than set Te and the drop in Paw is greater than 0.325 cmH2O. **B.** Representative tracing of a machine triggered breath where preceding Te is equal to the set Te and the drop in Paw is less than 0.325 cmH2O.

Annex 2. Diagram of the experiment set up and cuff electrodes



Annex 3. Calculation of Pressure-Time-Product in reverse triggered breaths



Annex 4. Western Blot protocol for Troponin I in serum samples

This protocol is modified from standard Western blot according to advice from Jeremy Simpson. See Simpson et al (2005) Clin Chem 51:6 and Foster et al (2012) Eur J Appl Physiol 112:3547. It uses a modified sample buffer with increased denaturants to assure separation of troponin from serum proteins, and a more alkaline transfer buffer due to the unusually high pI of skeletal troponin I. Modified sample buffer (MSB): 3.3 mg/mL SDS; 3.3 mg/mL CHAPS; 3.3 mg/mL NP-40; 1.4 mM urea, 50 mM Tris-HCl pH 6.8, 10% glycerol. This is a non-reducing sample buffer.

For 10 mL buffer (from stock solutions):

20% SDS	165 µL
10% CHAPS	330 µL
10% NP-40	330 µL
28 mM urea	500 µL
0.5M Tris pH6.8 (stacking gel buffer)	1.0 mL
Glycerol	1.0 mL
Water	6.7 mL

Few grains bromophenol blue (Na salt)

Store at 4C

Transfer Buffer: 10 mM CAPS pH 11, 10% Methanol

For 1 L (from stock solution)

100 mM CAPS pH11	100 mL
Water	800 mL
Methanol	100 mL

Make fresh, chill at 4C while preparing and running gel.

Western procedure:

1. Dilute serum samples 10X with modified sample buffer.
2. Heat at 95C for 10 min
3. Load 10 µl (for 10 well comb) on 12.5% SDS-PAGE gel, 1.5 mm gel
4. Run at 100 V for until dye front reaches bottom of gel (approx. 3 h?)
5. Transfer to PVDF in 10 mM CAPS (pH 11)/10% methanol for 45 min at 100 V.
6. Stain with Ponceau and cut off the albumin band (approx. 50 kD). Use the bottom half of the blot for immunodetection, troponin is approx. 25 kD.

Block: 5% milk, 5% BSA, 0.1% Tween in TBS overnight

Primary antibody: Dilute 1:1000 in 5% BSA/TBST. Antibody is NBP1-57842 from Novus Biologicals, a rabbit polyclonal raised against human peptide sequence PLHIPGSMSEVQELCKQLHAKIDAAEEEEKYDMEVVQKTSKELEDMNQKL. Stored in 10 ul aliquots at -20C

Incubate blot with primary antibody for 3-4 hr at room temperature.

Secondary antibody: goat anti-rabbit IgG FC-HRP linked (Jackson ImmunoResearch cat # 111-035-008) at 1:10,000 in blocking buffer, 1 hr at room temperature

Detection by ECL.